Carl von Ossietzky Universität Oldenburg

Institute of Physics

Sustainable Renewable Energy Technologies (SuRE)

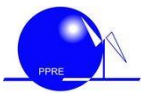

Master's Thesis

Title:

"Power-Grid-Friendly Placement of Large-Scale Hydrogen Production Facilities in the Northwest German High Voltage Grid"

Presented by:	Orlando Antonio PEREIRA LEON
First examiner:	Frank SCHULDT
Second examiner:	Prof. Dr. Carsten AGERT
Supervisors:	doc. dr. Mirza SARAJLIĆ
	Mahdi TAKACH
Host institution:	DLR Institute of Networked Energy Systems
Place, date:	Oldenburg, 09.08.2023

Acknowledgements

First and foremost, I extend my deepest gratitude to God, whose blessings have guided me through this endeavour.

My heartfelt thanks go to my wife, my constant source of strength and support. Without her unwavering faith in me, I wouldn't have made it this far. I am also incredibly grateful to my family, my mother and father, for their unconditional love and support.

To Mirza Sarajlić, my direct supervisor, I extend my sincerest appreciation. His expertise, mentorship, and guidance have been indispensable from the beginning of this project. His role as a reference point has inspired and motivated me throughout this journey.

I would like to extend my gratitude to the staff of the Flexibilities and Ancillary Services Group of the EST Department in the DLR, particularly to Mahdi Takach, Elena Memmel, Daniel Jung, Robert Beckman, and Nauman Beg. Their valuable feedback and advice have significantly enriched this work.

A special note of thanks goes to Frank Schuldt and Prof. Dr. Carsten Agert, the first and second examiners of this thesis, for dedicating their time and expertise to review and grade this scientific endeavour.

My appreciation also extends to the German Government, the DAAD, and by extension, the German people. Their generous funding has made my Master's studies in Renewable Energy possible.

Lastly, my deepest thanks to the lecturers and staff of PPRE and SuRE. Their vast knowledge and guidance have been pivotal in my academic and career growth, enabling me to reach this milestone.

Thank you all for making this journey possible.

Abstract

"Power-Grid-Friendly Placement of Large-Scale Hydrogen Production Facilities in the Northwest German High Voltage Grid"

This thesis presents a novel method for determining a strategic distribution of new large-scale Green Hydrogen (GH2) production plants across nodes of interest within the northwest German high voltage power grid. The research conducted in this thesis establishes a framework for gainfully connecting GH2 production plants to power grid nodes, with an emphasis on maintaining grid voltage stability and leveraging the advantages of large-scale GH2 facilities. The applied methodology uses a novel developed algorithm to determine the maximum GH2 plant size that can be connected to each node while keeping the secure steady state power system operation.

Through the utilization of Voltage-Power (V-P) characteristic analysis, this thesis successfully identifies connection points that can provide large amounts of power without causing voltage collapse, permitting the incorporation of GH2 loads of up to 7700 MW at an individual node, while maintaining reliable power system operation. This process involves constrained and optimal power flow calculations, facilitating the allocation of power to generators of different energy sources according to electricity generation costs.

Open-source data was utilized to develop a simulation model of the northwest German power grid, achieving the implementation of two different grid states: the current situation (scenario "Status Quo") and a future grid state (scenario "NEP2035"). Moreover, diverse operative conditions were applied to these grid scenarios, achieving a total of sixteen cases for steady state simulation and analysis. The obtained results indicate that the northwest German high voltage grid can accommodate new large-scale GH2 plants under various operating conditions.

The thesis concludes by acknowledging the importance of additional factors, such as gas infrastructure, storage capacity, and environmental regulations in determining the definitive distribution of GH2 plants, which could be incorporated in future extension to this work. However, even though further research is necessary, this thesis serves as a significant component in the identification of power capacity and optimal placement of new large-scale hydrogen production facilities in Germany, marking it an essential step toward a more sustainable future.

Keywords: power grid modelling, green hydrogen, load flow calculation, voltage-power (V-P) characteristic analysis, voltage stability limit, open-source data.

Contents

List of Figures

List of Tables

Symbols and abbreviations

AC	Alternating Current
API	Application Programming Interface
DC	Direct Current
GHG	Green House Gases
GH2	Green Hydrogen
HV	High Voltage
HVDC	High Voltage Direct Current
NEP	Grid Development Plan (germ. *Netzentwicklungsplan*)
OPF	Optimal Power Flow
PEM	Polymer electrolyte membrane
$\boldsymbol{PF}$	Power Factor
$\boldsymbol{P}_{\mathrm{m}}$	Maximum power that can be drawn from the bus while keeping its voltage in an acceptable value
$\boldsymbol{P}_{\mathrm{VSL}}$	Power at VSL
RES	Renewable Energy Sources
$\boldsymbol{RP}$	Required GH2 power for the interest area
VSL	Voltage Stability Limit
WEG	Wind Energy Generator

1. Introduction

The world is currently facing the threat of an imminent climate change crisis due to human-induced global warming as a consequence of the emission of greenhouse gasses (GHG) to the atmosphere [1]. This requires immediate corrective actions to reduce worldwide GHG emissions in every area of human activity. To address this issue, many countries, including Germany, have established ambitious climate change mitigation strategies, such as the Paris Agreement, which aims to limit global warming to well below 2°C compared to pre-industrial levels [2].

As part of its climate action plan, Germany is committed to increasing the share of renewable energy (GHG-emission free) in its electricity mix, with the goal of achieving at least 80 % of produced electricity from renewables by 2050 [3]. This commitment was demonstrated in the annual electricity mix of the year 2022, in which renewable energy sources reached 49.6 % of the total German electricity production [4]. Furthermore, through the adoption of the Federal Climate Change Act (2021), Germany has set the ambitious goal of achieving climate neutrality by 2045, which will require not only the reduction of GHG emissions in the electricity sector, but also from other sectors, such as transport and industry [5].

It is worth mentioning that the current installed power of solar and wind power plants in Germany totals roundabout 137 GW, which is almost twice the installed capacity of fossil-fuel fired power plants [6]. However, despite the amazing figures of installed power and electricity production, the intermittency of renewable energy sources poses a significant challenge to the power system's stability and its efficient operation. Since the output of renewable energy power plants (especially wind and solar) depends on environmental conditions and not on the power demand of loads, the natural fluctuation of wind speed and solar irradiance can result in periods of excess power supply when available power is greater than demand, as well as power shortages in the opposite case.

In order to solve this inherent problem, present in variable renewable energy sources (RES), flexibility solutions such as energy storage must be implemented to provide energy systems with the ability to store, transport and later utilize energy that can be produced in times of excess power supply from renewable sources [7].

In this context, “Green Hydrogen” (GH2), which is hydrogen produced utilizing renewable energy sources, has emerged as a promising energy storage solution, allowing the later utilization of energy produced from RES in the electric power

system, as well as in other sectors (transport, industry) [8]. In this line of application, GH2 can be used as energy source in fuel-cell-powered transport, or directly as a fuel in industrial applications, replacing fossil fuels and thus reducing GHG emissions related to their combustion. Moreover, given that hydrogen is already a component in the production of fuels, as well as a base substance for producing useful chemicals, GH2 can replace conventional hydrogen produced from fossil fuels (which generate GHG emissions [9]) with no adjustment being necessary [10].

"Green Hydrogen" can be produced through various methods, although water splitting via electrolysis is the most mature technology and the only one available at a market scale [11]. The most used technologies to carry out electrolysis for hydrogen production are alkaline electrolysers, polymer electrolyte membrane (PEM) electrolysers and high-temperature water electrolysers [11].

The current level of domestic hydrogen consumption in Germany is approximately 55 TWh per year (2021), and it is estimated to increase to approximately 90–110 TWh by 2030 under the National Hydrogen Strategy [10]. In order to partially cover this demand, Germany plans to incorporate 5 GW of GH2 production capacity by 2030, and increase this capacity to 10 GW by 2035 (or by 2040 at the latest) [10].

The expansion in the GH2 production capacity is also considered in the German Grid Development Plan 2035 (NEP 2035), which estimates that two thirds of the hydrogen electrolysis capacity will be allocated in the northern part of Germany, where exists a high penetration of wind energy power plants, while the remaining one third will be located in the south of Germany [12]. Applying this assumption to the target installed capacities proposed in the National Hydrogen Strategy results in approximately 3.3 GW and 6.6 GW to be achieved in the northern part of Germany by 2030 and 2035, respectively.

Although this distribution of GH2 production capacity is a rough estimation, special attention should be paid to the actual placement of these new large-scale electrolysers in the power grid, given that failing to do so could have a negative impact on the power system. In this regard, a study made in 2021 by the companies Gasunie, Tennet and Thyssengas identified five potential areas in the federal states of Lower Saxony and Schleswig-Holstein (Northwest Germany) for large-scale electrolysers, that would benefit the energy system for the current power grid status as well as for the NEP 2035 scenario [13]. In that study, a multi-criteria decision-making method based on Utility Analysis was applied, considering the impact of

new electrolysers in the categories of “Electricity”, “Gas” and “Environment”, suggesting not to install on-site electrolysers near industrial facilities in order to avoid contributing to the formation of grid bottlenecks. They also state that favourable locations for power-to-gas (GH2 production) plants can be found close to places where renewable energy is available, i.e. close to the coast in north-western Lower Saxony and Schleswig-Holstein.

After considering the recommendations made in the previously mentioned study, alongside the assumptions presented in the National Hydrogen Strategy and the NEP 2035, a subsequent logical step towards achieving the projected integration of new large-scale electrolysers into the power grid would be to identify the optimal power system nodes (buses) in the areas of interest for a power-system-friendly placement of the new electrolysers, i.e. where it allows satisfactory (safe and stable) operation of the power system. In other words, given the required installed power and “favourable” geographical areas for placing new large-scale electrolysers, it is yet necessary to determine the best connection points to the power grid within these “favourable” areas, which leads to the following question: are the suggested areas capable of receiving the required installed capacity of GH2 production plants while keeping satisfactory operating conditions, and how should the new load be distributed among the power system buses of these areas?

In order to address this question, this thesis proposes a method that can be utilized to determine a power-system-friendly distribution of large-scale electrolysers among nodes of interest in an existing power grid, while allowing satisfactory steady-state operating conditions. This method takes the desired total installed capacity of GH2 production plants and performs the automatic selection of the most convenient nodes to connect new loads in a predefined steady-state operative scenario, based on static (steady-state) voltage stability criteria. Subsequently, the automatic allocation of power to the selected nodes is carried out, based on keeping the power system under normal steady-state operating conditions.

The proposed method automatically allocates the highest possible amount of power to every selected node, assuming benefits in the implementation of ever larger GH2 production plants, due to economies of scale [14], considering at the same time steady-state operative constraints, such as branch element loading and bus voltage levels. The steady-state voltage stability criteria ensure earlier selection of the most voltage-stable nodes, which will firstly receive the new loads (GH2 production plants).

Voltage stability is defined as the ability to keep acceptable voltages in the power system buses when operating under normal conditions as well as after being subjected to a disturbance, such as load increase [15]. A power system is considered unstable when there is a continuous and progressive droop in voltage after a change in operating conditions. Due to voltage instability, the power transferred to the load becomes limited and voltage collapse can take place, at which point the power system is unable to supply power to the loads [15].

Indicators of voltage stability can be used to determine operative limits, such as maximum active power transfer values, which indicate the maximum power that can be delivered to a load connected to a power system bus. Techniques such as the *V-P* Characteristic Analysis help to identify stable and unstable operating points by establishing the relationship between the amount of power that can be delivered to a load and its terminal voltage, indicating the maximum active power value that can be supplied while keeping voltage at an acceptable level and without producing a voltage collapse.

Several studies have previously made use of the *V-P* Characteristic Analysis for voltage stability assessment. Linh in [16] has presented a method to find the maximum load power that allows operation within the steady-state voltage stability region for each bus of a test distribution power system with presence of wind energy generators. Besides, Thasnas and Siritaratiwat in [17] have applied *V-P* Characteristic curves to evaluate static voltage stability margin enhancement in an IEEE 14-bus test power system by placing reactive power compensation elements in the weakest bus of the power system. Moreover, in [18] the authors have presented a method that uses the active power margin (from the *V-P* characteristic) to determine weak buses (in terms of voltage stability) in a power system.

In this thesis, the *V-P* Characteristic Analysis will be utilized to determine the most stable buses in terms of voltage stability, i.e. the buses that allow the highest amount of power to be delivered to loads connected at their terminals, and the highest increase in power demand with the smallest change in voltage as a result. The points of connection (buses) for the new large-scale electrolysers in the northwest German high voltage grid will be then selected according to their voltage stability, prioritizing the most stable buses.

The method developed in this thesis will be tested on a simulation model of the Northwest German High Voltage Grid, which includes buses, transmission lines, transformers, generators, and loads at 110 kV, 220 kV, and 380 kV, located in the federal states of Hamburg, Bremen, Lower Saxony, and Schleswig-Holstein. Two

power grid development scenarios: the current status ("Status Quo") and the "NEP2035" grid scenario, will be examined in this thesis. Moreover, various operative scenarios will be considered, portraying different wind energy availability conditions as well as multiple power demand scenarios.

The aim of the aforementioned method is to serve as a fundamental component in the process of identifying the power capacity and optimal placement of new large-scale hydrogen production facilities in Germany, allowing steady-state analysis of different critical operation scenarios, which requires less modelling detail, computational power and is therefore less time consuming than dynamic time-domain analysis [15]. Thus, further testing and studies using dynamic simulations are reserved for the most relevant cases, for which initial conditions and a distribution of electrolysers among the power system nodes would be available by applying the method to be presented in this thesis, enabling future investigation of transient stability or dynamic voltage stability analysis under different contingencies.

Finally, the purpose of this thesis can be condensed as the formulation of a strategic distribution of GH2 production plants across the power grid buses (nodes) of the designated area, which will allow maximum power delivery at the selected nodes without producing element overloads or voltage collapse, i.e. keeping acceptable steady-state operating conditions. Additionally, it is of interest to investigate whether the required installed power of GH2 production plants can be effectively assigned to the Northwest German region.

The outcomes of this thesis will offer insights into the Northwest German Power Grid's potential to accommodate new large-scale GH2 production facilities, revealing possible restrictions on the maximum allowable size and overall installed capacity of these plants within the analysed areas.

2. Theory

This chapter explores the theoretical background of this thesis, covering the basic concepts related to power systems, as well as different methods of analysis and simulation, which include dynamic and static analysis, power flow calculation, voltage stability and V-P characteristic analysis.

2.1. Power Systems

Power systems are complex networks that involve various components such as generators, transmission lines, substations (buses), transformers, and loads, which work together to ensure the reliable and efficient delivery of electricity to consumers in the industrial, commercial and residential sectors [19]. Understanding the behaviour of these components and the overall power system is crucial for maintaining the stability and reliability of the power grid [19]. Figure 2.1 presents a diagram of an electric power system, depicting various interconnected components.

Generators are responsible for converting different types of energy (traditionally mechanical energy) into electrical energy. They are typically driven by turbines, or internal combustion engines and are usually found grouped in power plants. Large power plants are primarily connected to the transmission grid in high voltage, forming the backbone of electricity production. On the other hand, smaller plants can be found in the subtransmission or distribution grids, close to load centres [15].

Nowadays, the ever-increasing number of independent and decentralized renewable power plants (such as solar PV and wind generators), which are geographically distributed, has enlarged the number of power plants with a direct connection to the subtransmission or distribution system [20].

Transformers are used to step up or down AC voltage for efficient transmission and distribution of electricity. They can increase voltage for long-distance transmission or decrease voltage for local distribution, minimizing energy losses [19].

Transmission lines are the links to transport electricity over long distances between substations and from power plants to the distribution system. They operate at high voltages and their design allows to minimize power losses during power transfer [15].

Substations (also known as buses) are junction points in the power system where transmission lines, transformers, generators and other equipment are interconnected. They serve as distribution centres for routing electricity to different regions or areas [15].

Loads represent electrical devices and systems that consume power, which can be classified in residential, commercial, and industrial users. Loads determine the power demand (both active and reactive) of the system [15]. Industrial loads generally employ three-phase systems, whereas single-phase systems serve residential and commercial loads [15]. In this thesis, loads will be clustered in mathematical equivalents, connected to high voltage substations.

Special loads known as reactive power compensation devices are also commonly found in electric power systems, being used to maintain power factor and voltage in the system at desired levels by consuming or injecting reactive power. For example, reactive power consumed by inductive elements in the grid can cause the voltage to drop under acceptable values. Devices like capacitors and static compensators are used to regulate reactive power, improve voltage stability, and reduce line losses [20].

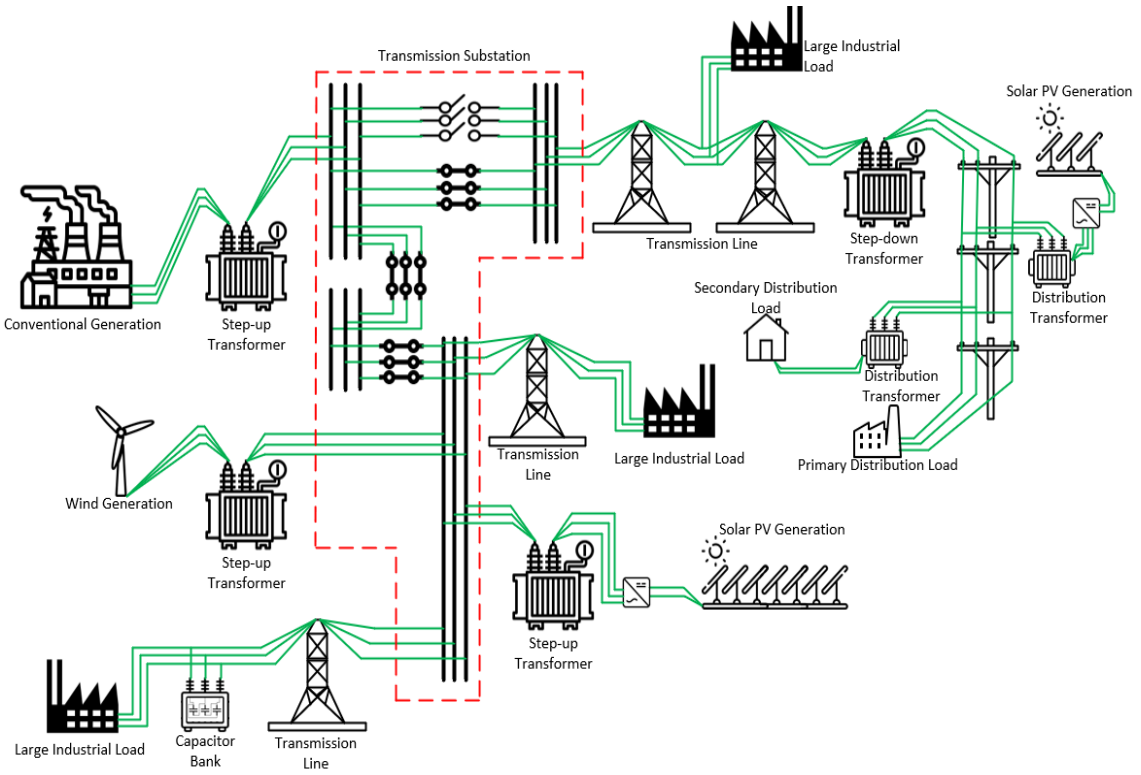

Figure 2.1. Diagram of an electric power system, with its basic components.

2.1.1. Structure of the Power System

The power system is typically categorized into three main subsystems: transmission, subtransmission, and distribution systems [15]. Figure 2.2 illustrates the different category levels of a power system.

2.1.1.1. Transmission system

The transmission system links all major power generation facilities and primary load centres in a power grid, functioning as the backbone of the integrated power system and operating at the highest voltage levels with the aim of minimizing power losses [15]. The usual nominal voltages in Germany for AC power transmission are 220 kV and 380 kV [21]. High voltage direct current (HVDC) transmission is also used nowadays for transporting large blocks of power over a long distance, having comparative advantages to AC power in specific cases [15].

Generator voltages typically fall within tens of thousands of volts, which are increased (using transformers) to the transmission voltage level for transportation to transmission substations. Here, the voltages are reduced to the subtransmission level [15]. Renewable energy sources such as PV and wind tend to be more geographically distributed, leading to a spread-out generation landscape, which has led to their incorporation into distribution and subtransmission systems, a shift from their conventional placement at the transmission level [20].

2.1.1.2. Subtransmission system

On the other hand, the subtransmission system transfers AC power in smaller amounts from the transmission substations to the distribution substations [15], as well as to large industrial loads. In Germany, direct supply from the transmission system is often provided to large industrial customers at a voltage level between 60 kV and 220 kV [21]. In certain cases, there is no distinct boundary between subtransmission and transmission circuits [15].

2.1.1.3. Distribution system

The distribution system represents the final stage in the transfer of power to the individual customers [15]. The primary distribution voltage in Germany is typically between 6 kV and 60 kV [21], with small industrial customers being supplied by primary feeders at this voltage level [15]. The secondary distribution feeders supply residential and commercial customers at a low voltage level, being 230 V and 400 V the standard values in Germany [21].

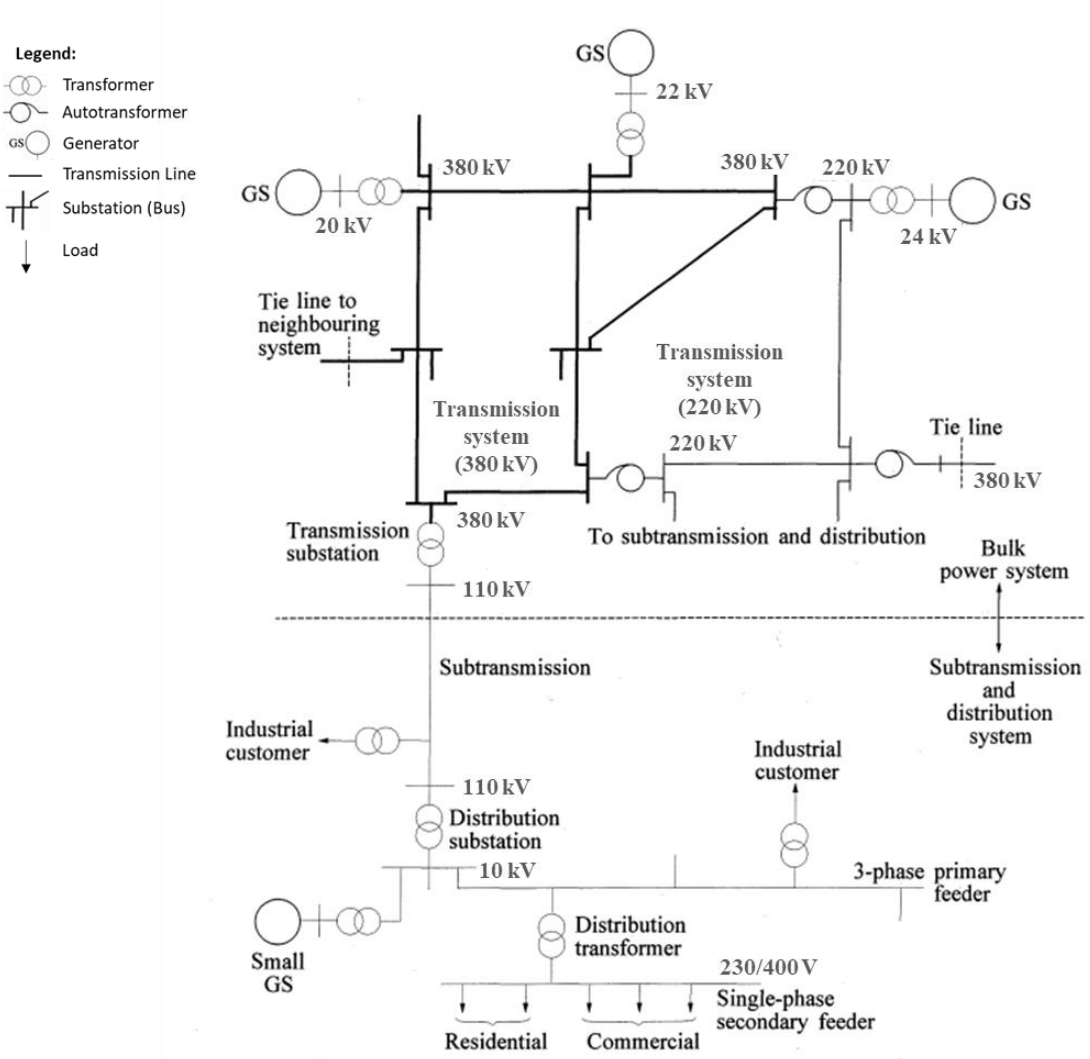

Figure 2.2. Single-line diagram of a sample three-phase AC power system. Depicted from [15].

2.1.2. Electric power in AC Systems

In an AC system, voltage and current vary sinusoidally over time with an almost constant frequency [19]. The standard frequency values for AC power in Germany is 50 Hz. Electric power in AC systems can be divided into two components: real power (P) and reactive power (Q). Real power is the actual power that performs useful work, such as lighting a bulb or operating machinery and its measurement unit is the watt [W] [19]. On the other hand, reactive power is the power exchanged with inductive and capacitive elements in a circuit, maintaining magnetic and electric fields; therefore, the reactive power can be inductive or capacitive, and it is measured in volt-amperes reactive [var] [19]. Complex power (S) represents the combination of real power and reactive power and is measured in volt-amperes [VA] [19].

According to reference [19], the following equations can be used to describe the relationships between S, P and Q:

$$S = P + jQ \tag{2.1}$$

$$|S| = \sqrt{P^2 + Q^2} \tag{2.2}$$

$$P = |S| \cdot cos\,\theta \tag{2.3}$$

$$Q = |S| \cdot sin\,\theta \tag{2.4}$$

where: S is complex power, P is active power, Q is reactive power, $|S|$ is magnitude of the complex power, also called apparent power, θ is phase angle (angular difference between AC current and voltage sinewaves) and $\cos\theta$ is power factor (PF).

2.1.3. Power System Analysis and Simulation

Power system analysis and simulation techniques are used to understand the behaviour of the power system under different operating conditions. Two types of analysis are commonly used: dynamic analysis and static analysis.

Dynamic analysis involves modelling the time-varying behaviour of the power system components and studying the system response to disturbances such as faults or sudden changes in load [15]. Large-disturbance voltage stability and transient stability analysis are examples of dynamic analysis used to study the stability of the power system during transient events [15].

Static analysis, on the other hand, involves analysing the steady-state behaviour of the power system [15]. Two common techniques used in static analysis are power flow calculation and V-P Characteristic for static voltage stability analysis.

2.1.4. Power Flow Analysis

Power flow analysis, also known as load flow analysis, is used to determine power flows (P and Q) in branch elements, as well as voltages (V) and their angles (θ) in buses of a power system under specified steady-state conditions [15]. For the solution of a power flow problem, each one of the system buses must be classified into one of the following representations: Voltage-controlled (PV) bus, Load (PQ) bus or Slack (swing) bus [15].

The PV bus is characterized by the specification of active power and voltage magnitude. It also includes limits on reactive power, which depend on the specific

characteristics of the devices connected to the bus. Examples of such devices include generators, synchronous condensers, and static var compensators.

On the other hand, the PQ bus is defined by the specification of both active and reactive power. Typically, loads are assumed to have constant power, and they are considered to be supplied by transformers that can adjust the output voltage accordingly [15].

Finally, the slack bus is distinguished by the specification of both voltage magnitude and phase angle. Since the power losses within the system are not initially known, at least one bus must have unspecified values for active power and reactive power (P and Q). Consequently, the slack bus becomes the only bus in the system with a known voltage [15].

A nonlinear problem is formed when trying to determine the two missing variables at each bus. As a result, power-flow equations are solved through iterative techniques like the Gauss-Seidel or Newton-Raphson methods. The detailed principles and application of these iterative methods can be found in reference [22].

2.1.4.1. Optimal Power Flow (OPF)

An OPF analysis represents a power flow problem where specific control variables need to be optimized to minimize an objective function, such as the cost of active power generation. This optimization is conducted while ensuring that physical and operational constraints on various dependent variables are met [23].

2.1.5. Voltage Stability

Voltage stability in power systems refers to the system's capability to maintain voltage levels within the acceptable range at all nodes under specific operating conditions or in the aftermath of a disturbance [24]. Voltage instability in a system becomes evident when there is a continuous decline or gradual decrease in bus voltages, which can occur due to various factors such as disturbances, load increase or changes in operating conditions [24].

The primary objective of a power system is to ensure the reliable delivery of electrical energy to the consumer (load). However, voltage instability can restrict the power transferred to the load, and during a voltage collapse, the system becomes incapable of supplying power to the load [24]. Consequently, voltage instability can lead to undesirable outcomes such as the activation of protective systems causing cascading outages, including the tripping of transmission lines and other elements

[25]. Additionally, loss of synchronism among generators may occur as a result of these outages or due to operating conditions that violate field current limits [25].

A significant contributing factor to voltage instability is the voltage drop that occurs when active and reactive power flow through inductive reactances in the transmission grid. This limits the power transfer capability and voltage support within the network [25].

2.1.5.1. Voltage Stability Classification

Voltage stability of a system can be categorized into long-term voltage stability and short-term voltage stability. The classification of long-term and short-term is based on the duration it takes for the system to transition into voltage instability following a disturbance or a change in the operating point [24].

The assessment of long-term voltage stability refers to durations ranging from a few minutes to a few tens of minutes, and in unusual cases, it can be prolonged to a few hours if voltage instability goes undetected. A classic example of long-term voltage instability is voltage collapse, which is a critical condition in a power system, where the voltage levels experience a rapid and significant decline, leading to a severe drop or even a complete collapse in voltage, being its primary cause a loss of generation or an increase in load [24]. Static analysis can often be employed in long-term stability analysis to estimate stability margins, identify factors influencing stability, and evaluate numerous system conditions and scenarios [24]. Voltage stability indicators used in this thesis belong to the long-term classification.

Voltage stability within a time frame of up to 30 seconds is known as short-term voltage stability. This aspect of voltage stability differs significantly from long-term voltage stability in terms of dynamics and involved components. Short-term voltage stability is associated with the rapid behaviour of load components such as induction motors, electronic loads, HVDC links, and generator resources based on inverters. The study duration of interest typically spans several seconds, necessitating the use of detailed models that accurately represent transient dynamics within the power system [24]. The analysis of short-term voltage stability requires solving relevant system differential equations. Therefore, accurate modelling of load dynamics becomes crucial in this context [25].

2.1.5.2. Static and Dynamic Voltage Stability Analysis

There are two main types of tools used for voltage stability analysis: dynamic and static. Dynamic analysis involves solving nonlinear system differential algebraic

equations through time-domain simulations. On the other hand, static analysis relies on solving conventional or modified power flow equations [26].

Static analysis, which only requires solving algebraic equations, is computationally more efficient compared to dynamic analysis. It is particularly suitable for studying a large number of cases and determining voltage stability limits for pre-contingency and post-contingency scenarios [26]. Static methods effectively analyse various aspects of the voltage stability problem by examining the viability of the equilibrium point represented by a specific operating condition of the power system. By exploring a wide range of system conditions, static analysis techniques provide valuable insights into the nature of the problem and identify key contributing factors [15]. This analysis is typically performed using power flow solutions and can determine vulnerable regions of the power system in terms of voltage stability margins for different power transfers [24].

Dynamic analysis offers the most accurate representation of the time responses of the power system. It accurately captures the sequence of events leading to voltage instability, enabling post-mortem analysis and coordination of protection and control measures. However, dynamic analysis is computationally intensive, both in terms of CPU (central processing unit) time and engineering effort required to analyse the results. Furthermore, it does not readily provide information on sensitivity or the degree of instability, making it impractical for studying a wide range of system conditions or determining stability limits [26].

Dynamic analysis is beneficial for detailed studies of specific voltage collapse scenarios, coordination of protections and controls, and testing of remedial measures. It investigates whether and how the steady-state equilibrium point will be reached [15].

In this thesis, static voltage stability analysis will be applied to determine indicators of long-term voltage stability, with a focus on load increase as the cause of instability risk. The use of the words “voltage stability” will therefore refer to the long-term type, evaluated by applying static analysis.

2.1.5.3. *V-P* Characteristic Analysis

The *V-P* characteristic curve (presented in Figure 2.3) is produced by performing a series of power flow calculations for different load power demand values. This curve is used to represent the relationship between voltage and active power in a power system [15].

Figure 2.3 shows an example for a radial network formed by a source, a transmission line, a bus and a load, depicting the *V-P* characteristic curve at the bus. It can be noted that different values of load power demand (P_R) produce in turn different values of bus voltage (V_R).

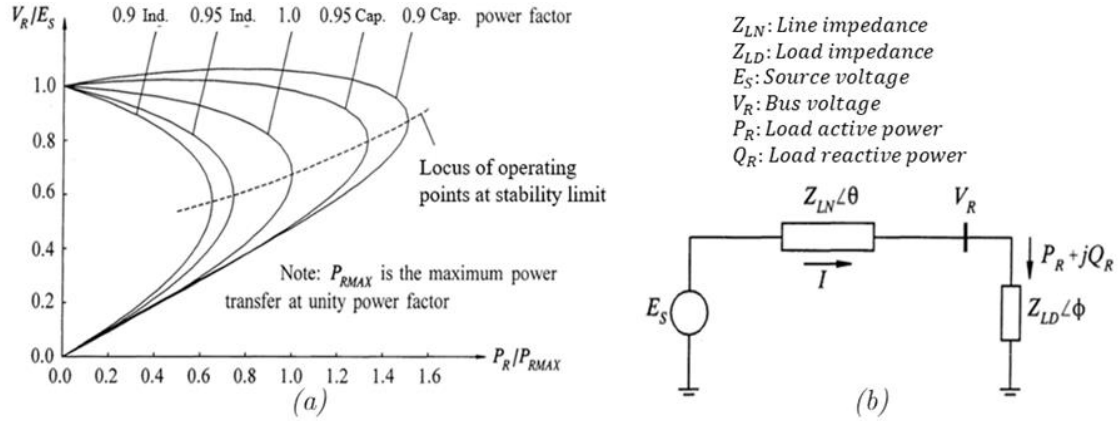

Figure 2.3. V-P Characteristic (*a*) for a bus in a radial network (*b*), for different values of load power factor. Depicted from [15].

In the example presented in Figure 2.3, maximum power transmitted is reached when voltage drop in Z_{LN} and Z_{LD} are the same, i.e. $\boldsymbol{Z_{LN} = Z_{LD}}$ (maximum power transfer theorem) [15], where Z_{LN} represents the transmission line impedance and Z_{LD} represents the load impedance.

The conditions corresponding to maximum power represent the limits of satisfactory operation [15]. Power flow solutions fail to converge beyond the maximum power operation point (i.e. "knee" of the *V-P* characteristic curve), which is indicative of voltage instability [15]. The Voltage Stability Limit (VSL) is then at the maximum power operation point. Practical power systems consisting of many voltage sources and load buses also exhibit similar relationships between active power transfer and load bus voltages [15].

Finally, another concept to consider is the power margin or the loading limit of the system for the given operating conditions, which is the power from a given operation point to the point of maximum power transfer [24]. Satisfactory operating condition is ensured by allowing sufficient power margin [15].

3. Green Hydrogen as a Clean Energy Carrier

Green hydrogen, produced from renewable energy sources, is gaining importance as a clean energy carrier, especially for sectors challenging to electrify like industry, buildings, and transport. This energy medium enables renewable energy to be channelled from power systems to end-use sectors.

Extracted from water via electrolysis, green hydrogen can be combined with the natural gas network, reducing natural gas usage and CO_2 emissions. It also offers storage capabilities, extending its use to marine, aviation, and other transport systems [8].

The 2020s are pivotal for maturing green hydrogen technology, with electrolyser technologies like alkaline and proton exchange membrane (PEM) expected to scale up. However, large-scale green hydrogen integration introduces challenges in power system planning and operation, including increased flexible demand and network security considerations. Despite the challenges, the introduction of green hydrogen offers benefits such as reducing renewable energy curtailment and promoting decarbonization strategies while maximizing electricity market revenue [8].

This thesis explores the integration of large-scale electrolysers for green hydrogen production into the power grid, examining how the grid responds to demand surges under various operational scenarios.

3.1. Renewable Energy and the Need for Storage Flexibility

The inherent variability, unpredictability, and location-specific characteristics of renewable energy sources, especially solar and wind energy, require flexibility within power systems for their effective integration. Flexibility, in this context, refers to the capability to balance the remaining load after accounting for variable renewable energy production. Multiple sources can provide this flexibility, including curtailment, demand-side management and notably, electrical energy storage [7].

Examples of flexible storage solutions are batteries, pumped-hydro plants, compressed air energy storage, and green hydrogen with a potential for reconversion to electricity or sector coupling. A common consensus is that no single storage solution excels in every aspect, leading to the natural conclusion that a combination of storage options should be considered in planning strategies.

Batteries for example, have the ability of shifting load to times when renewable energy is abundant. Electrolysers, on the other hand, can convert excess electricity into hydrogen which can be stored for long periods and used in various sectors like transportation and industry, or even reconverted back into electricity when needed by using fuel cells [7].

Finally, the implementation of energy storage systems has the potential to enhance the reliability, efficiency and resilience of the power system as it accommodates higher penetrations of renewable energy sources.

3.2. Water Electrolysis for Green Hydrogen Production

Water electrolysis is a process used to produce green hydrogen by splitting water molecules into hydrogen and oxygen using electrical energy. Electrolysers technologies come in various types, including alkaline electrolysers and polymer electrolyte membrane (PEM) electrolysers, which are nowadays the technologies with the highest penetration in GH2 production projects for commercial purposes [11].

3.2.1. Electrolyser Technologies

Alkaline electrolysers are the most common type of electrolyser and are widely used in industry due to their low cost and high efficiency [27]. Large-scale systems often utilize this particular type of electrolyser due to its cost-effectiveness, straightforward implementation, and extended operational lifespan compared to other technologies [11]. However, one important drawback of alkaline electrolysers is the need of constant power supply to ensure stable operation [27].

Conversely, despite being more expensive, PEM electrolysers are able to operate under a variable supply of power [28]. This technology is mainly used for low-scale plants due to their shorter lifetime [11]. Table 3.1 presents a summary of these two electrolyser technologies, their efficiency and costs.

Table 3.1. Electrolyser Technologies [11].

Electrolyser Type	**Common Application**	**Electrolyser Efficiency**	**Investment Cost [€/kW]**
Alkaline	Large-scale applications with low dynamic reaction needed	70 %	1000
PEM	Small-scale application coupled with fluctuating power source	60 %	2000

3.2.2. Representation of Electrolysers in Dynamic and Static Power System Analysis

The representation of electrolysers in dynamic and static power system analysis depends on the type of electrolyser technology and the level of detail required for the analysis. In dynamic analysis, the electrolyser is typically modelled as a nonlinear dynamic element [29]. Meanwhile in static analysis, the electrolyser is modelled as a constant power or constant current load [30].

Figure 3.1 depicts the fundamental electrical power configuration of an electrolyser suitable for power system analysis, along with its equivalent representation as an equivalent load for static analysis. In this thesis, electrolysers will be treated as equivalent constant power loads. Their impact on the power system will be examined through steady-state analysis, with power consumption as the primary variable of interest. As a result, all the components involved in adapting the electric power supply will be consolidated into a single equivalent load.

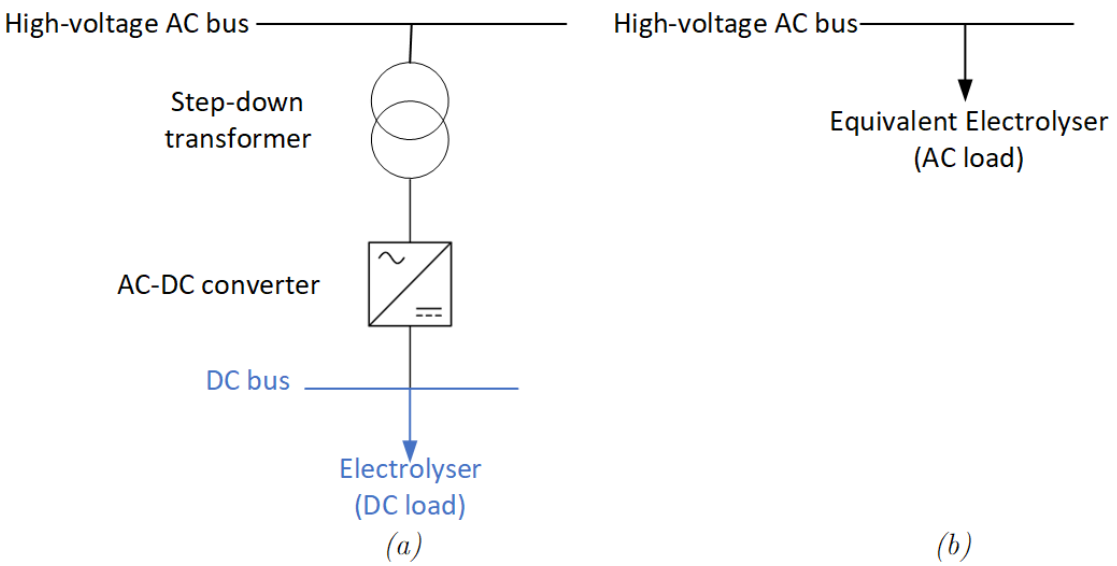

Figure 3.1. Representation of basic power components associated to an electrolyser in power system analysis. (*a*): Representation of an electrolyser as a DC load, considering basic power equipment. (*b*): Lumped AC equivalent load.

4. Methodology

This chapter details the methodology employed to achieve the research goals of this thesis, which can be summarized in the formulation and implementation of a strategy to determine a power-system-friendly distribution of new GH2 production facilities across target areas in the northwest German high voltage grid. The process encompasses three key steps. First, the development of an algorithm that takes a power grid model in a certain steady-state operative scenario and performs the automatic connection of the necessary new electrolysers to selected buses of an interest area within the power grid, all while adhering to steady-state operational constraints. Second, the development of the northwest German high voltage grid model. Finally, the algorithm is tested on the developed model under a variety of operational scenarios.

4.1. Algorithm Development

The algorithm will be designed to work on a power grid model, operating in steady-state conditions. It will receive as input data the buses of interest (substations within an interest area, to be considered as possible locations for the incorporation of new loads), as well as the required GH2 power to be allocated in the area under evaluation (RP) and the minimum desired GH2 plant size ($MinGH2$) in MW.

In terms of outputs, this algorithm will determine whether the required GH2 power (RP) can be incorporated to the buses of interest while keeping satisfactory steady-state operating conditions. Should the former not be possible, the maximum allowable GH2 power demand will be indicated. Additionally, the algorithm will show the substations that have been selected to receive the new loads (GH2 plants) along with their power demand. Finally, the geographic distribution of the newly allocated GH2 plants in the power grid will be presented.

The flow diagram in Figure 4.1 depicts the algorithm's general functioning process, which leads to generating the previously mentioned outputs. The initial step involves specifying the desired minimum size of GH2 plants, as well as indicating the buses of interest within the power grid being analysed. These buses are then sorted considering voltage stability indicators, from the most to the least stable bus, forming a "Bus Ranking". A static voltage-stability analysis is conducted to achieve this goal, which involves determining and evaluating the voltage-to-active-power (V-P) characteristic for each specified bus. This will ensure the new loads

(GH2 plants) to be incorporated to the power grid will be added to the most stable buses first.

The *V-P* characteristic will indicate the maximum power that can be connected to a specific bus while keeping voltage stability in the system (avoiding voltage collapse), as well as the maximum power at steady-state normal operating voltage. In addition, examining the *V-P* curves at each bus allows for observations regarding the sensitivity of voltage changes in response to power increases.

Subsequently, the algorithm will create a new GH2 load (which symbolizes a GH2 production plant) and will connect it to the first bus listed in the "Bus Ranking". The initial power demand assigned to this new load will correspond to the maximum power that can be delivered at this bus while keeping its voltage within the acceptable range for normal operation.

Verification of satisfactory steady-state operating conditions (line loading and bus voltages within acceptable range) in the entire grid will follow, revealing whether the assigned power demand allows for normal steady-state operation of the system. In case of not achieving satisfactory operating conditions, an adaptation (reduction) of the GH2 load power demand is carried out. This iterative process of verification of system conditions and adaptation of the GH2 load power demand will continue until satisfactory steady-state operation of the system is achieved. At this stage, if the achieved GH2 load power demand is greater than zero, the grid model will be changed, with a new load (GH2 production plant) connected to the bus under evaluation.

With the target set at achieving the required GH2 power (*RP*), the algorithm will execute the same steps of connecting a new GH2 load and finding the right power demand value (allowing normal steady-state operation), with the buses that follow in the ranking, until the specified *RP* has been reached or all buses of interest have been tried.

The implementation of this algorithm will be realized using python. Load flow calculations to determine the *V-P* characteristic of each bus and ensure satisfactory steady-state operating conditions will be conducted using PowerFactory, a software tool developed by DIgSILENT GmbH. Within the python environment, various tasks such as data analysis, filtering, and plotting will be performed, as well as, instructions for executing calculations requiring the use of PowerFactory. The data exchange between the python environment and PowerFactory will be facilitated through an API (Application Programming Interface), enabling seamless interaction and allowing for automation of repetitive tasks.

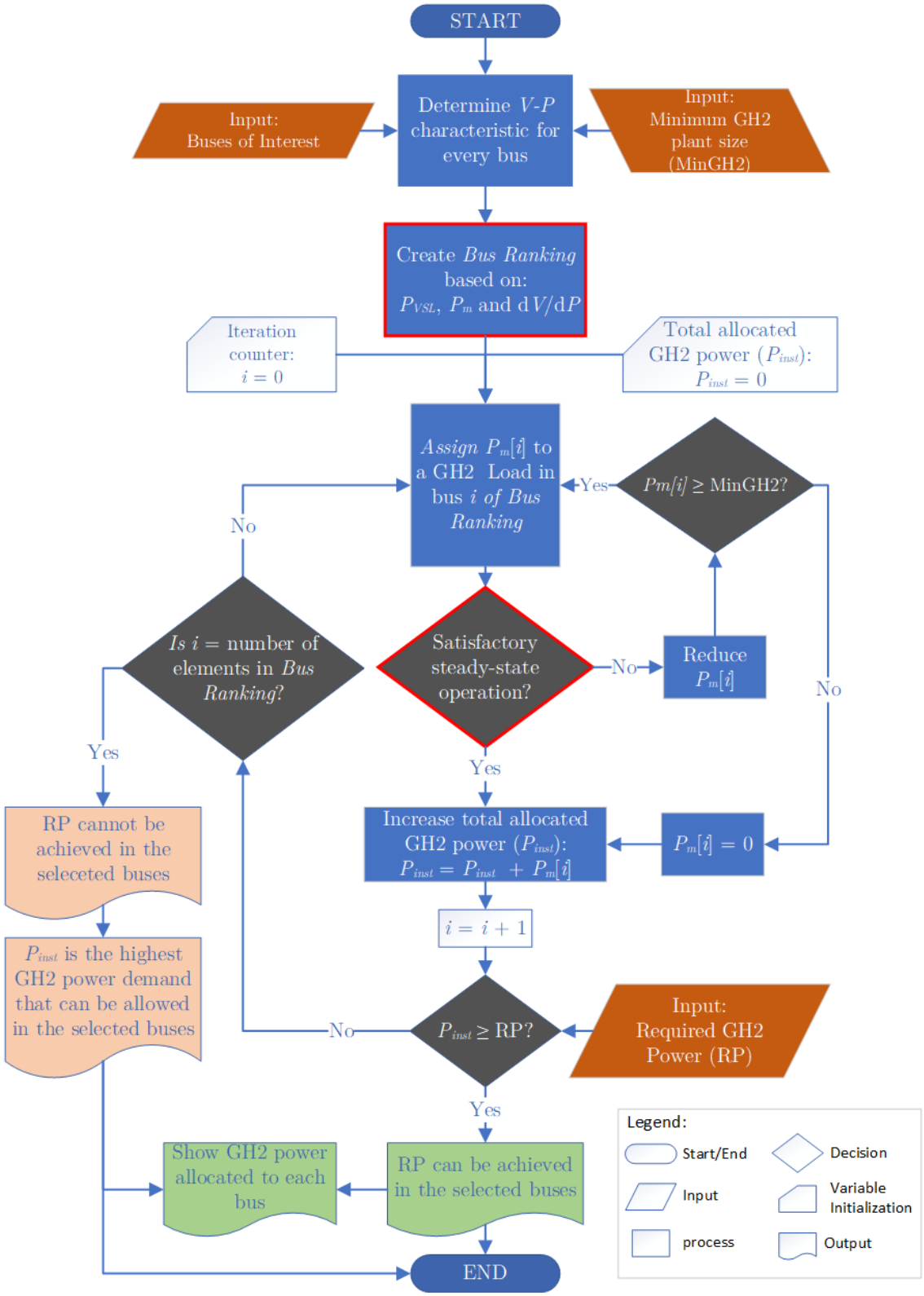

Figure 4.1. Flow diagram of the Algorithm to determine the distribution of new electrolysers among buses of interest in an area of the power grid.

4.1.1. Bus Ranking

The purpose of the Bus Ranking is to organize the buses of interest into a list-like structure, sorted form the most to the least stable in terms of voltage stability. This provides a hierarchy of preference when it comes to selecting the connection points for the new GH2 plants in the power grid, ensuring the most voltage stable buses are evaluated first.

The Bus Ranking is formulated based on key indicators derived from an analysis of the *V-P* characteristic curves of the buses of interest, which provide insights into their voltage stability. Upon determining the key indicators for each bus, they are arranged in descending order of voltage stability. Figure 4.2 shows the *V-P* characteristic of a bus, along with the key indicators for consideration.

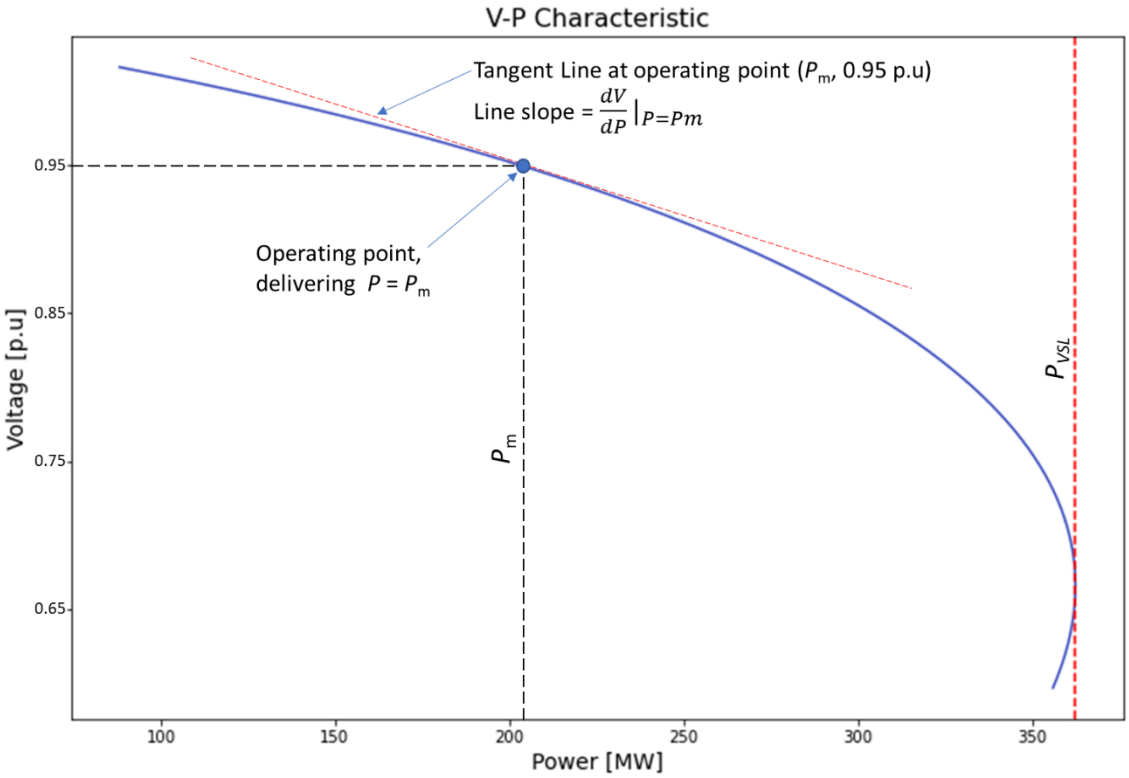

Figure 4.2. Example of a V-P characteristic of a system bus and its key indicators.

These key indicators influencing the formation of the Bus Ranking, in order of significance in terms of voltage stability, are as follows:

- P_{VSL}: this is the value of power at the Voltage Stability Limit (VSL). This indicators' value represents the maximum power demand that can be connected to the respective bus, without provoking a voltage collapse. A

higher value of this indicator corresponds to greater voltage stability at the respective bus.

- P_m: this represents the maximum power that can be delivered at the bus while maintaining a voltage value equal or greater to the lower limit of the predefined range of acceptable voltages at normal operating conditions. As an example, Figure 4.2 shows P_m as the maximum power that can be delivered without causing the bus voltage to fall below 0.95 p.u.
- $\frac{dV}{dP}|_{P=P_m}$: this is the slope of the tangent line to the *V-P* characteristic curve evaluated at P_m, which indicates the rate of change in the voltage to the change in power. A pronounced slope indicates rapid variation in voltage for a change in power demand, which may lead bus voltage to quickly fall out of the acceptable range due to small changes in the load.

4.1.1.1. *V-P* Characteristic at each bus of interest

In order to determine the *V-P* characteristic for a bus, repeated power flow calculations are carried out using different values of power demand for a test load connected to the bus, storing the resultant bus voltage for each calculation.

In this thesis, power demand values used to determine the *V-P* characteristic at each bus of interest will start at the minimum allowable GH2 plant size (*MinGH2*), which must be specified as an input. Incremental steps of the same size (*MinGH2*) in power demand are carried out for each consecutive power flow calculation until the value at which the power flow solution fails to converge has been achieved, which indicates the voltage stability limit has been reached or surpassed. In any case, the VSL will be within the range between the last recorded value of power demand that allows convergence of the power flow solution and the value that causes convergence failure. It is also worth mentioning that the power factor of the test loads will be assumed to be 0.95 p.u. inductive, based on what is indicated in [31] as general requirements of power-to-hydrogen power converters.

Figure 4.3 presents two *V-P* characteristic curves corresponding to two buses from the power grid model used in this research, for a high load operative scenario. It can be noted in this picture that in bus B exists a higher capacity than in bus A to deliver active power without producing a voltage collapse (P_{VSL}), as well as for keeping voltage above 0.95 p.u., therefore indicating higher stability in bus B.

4.1.1.2. Determining P_{VSL}

As previously mentioned, the active power at the VSL will be situated within the range that extends from the last recorded power demand value, which allows

convergence of the power flow solution, to the value that triggers convergence failure. For the purposes of this thesis, it is enough to know the maximum active power for which the power flow converges at each bus, which will be considered as the indicator P_{VSL}, as shown if Figure 4.3.

Given that the increments in load demand to determine the *V-P* characteristic are of the same size for all buses (equivalent to *MinGH2*), the indicator P_{VSL} will be in all cases a multiple of *MinGH2*, allowing comparison between system buses. The main criterion for ranking the buses of interest will be based on this indicator. In cases where two buses share the same value, the other two indicators will determine their respective positions in the ranking.

4.1.1.3. Determining P_{m}

As previously described, the indicator P_{m} is defined as the power that can be supplied while maintaining the voltage at or above the lower limit of the acceptable voltage range. This indicator is obtained from the *V-P* characteristic, where active power (the independent variable) is provided as discrete inputs to the algorithm. Conversely, voltage represents the system's response, and since the calculated values may not precisely align with the selected lower limit of the acceptable voltage range, cubic spline interpolation as defined in [32] is utilized to estimate the active power value corresponding to the lower limit of the acceptable voltage range. The interpolation is executed in python, applying the function “interpolate” of the python SciPy library [33].

4.1.1.4. Determining $\frac{dV}{dP}|_{P=P_m}$

The slope of the *V-P* characteristic curve at the point where active power equals P_{m} (where $P = P_{\mathrm{m}}$) can be determined by calculating the derivative of the function $V(P)$ and evaluating it at $P = P_{\mathrm{m}}$. This is achieved using a numerical differentiation method known as the finite difference method, detailed in reference [34]. This method provides an approximate value of the function derivative at the specified point. The derivative approximation is computed using python, specifically employing the “gradient” function from the python NumPy library [35].

4.1.1.5. Advantages of implementing the Bus Ranking

Employing the Bus Ranking enables prioritizing the connection of new GH2 loads to the grid's most stable buses. This concept can be observed in Figure 4.3: if a new GH2 load of 200 MW was connected to bus A, the voltage would dip slightly below the acceptable operational limit of 0.95 p.u. However, connecting the same

load to bus B would maintain the voltage near its original 1.0 p.u. value. Furthermore, the power margin would vary for each bus post-connection of the new 200 MW load: bus A would have a power margin of 300 MW, compared to a robust 3400 MW margin at bus B. Thus, if the power margin were to be further reduced by an increase in GH2 power demand, bus B could accommodate a higher power demand than bus A, without producing a voltage collapse situation, allowing for higher GH2 production.

This strategic prioritization allows for the incorporation of new GH2 loads to buses that are able to deliver higher amounts of active power while keeping voltage levels within operational standards. This enables the deployment of larger plants at selected substations among the buses of interest, having a positive impact in the economies of scale to achieve cost reductions [14], [36].

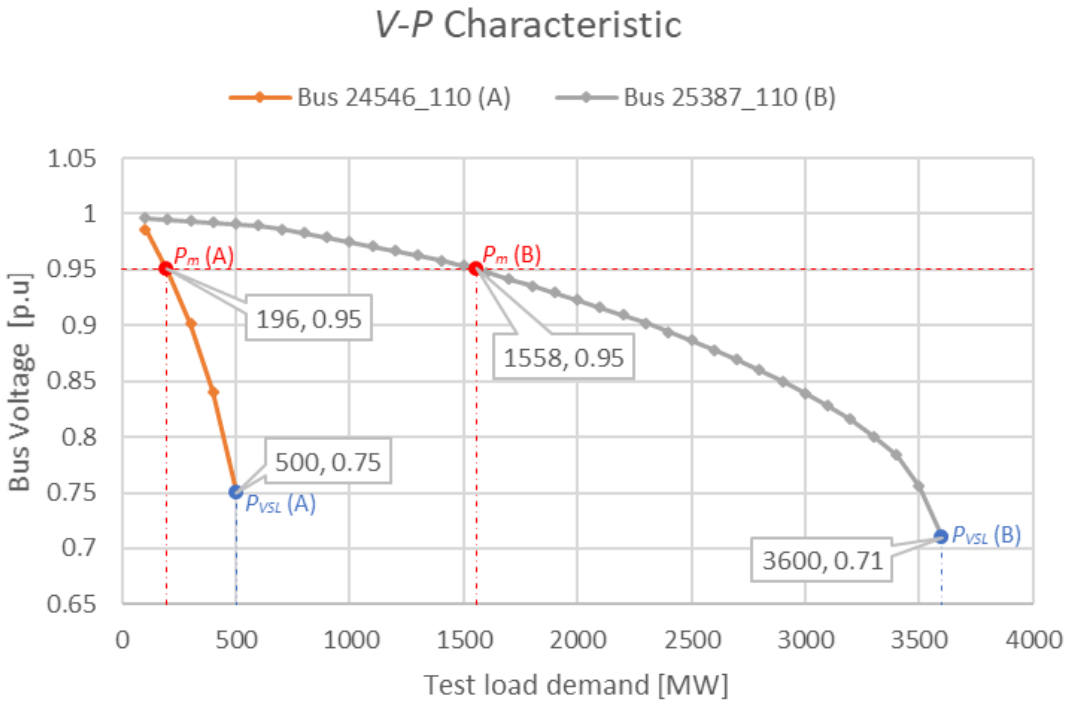

Figure 4.3. V-P Characteristics of two buses, depicting indicators P_{VSL} and P_m (dash-dotted lines). Bus voltage of 0.95 p.u. is considered as the minimum acceptable operational voltage (red dashed line).

4.1.2. Verification of satisfactory steady-state operation

Immediately after adding a GH2 load to a bus, an optimal power flow (OPF) calculation is performed in order to verify satisfactory operation in steady state for the modified grid (with a new load). The goal is to avoid overloads in transmission lines and optimize generation for cost minimization in the new operating conditions.

The OPF calculation is executed in PowerFactory utilizing the “DC Optimization” function. This feature performs a constrained load flow calculation using PowerFactory's linear DC load flow methodology. It first determines the feasibility of a solution to the power flow problem and then optimizes all generator power injections to minimize cost [37]. The constraints dictating this load flow calculation include the maximum permissible line loading and the upper limit of active power that generators can produce, while the optimization of generation costs requires the electricity production costs of each generator as input.

The DC load flow method, contrary to its name, is not primarily for DC systems, but is essentially used for AC systems. It provides a swift analysis tool for intricate transmission networks where an adequate approximation of the system's active power flow is required. This method simplifies the non-linear system emerging from nodal equations, capitalizing on the predominant relationship between voltage angle and active power flow in high voltage networks. Thus, a set of linear equations is formed, linking the voltage angles of the buses directly to the active power flow through the reactance of individual components [37]. As the DC load flow method circumvents the need for an iterative solution process due to the use of linear equations, it significantly boosts calculation speed [37]. However, one important disadvantage is the loss of information regarding reactive power. The results provided with this method only comprise active power flow and voltage angles.

The decision of using the DC load flow method is based on the fact that the simulation model of the Northwest German high voltage grid (Section 4.2) does not comprises reactive power (Q) compensation elements (such as shunt and series capacitors, reactors, and static var compensators), nor generator reactive power controllers, and therefore it is not possible to determine meaningful Q values for generators or the reactive power flow through the system branch elements.

4.2. Simulation Model of the Northwest German High Voltage Grid

A model of the Northwest German High Voltage Grid was built in the software tool PowerFactory, using open-access data from the open_eGo Project [38]. This model is formed by the high voltage (HV) grids located within of the federal states of Lower Saxony, Schleswig-Holstein, Hamburg and Bremen at three different voltage levels (110 kV, 220 kV and 380 kV).

This model reproduces two different power grid development scenarios: the current grid state, referred in this document as “Status Quo”, and the grid development plan for the year 2035 or “NEP2035”.

4.2.1. Simulation model development

The data for building this model in PowerFactory was directly downloaded in .csv (comma-separated values) format from the Open Energy database (open_eGo project) [38]. All datasets of buses, lines, transformers, generators and loads undergo an adequation process, carried out using python, in order to match format requirements that are necessary for their subsequent incorporation to PowerFactory.

Once the data format has been filtered and adapted, it is exported to PowerFactory using a python API to create the power grid simulation model. Figure 4.4 presents a diagram that illustrates the process of generating the power grid model.

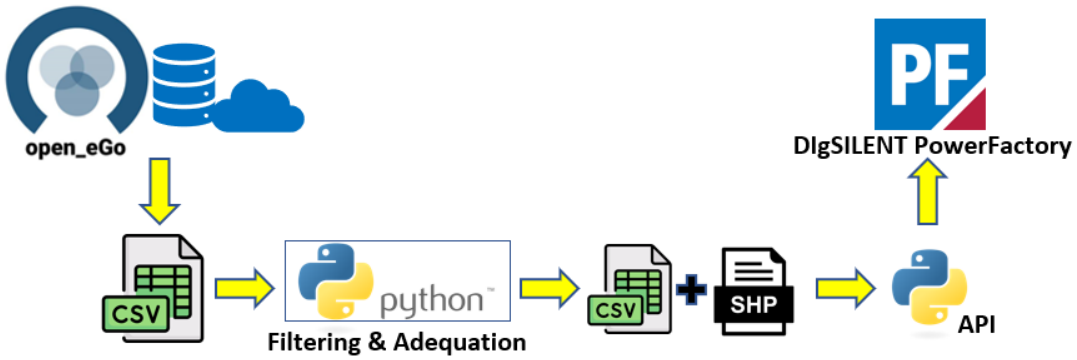

Figure 4.4. Grid simulation model development process.

The Open Energy platform is a set of open-source tools aimed to ensure quality, transparency and reproducibility in energy system research [38]. It provides a publicly accessible database and is maintained by a team of developers from different research institutes [38]. This database comprises three development scenarios of the German power grid [39], two of them being used for the purpose of this thesis, namely: “Status Quo” and “NEP2035”. The “Status Quo” scenario is based on high-resolution data of the German grid for the year 2015. On the other hand, the scenario “NEP2035” is based on the first draft of the German Grid Development Plan “NEP Strom 2015”, specifically scenario B2 2035, released by the four transmission system operators (TSO) that operate in the country [39].

The developed grid model is comprised by various components, which are interconnected to form a power grid. These components include buses, transmission lines, transformers, generators and loads. Each of these elements requires the parametrization of its essential characteristics in order to perform its intended role in the power system model. The data associated to the characteristics of these

elements is provided in the Open Energy database and can be downloaded as readily available .csv files.

For every element, basic electrical characteristic data such as nominal voltage, rated power or current, and impedance are supplied. In the case of buses and lines, geographic location and route coordinates are also provided. Table 4.1 summarizes the available data in the Open Energy database for each component type.

Table 4.1. Summary of component characteristics provided by the Open Energy database.

Component	Provided data
Bus	Bus ID (unique name)
	Geographic location coordinates
	Nominal voltage [kV]
Transmission line	Line ID (unique name) and terminal buses ID
	Route coordinates
	Length [km]
	Resistance per unit length [Ω/km]
	Inductive reactance per unit length [Ω/km]
	Capacitive susceptance per unit length [S/km]
	Nominal apparent power [MVA]
Transformer	Transformer ID (unique name) and terminal buses ID
	Inductive reactance [Ω]
	Nominal apparent power [MVA]
Generator	Generator ID (unique name) and terminal bus ID
	Nominal power [MW]
	Energy source
Load	Load ID (unique name) and terminal bus ID
	Active power demand [MW]

Within the data utilized in the development of the model used for this thesis, loads are represented as aggregated equivalent loads, representing “load areas” (geographic units which are assigned annual electricity consumption characteristics), and are assigned to different nodes in the system in the 110-kV grid. Time series of power demand with 1-hour resolution are provided, which are based on the annual electricity consumption and standard load profiles from the German Association of Energy and Water Industries (BDEW). They represent the consumption characteristics of geographic areas for the year 2011 (in MW), considering a power factor of 0.95 p.u. inductive.

In both grid development scenarios ("Status Quo" and "NEP2035"), the same power demand is considered. This assumes load-stabilizing measures like demand-side management, compensation systems, increased efficiency, etc. [39]

4.2.2. Model characteristics

The power grid model developed for the purpose of this research is a comprehensive representation of the HV grid of the Northwest German region, which includes the federal states of Lower Saxony, Schleswig-Holstein, Bremen and Hamburg. This region's location within Germany is illustrated in Figure 4.5.

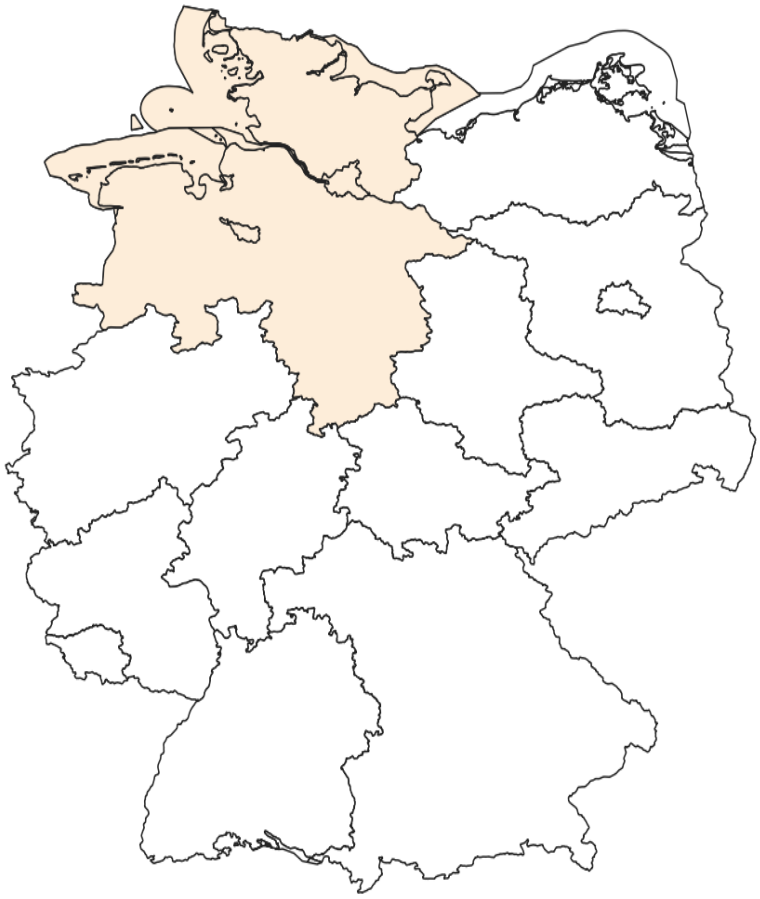

Figure 4.5. Location of the Northwest region within Germany.

The model comprises generators, loads, buses, transmission lines and transformers, that are located within this region and are interconnected to form a complex network in three different voltage levels (110 kV, 220 kV and 380 kV), allowing for steady-state simulation and analysis of this power system under different operative configurations. As previously stated, two grid development scenarios will be considered: "Status Quo" representing the current grid configuration, and "NEP2035" representing a future grid configuration. The resultant grids are presented in Figure 4.6, showing a geographic representation of both scenarios.

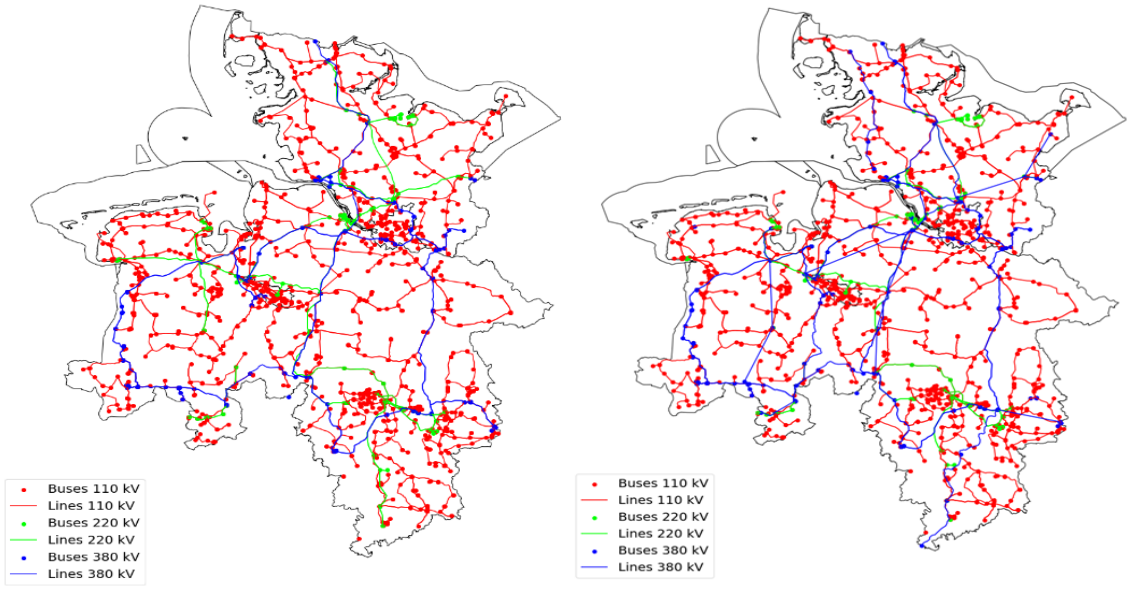

Figure 4.6. Geographic representation of the Northwest German HV grid for the scenarios a) "Status Quo" and b) "NEP2035".

A summary of the installed generation capacity, load power demand and number of components involved in this power grid model, considering both grid development scenarios, is presented in Table 4.2. Moreover, Figure 4.7 presents a graphic comparison of the number of buses in both scenarios, while Figure 4.8 compares the number of transmission lines.

By comparing the data of both scenarios presented in Table 4.2, it can be noted a small increase in the total number of buses as the grid changes from "Status Quo" to "NEP2035" (see also Figure 4.7). On the other hand, the number of transmission lines at 110 kV and 220 kV slightly decreases from "Status Quo" to "NEP2035", while there is an increment in the number of lines at 380 kV (see also Figure 4.8).

Table 4.2. Summary of Grid Components of scenarios "Status Quo" and "NEP2035".

Voltage level [kV]	Number of Buses		Number of Lines		Peak Power Demand [MW]		Generation Installed Power [MW]	
	Status Quo	NEP2035	Status Quo	NEP2035	Status Quo	NEP2035	Status Quo	NEP2035
110	1554	1552	2838	2814	12421	12421	22713.3	38480.6
220	172	172	310	257	0.0	0.0	4075.6	2145.2
380	160	197	312	325	0.0	0.0	8824.3	20295.3
Total	1886	1921	3460	3396	12421	12421	35613.2	60921.1

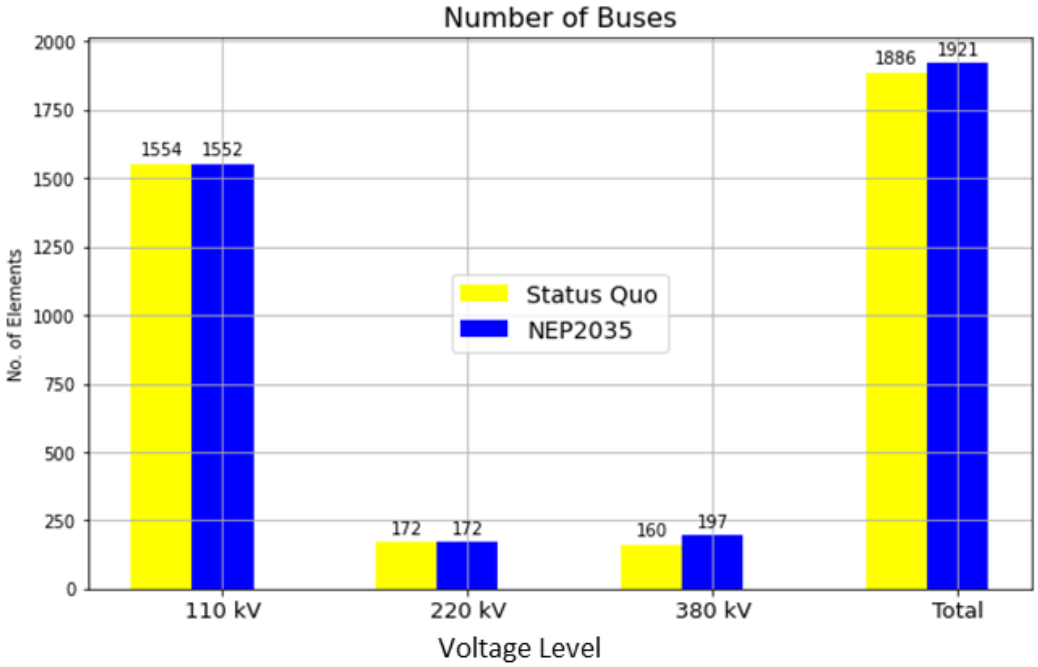

Figure 4.7. Number of buses in the Northwest German power grid model, for both grid development scenarios.

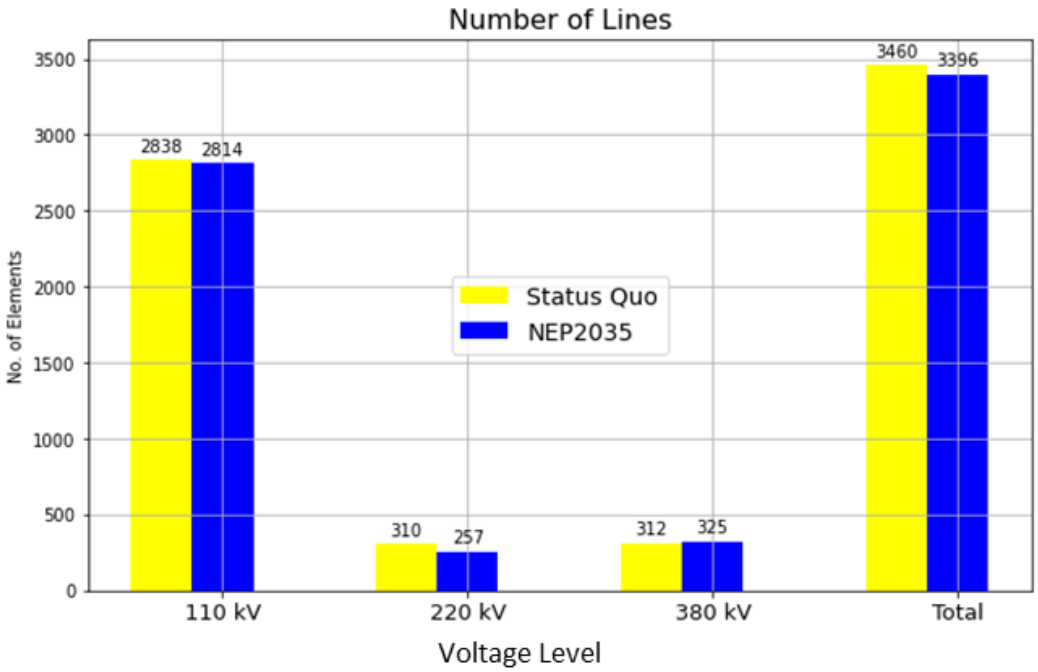

Figure 4.8. Number of transmission lines in the Northwest German power grid model, for both grid development scenarios.

Furthermore, generation installed power increases by 1.7 times as the grid evolves from "Status Quo" to "NEP2035". In both grid scenarios the highest generation installed power can be found connected to the 110 kV grid, followed by the 380 kV grid. Moreover, as it can be noted from Table 4.3, scenario "NEP2035" presents an

important increase of about 2.5 times in installed wind power with respect to "Status Quo". On-shore wind generation capacity almost doubles, while off-shore power becomes five times greater. In turn, solar power installed capacity also increases by 80 % in "NEP2035" as compared to "Status Quo".

Figure 4.9 illustrates the distribution of installed power generation for both scenarios. It is evident that the "NEP2035" scenario not only exhibits higher installed power capacity from renewable sources, as indicated in Table 4.3, but also showcases a greater share of renewable energy in the overall generation installed capacity. It is important to highlight that the proportion of wind-based power in the total installed capacity undergoes a substantial change, rising from 47 % (38.4 % onshore and 8.6 % offshore) in the "Status Quo" to almost 70 % (42.6 % onshore and 27.2 % offshore) of the total installed capacity in "NEP2035".

Conversely, gas-based installed power (non-renewable) slightly increases in the "NEP2035" scenario, although its contribution to the total installed generation is lower. Notably, other non-renewable sources such as oil and coal witness a substantial reduction in their presence within the "NEP2035" scenario, compared to the "Status Quo" situation.

Table 4.3. Generation installed power by energy source.

	Scenario "Status Quo"		**Scenario "NEP2035"**	
Energy source	**Installed power [MW]**	**Share of total installed power [%]**	**Installed power [MW]**	**Share of total installed power [%]**
Biogas	1953.3	5.5	2261.8	3.7
Coal	4940.3	13.9	2322.5	3.8
Gas	4450.4	12.5	4630.1	7.6
Hydro	87.2	0.2	123.0	0.2
Nuclear	1329.0	3.7	0.0	0.0
Oil	759.3	2.1	40.8	0.1
Other Static	502.1	1.4	384.0	0.6
Solar	4838.0	13.6	8647.2	14.2
Wind onshore	13681.5	38.4	25929.7	42.6
Wind offshore	3072.2	8.6	16582.0	27.2
Total	35613.3	100.0	60921.1	100.0

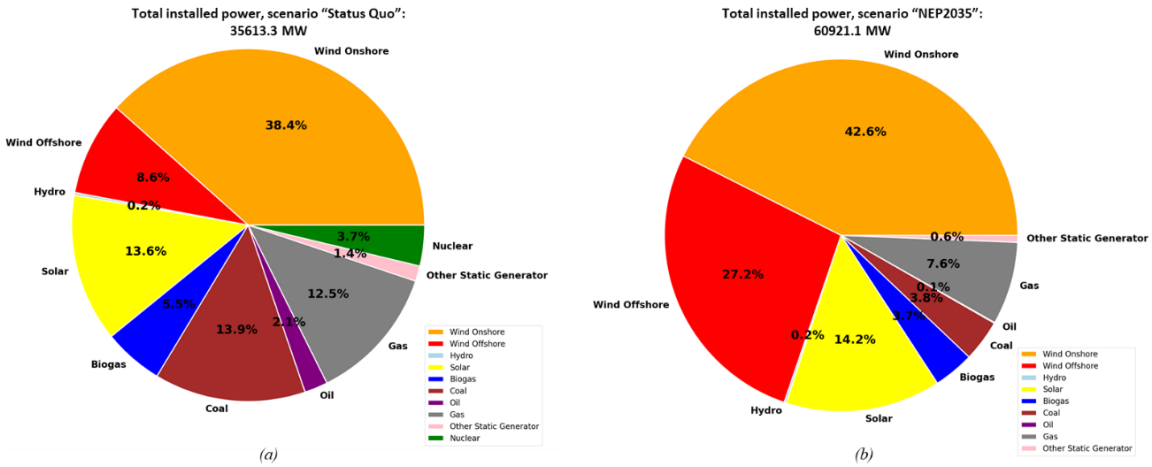

Figure 4.9. Share of generation installed power by source for the scenarios: "Status Quo" (*a*) and "NEP2035" (*b*).

In addition, Figure 4.10 and Figure 4.11 depict the installed generation power connected to each voltage level, categorized by energy source in both grid scenarios. Since the GH2 production in the northwest German region will mostly rely on wind energy, due to its preponderance respect to other RES (higher installed power and capacity factor), it is important to highlight that in both grid scenarios onshore wind energy generators are almost exclusively found in the 110 kV grid, while offshore wind is entirely connected to the 380 kV grid.

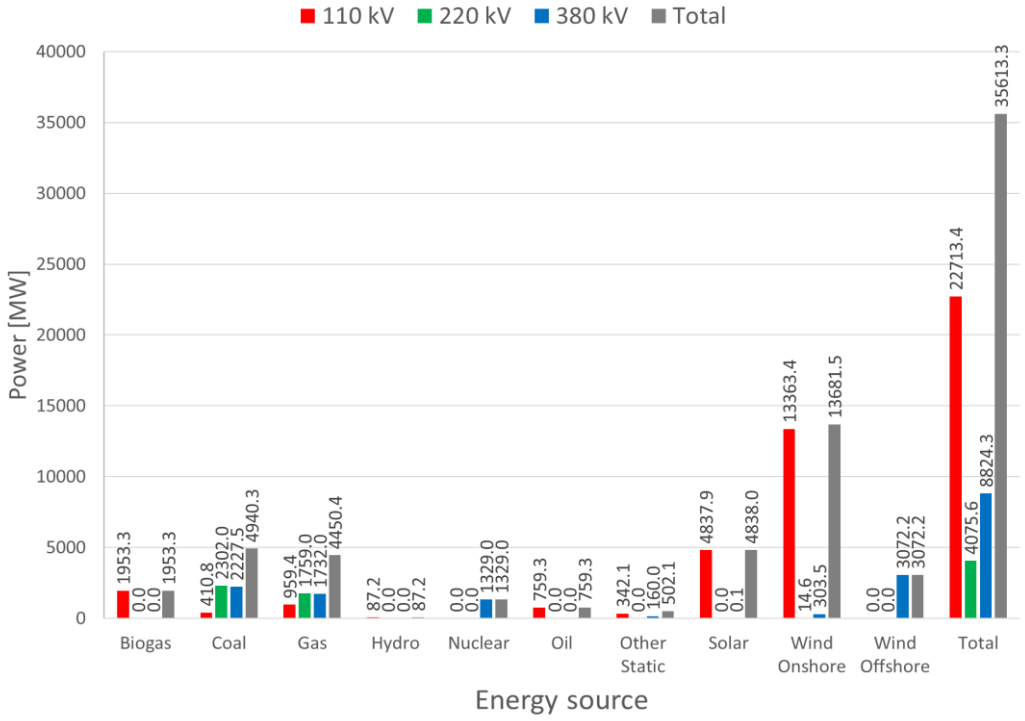

Figure 4.10. Generation installed power by energy source, at different voltage levels for the scenario "Status Quo".

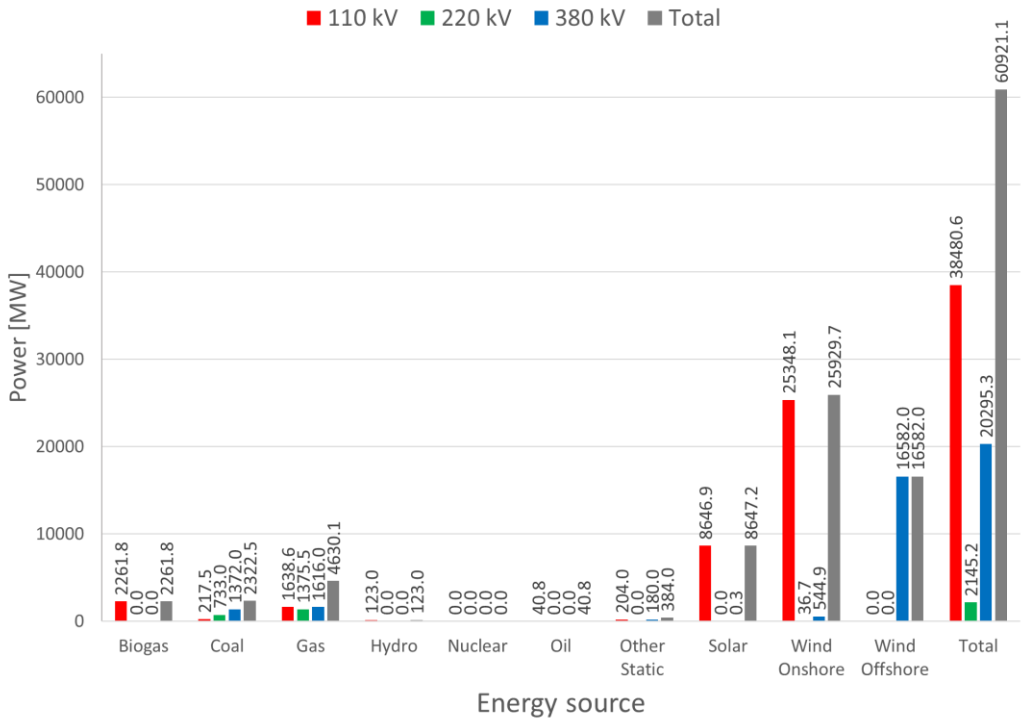

Figure 4.11. Generation installed power by energy source, at different voltage levels for the scenario "NEP2035".

4.2.3. Model data validation

In order to assess the accuracy of the data used for developing the power grid model, the generation installed power of the "Status Quo" scenario was compared to equivalent data from the MaStR platform (germ. *Marktstammdatenregister*) from the German Federal Network Agency (germ. *Bundesnetzagentur*), corresponding to December 2022. The results of this comparison were quite satisfactory, with very similar installed capacities for each type of energy source. A difference of just 3.9 % in the total installed generation power was found (relative to the Open Energy database). This is illustrated in Figure 4.12, which shows a comparison of installed generation power from both data bases. Additionally, Figure 4.13 showcases a comparison of the proportion that each type of energy source has in the overall generation capacity.

Several notable observations can be made from this comparison. Firstly, the total installed power in the MaStR database is slightly higher, with an approximate difference of 1.3 GW compared to the Open Energy database. Moreover, the installed wind power in the MaStR database is lower, with a difference of around 1 GW compared to the Open Energy database, also resulting in a lower share of the total installed power for wind generation. Conversely, the installed solar power in the MaStR database is higher by approximately 1.8 GW, leading to a higher

share of the total installed power of solar generation. Additionally, in all other source categories, the installed power is marginally higher in the MaStR database.

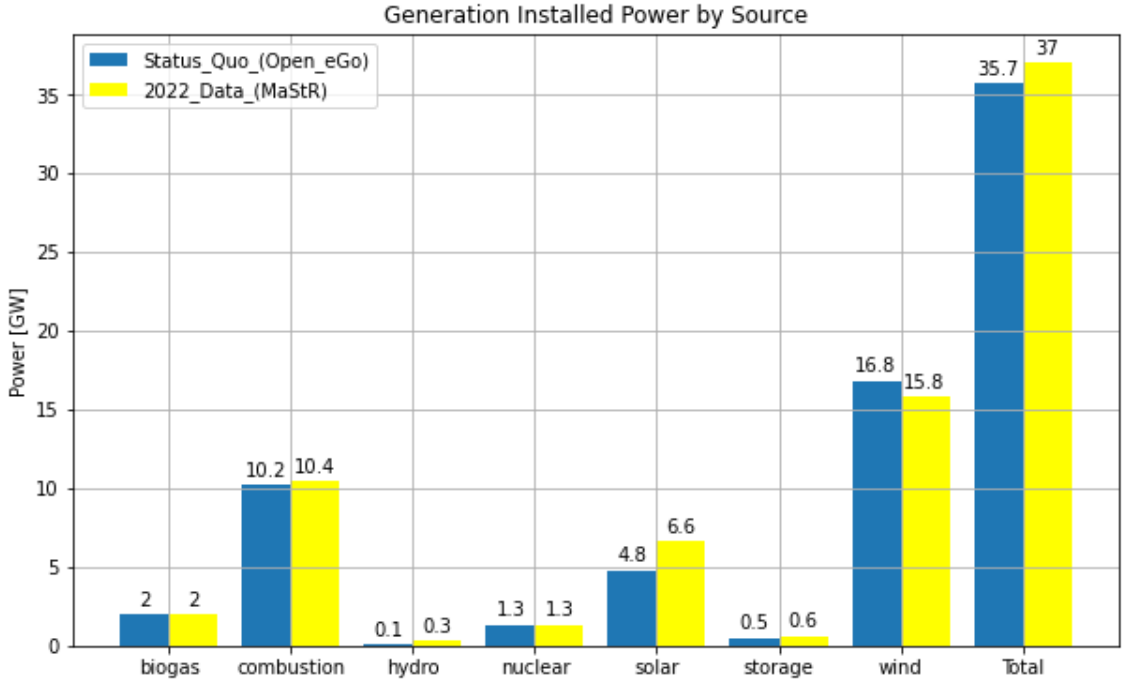

Figure 4.12. Generation Installed Power by Source, in [GW].
Comparison between the Open Energy database ("Status Quo") and MaStR data.

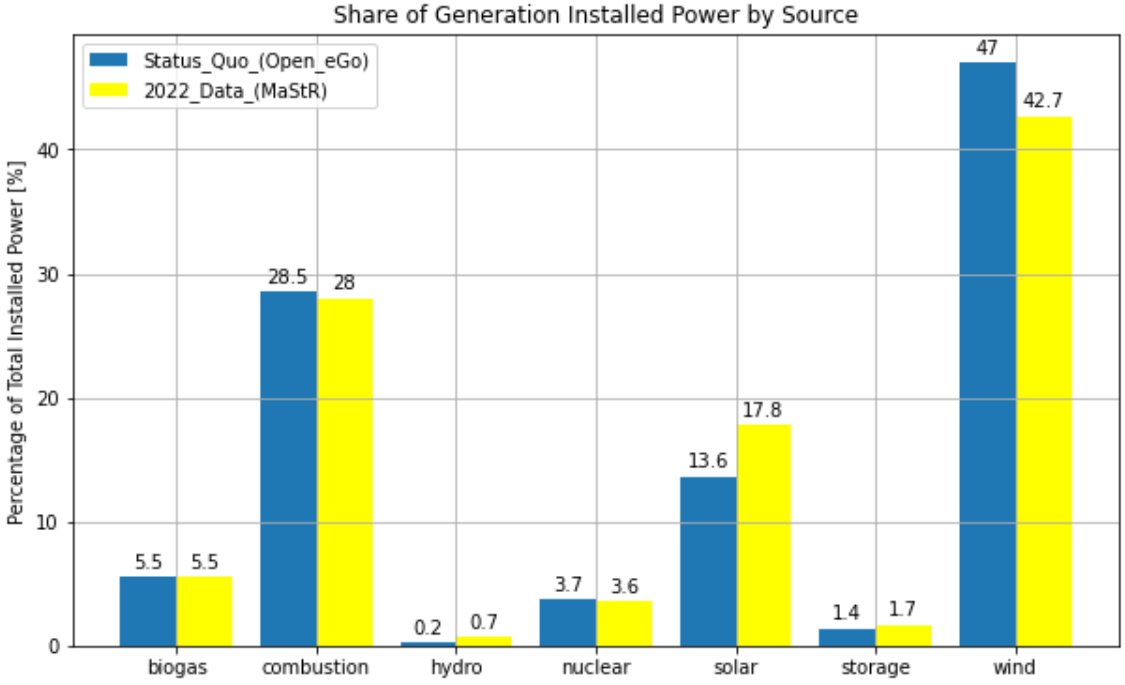

Figure 4.13. Share of Generation Installed Power by Source, in [%].
Comparison between Open Energy database ("Status Quo") and MaStR data.

4.3. Algorithm Testing on Grid Model

In order to achieve the objectives of this thesis, it is fundamental to test the developed algorithm on the HV grid model of Northwest Germany. This serves the purpose of generating a power-system-friendly distribution of new GH2 plants within the buses of interest, as well as assessing the adequacy of the subject grid to accommodate these new loads. The results obtained from this testing phase will provide valuable insights into the behaviour of the grid under different scenarios and will enable the formulation of meaningful conclusions about the feasibility of integrating green hydrogen production into the power system.

4.3.1. Operative conditions

In order to execute the developed algorithm using the northwest German power grid model, multiple steady-state operative conditions were implemented for both the "Status Quo" and "NEP2035" grid development scenarios. These operative conditions include different wind energy availability and load power demand situations, resulting in four cases for evaluation in each grid scenario, as depicted in Table 4.4. The operative conditions include high wind availability (HW) and limited wind availability (LW) in terms of wind energy generation capacity. Furthermore, two initial load power demand conditions are considered, high load (HL) and low load (LL). These demand conditions represent system load situations before incorporating any GH2 load.

Moreover, for all cases the availability of solar power plants will be intentionally limited to 10 % of their rated capacity to simulate poor solar irradiance conditions. Additionally, nuclear power plants are put out of service, following the face out of nuclear power in Germany since 15.04.2023.

In order to recreate a condition of high wind energy availability (HW) for the simulations, wind energy generators will be allowed to operate at 100 % of rated capacity when required. On the other hand, for simulating the condition of limited wind energy availability (LW), onshore and offshore wind generators are only allowed to operate at a maximum of 35 % and 45 % of their rated capacity, following average capacity factors for these types of generators [40]. Besides, the high and low power demand conditions correspond to the highest and lowest hourly average power demands of the modelled power grid loads, obtained from the time series data provided by the Open Energy database, which account for 12421 MW and 5279 MW.

Distinct conditions of wind energy availability and initial load power demand are intended to affect differently the power grid's ability of to accommodate new GH2 loads. Loading of transmission lines is increased when power demand is higher, therefore reducing the capacity to convey power to new GH2 loads. Additionally, increases in power demand by the incorporation of these GH2 loads must only be covered by increases in renewable energy generation, with a crucial role being played by wind energy, after the limitations imposed over solar-based generation.

Table 4.4. Operative conditions for steady-state simulations.

Operative condition	Abbreviation	Description
High load power demand, high wind energy availability.	HLHW	Load power corresponding to highest demand condition. Wind-based generators are allowed to operate at 100 % rated capacity.
Low load power demand, high wind energy availability.	LLHW	Load power corresponding to lowest demand condition. Wind-based generators are allowed to operate at 100 % rated capacity.
High load power demand, limited wind energy availability.	HLLW	Load power corresponding to highest demand condition. Onshore and offshore wind-based generators are allowed to operate at a maximum of 35 % and 45 % of their rated capacity, respectively.
Low load power demand, limited wind energy availability.	LLLW	Load power corresponding to lowest demand condition. Onshore and offshore wind-based generators are allowed to operate at a maximum of 35 % and 45 % of their rated capacity, respectively.

4.3.1.1. Simulation constraints

The execution process of the developed algorithm involves constrained power flow calculations in order to verify satisfactory steady state operation of the grid. The main constraint being the maximum loading of transmission lines, which will be considered at 100 % of the rated value.

Additionally, the power supplied by each generator in the simulations will be determined using OPF, with minimization of generation costs as the objective function. To accomplish this, the generation costs for different energy sources indicated in Table 4.5 will be used.

4.3.1.2. Base cases for simulation

Initial conditions, referred here as base cases, for the execution of the developed algorithm will be generated using the four operative situations shown in Table 4.4,

for both grid development scenarios, “Status Quo” and “NEP2035”, for a total of eight base cases, which are summarised in Table 4.6.

These base cases follow the previously explained simulation constraints, with a maximum line loading of 100%, and the power output of each generator according to OPF calculations for minimum generation costs.

Table 4.5. Generation marginal costs by energy source.

Energy Source	**Fuel cost [€/MWh]**	**CO_2 emissions cost [€/MWh]**	**Total cost [€/MWh]**
Wind onshore	0*	0	0
Wind offshore	0*	0	0
Solar PV	0*	0	0
Hydro	0*	0	0
Biogas	60**	0	60
Coal	20***	60***	80
Gas	60***	40***	100
Oil	60**	40**	100

* Assumed to be zero, according to [41].

** Assumed equal to gas generation cost.

*** Costs in 2021, according to [42].

Table 4.6. Summary of simulation base cases.

N°	**Base case designation**	**Grid scenario**	**Operative condition**
1	“BC HLHW SQ”	Status Quo	HLHW
2	“BC LLHW SQ”	Status Quo	LLHW
3	“BC HLLW SQ”	Status Quo	HLLW
4	“BC LLLW SQ”	Status Quo	LLLW
5	“BC HLHW NE”	NEP2035	HLHW
6	“BC LLHW NE”	NEP2035	LLHW
7	“BC HLLW NE”	NEP2035	HLLW
8	“BC LLLW NE”	NEP2035	LLLW

Resultant loading of transmission lines in the base cases corresponding to the “Status Quo” are illustrated in Figure 4.14, while Figure 4.15 showcases the corresponding line loading for “NEP2035”. From these figures it is evident that in all cases, maximum line loading does not go beyond 100 %, which is a consequence of applying a constrained load flow calculation. In both grid scenarios high load cases produce higher utilization of transmission lines than low power demand cases. Besides, a scenario-wise comparison indicates that scenario “NEP2035” presents higher utilization in greater number of elements than scenario “Status Quo” in all

operative conditions, evidenced by increases in the size of interquartile ranges and superior whiskers.

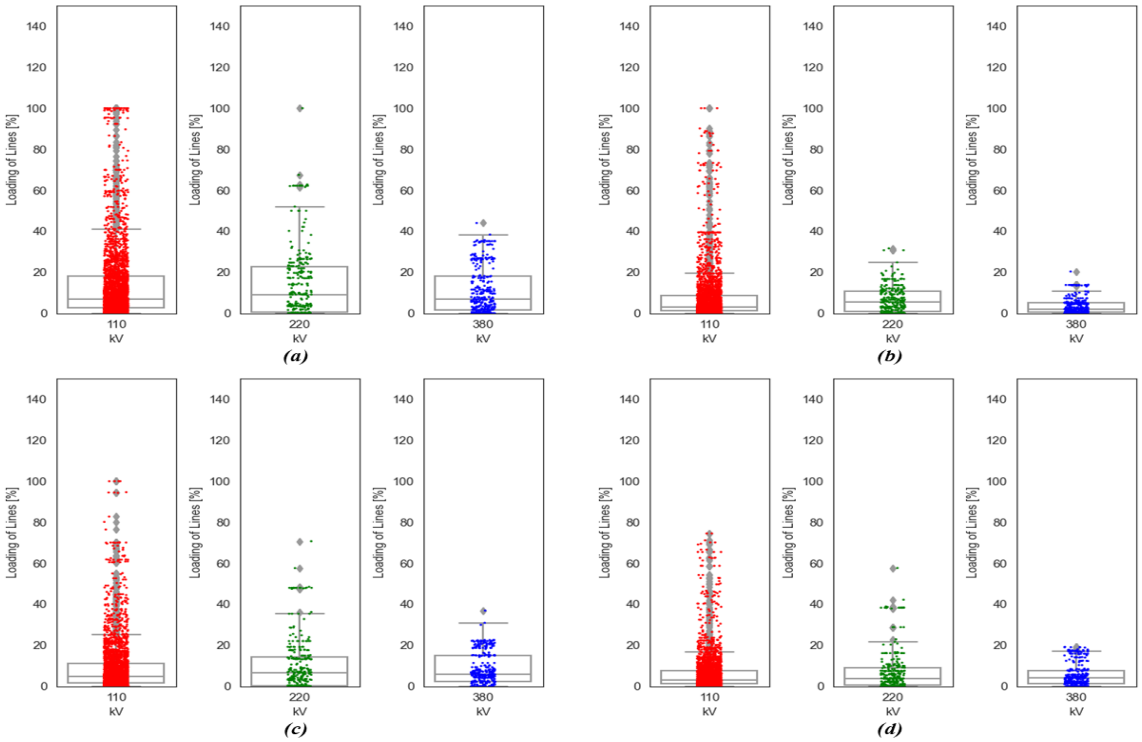

Figure 4.14. Line loading in base cases of scenario "Status Quo":
(*a*) "BC HLHW SQ", (*b*) "BC LLHW SQ", (*c*) "BC HLLW SQ", (*d*) "BC LLLW SQ".

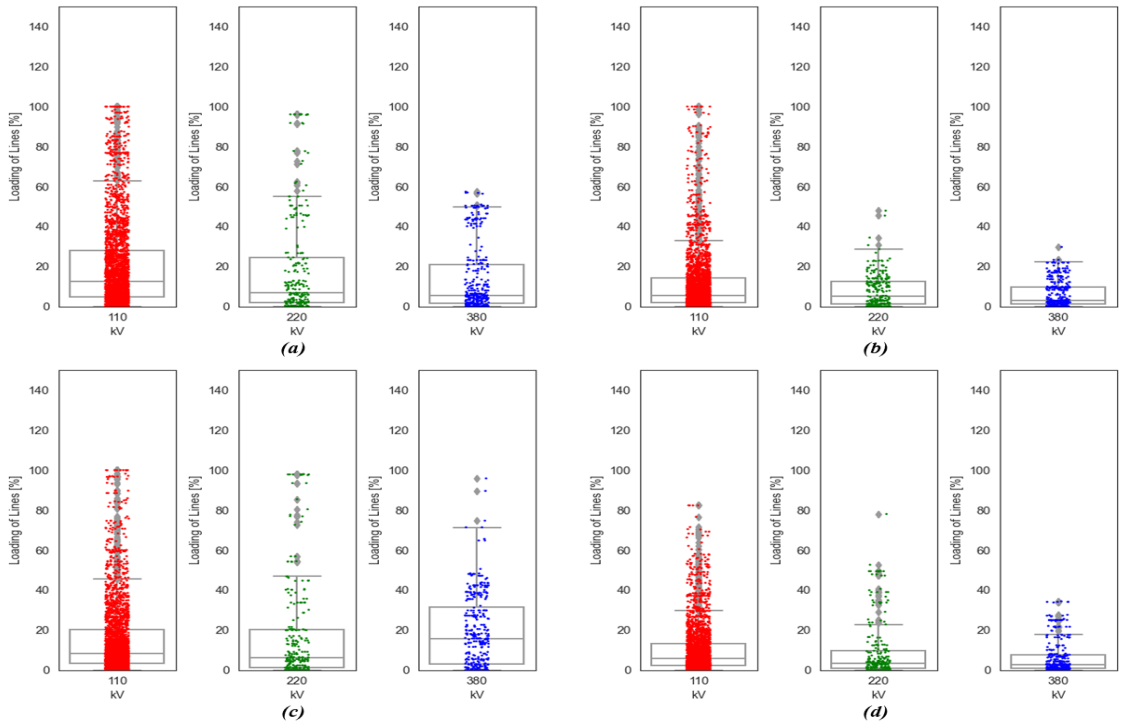

Figure 4.15. Line loading in base cases of scenario "NEP2035":
(*a*) "BC HLHW NE", (*b*) "BC LLHW NE", (*c*) "BC HLLW NE", (*d*) "BC LLLW NE".

Furthermore, Figure 4.16 illustrates the active power generation resulting from the base cases of the "Status Quo" scenario, while Figure 4.17 displays the corresponding values for the base cases of the scenario "NEP2035". From these figures it can be noted that in high wind availability cases of scenario "Status Quo" ("BC HLHW SQ" and "BC LLHW SQ") as well as in the "BC LLLW SQ" case, the power demand is fed by employing mostly wind energy. Conversely, in the case of high load and limited wind energy availability ("BC HLLW SQ"), overall coal-fired power plants use reaches 75 % of these plants' installed power, and Biogas plants are operated at full capacity, provided that onshore and offshore wind generators reach their pre-set limit of 35 % and 45 % of their installed power. On the other hand, in all the base cases of the "NEP2035" scenario, the load demand can be fulfilled predominantly using renewable sources, with wind energy accounting for over 90 % of the power in each case.

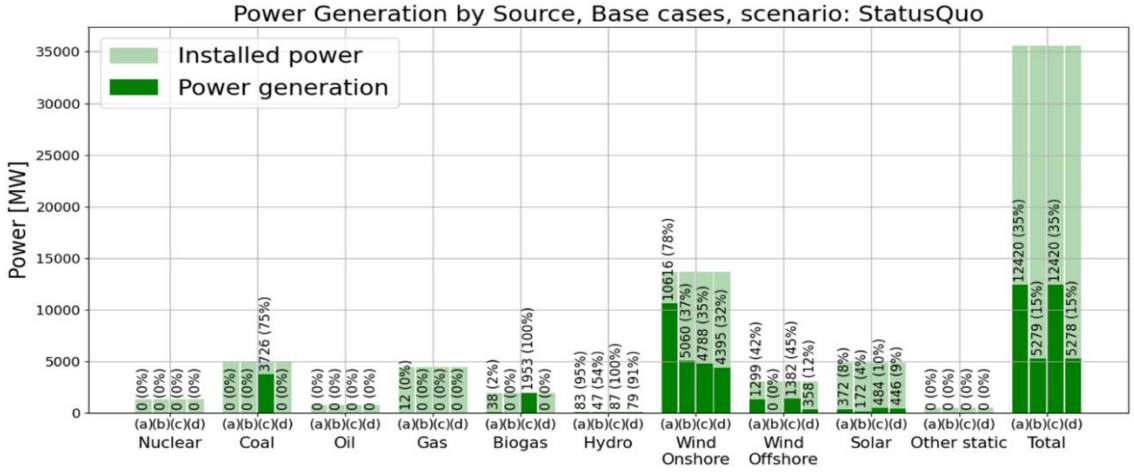

Figure 4.16. Generated active power in base cases of scenario "Status Quo":
(a) "BC HLHW SQ", (b) "BC LLHW SQ", (c) "BC HLLW SQ", (d) "BC LLLW SQ".

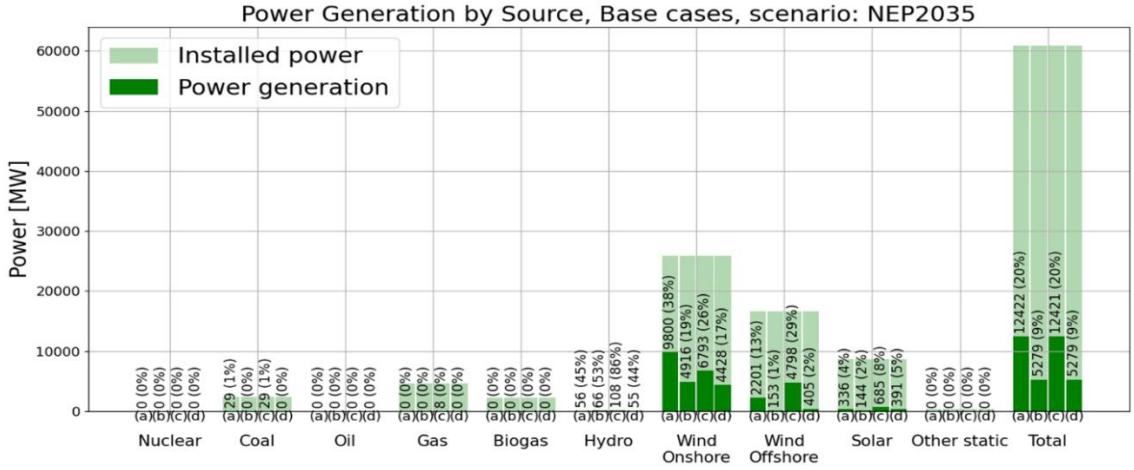

Figure 4.17. Generated active power in base cases of scenario "NEP2035":
(a) "BC HLHW NE", (b) "BC LLHW NE", (c) "BC HLLW NE", (d) "BC LLLW NE".

4.3.2. Simulation cases

The simulations to determine the connection points and maximum sizes of new GH2 plants in the power grid model by executing the de developed algorithm will be carried out considering both grid development scenarios ("Status Quo" and "NEP2035") and the various operative conditions described in Table 4.4. Moreover, two different groups of buses will be targeted among the interest buses to be considered as possible connection points for new GH2 plants: buses in the 110 kV grid and buses in all voltage levels. Table 4.7 presents a summary of all simulation cases that are to be evaluated.

Table 4.7. Summary of simulation cases.

N°	Case designation	Associated base case	Grid scenario	Operative conditions	Target grids
1	"HLHW SQ 110"	"BC HLHW SQ"	"Status Quo"	HLHW	110 kV grid
2	"HLHW SQ All"				All voltage levels
3	"HLHW NE 110"	"BC HLHW NE"	"NEP2035"		110 kV grid
4	"HLHW NE All"				All voltage levels
5	"LLHW SQ 110"	"BC LLHW SQ"	"Status Quo"	LLHW	110 kV grid
6	"LLHW SQ All"				All voltage levels
7	"LLHW NE 110"	"BC LLHW NE"	"NEP2035"		110 kV grid
8	"LLHW NE All"				All voltage levels
9	"HLLW SQ 110"	"BC HLLW SQ"	"Status Quo"	HLLW	110 kV grid
10	"HLLW SQ All"				All voltage levels
11	"HLLW NE 110"	"BC HLLW NE"	"NEP2035"		110 kV grid
12	"HLLW NE All"				All voltage levels
13	"LLLW SQ 110"	"BC LLLW SQ"	"Status Quo"	LLLW	110 kV grid
14	"LLLW SQ All"				All voltage levels
15	"LLLW NE 110"	"BC LLLW NE"	"NEP2035"		110 kV grid
16	"LLLW NE All"				All voltage levels

4.3.3. Buses of Interest

Good locations for placing new electrolysers can be found close to places where renewable energy is generated. In the case of the Northwest German region, locations on the coastal areas of north-western Lower Saxony and Schleswig-Holstein offer favourable conditions [13]. Figure 4.18 shows the installed power of wind energy generation divided by districts in northwest Germany, according to the data obtained from the Open Energy database for scenarios "Status Quo" and "NEP2035".

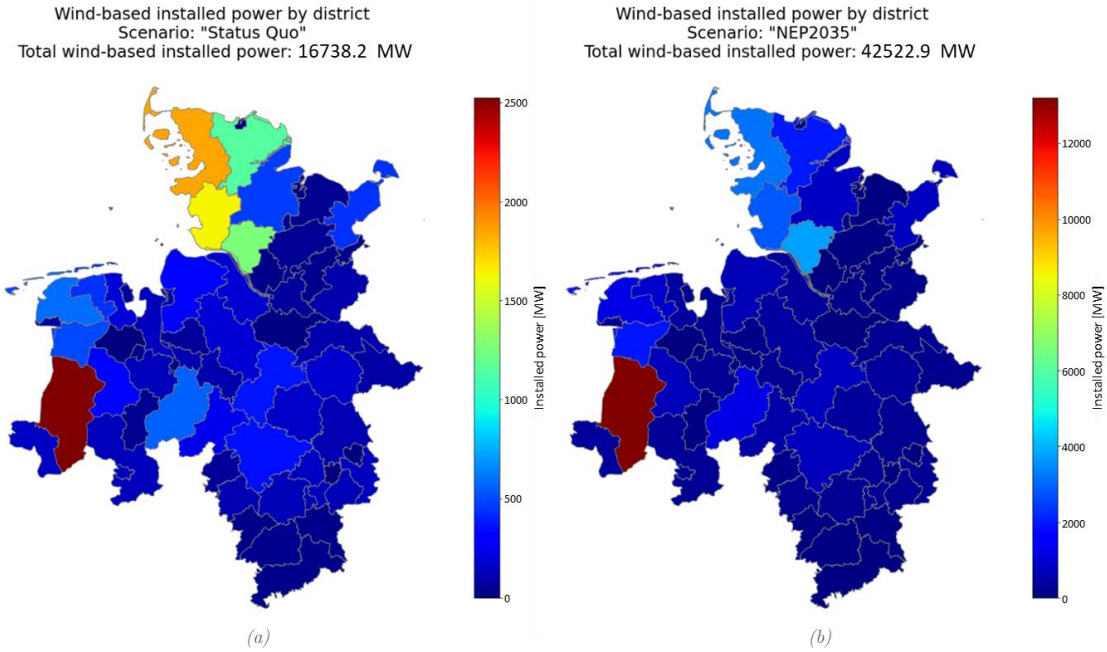

Figure 4.18. Installed power of wind energy generators for scenarios: (*a*) "Status Quo" and (*b*) "NEP2035".

Based on the previous considerations, the Buses of Interest in the simulations will exclusively include buses directly connected to wind energy generators within the specified regions. A map of the northwest German region, shown in Figure 4.19, highlights the districts (germ. *Landkreis*) corresponding to the area where these Buses of Interest are situated. Additionally, Figure 4.20 displays the geographic location of the Buses of Interest, and Appendix A presents a list of these buses.

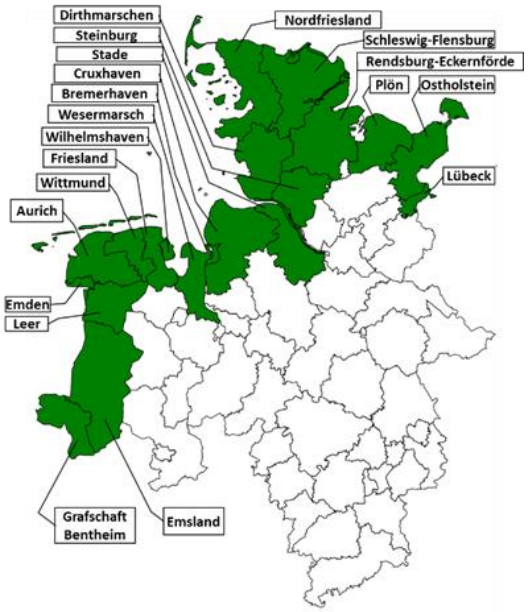

Figure 4.19. Districts (germ. *Landkreis*) of interest.

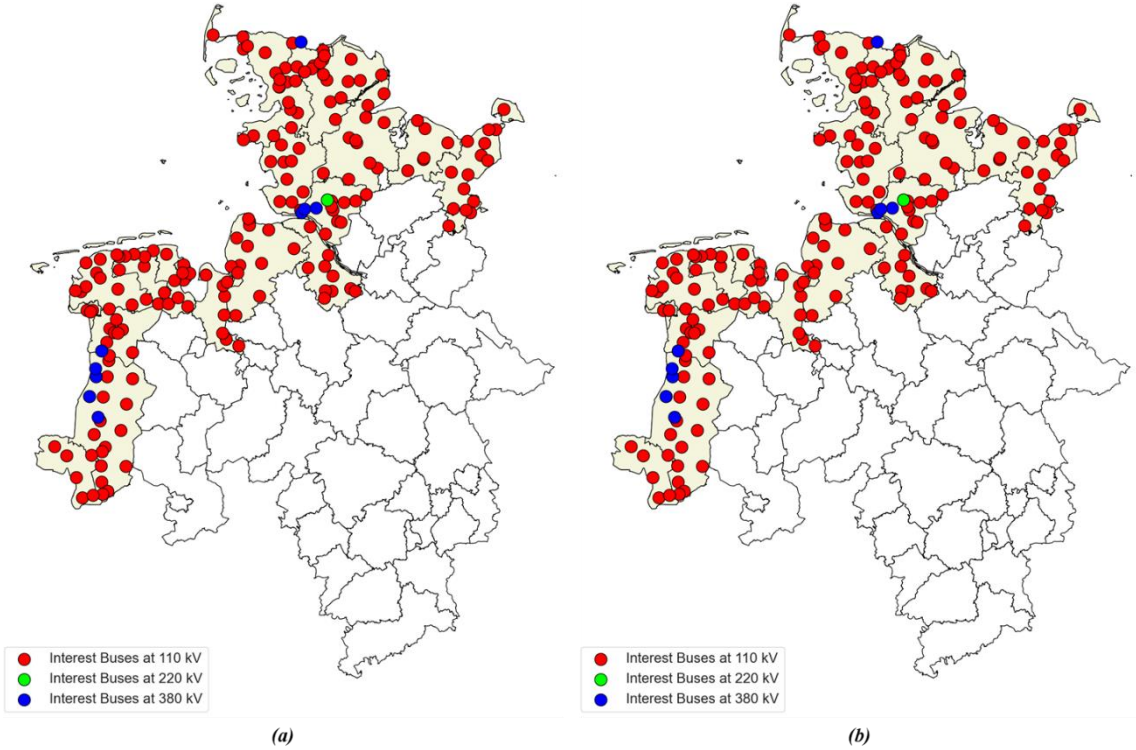

Figure 4.20. Buses of Interest: geographic representation for (*a*) Scenario "Status Quo" and (*b*) Scenario "NEP2035".

4.3.4. GH2 power demand target and minimum plant size

The incorporation of new GH2 plants will be made aiming to a target of 10 GW as Required GH2 Power (*RP*), being this the target installed capacity of GH2 production in Germany for the year 2035 [12]. Moreover, the minimum plant size (*MinGH2*) will be considered at 100 MW.

5. Results and Discussion

This chapter describes the outcomes obtained from implementing the developed algorithm, using the simulation scenarios from Table 4.7. A variety of graphic representations are employed to showcase key aspects such as the achieved GH2 power and the necessary count and power demand of the respective GH2 plants across each simulation case. Additionally, it elaborates on the changes in power generation required to accommodate the new GH2 power demand. The chapter also includes geographic representations of both studied grid development scenarios, that visually convey the positioning of the GH2 plant connection points.

5.1. Simulation Results

This section showcases the results derived from all the simulation scenarios outlined in Table 4.7. It also delivers comprehensive analyses and pertinent observations that offer valuable perspectives into the resulting distribution of GH2 plants across each simulation case.

5.1.1. High power demand and high wind energy availability: Simulation cases 1 to 4

This subsection presents the findings derived from simulation cases 1 through 4, corresponding to the following designations as described in Table 4.7: “HLHW SQ 110”, “HLHW SQ All”, “HLHW NE 110”, “HLHW NE All”, which depict conditions of high initial power demand coupled with high availability of wind energy. These results show the maximum GH2 power demand and required distribution for the abovementioned cases.

As it can be observed from Figure 5.1, the target *RP* of 10000 MW could not be achieved for high power demand and high wind energy availability (HLHW) conditions in the “Status Quo” scenario, reaching a maximum of 6500 MW when only allowing connection of new GH2 loads to the 110 kV grid (case 1: “HLHW SQ 110”) and 6600 MW when connection to all voltage levels (case 2: “HLHW SQ All”) is permitted. In order to achieve this GH2 power, the incorporation of fourteen GH2 plants is required as per case “HLHW SQ 110”, while in case “HLHW SQ All” the number of GH2 loads reaches thirteen.

Simulation case “HLHW SQ 110” (connections allowed at 110 kV grid only), results in the incorporation of two major GH2 loads of 2900 MW and 1800 MW, in

addition to twelve other smaller loads ranging from 100 MW to 300 MW. On the other hand, simulation case "HLHW SQ All" results in connection points distributed across 110 kV and 380 kV, with a major GH2 load of 4600 MW incorporated to the level of 380 kV and other smaller loads that range from 100 MW to 300 MW. Therefore, the approach of considering possible connection points in all voltage levels results in higher centralization of GH2 power demand than only permitting GH2 incorporation at 110 kV in scenario "Status Quo".

The required power to supply the new GH2 demand in these two simulation cases of scenario "Status Quo" is obtained from RES, as illustrated in Figure 5.2. Onshore wind generation increases from 10616 MW (in the corresponding base case scenario) to more than 13000 MW. In turn, offshore wind generation goes from 1299 MW to 3072 MW. Moreover, this is accompanied by the ramping up of biogas plants, which now deliver 1843 MW, compared to only 38 MW in the base case, and marginal increases in hydro and solar generation.

As it can be inferred from Figure 5.2, as well as from the summary presented in Table 5.1, the available power from RES that could be used to feed new GH2 loads in cases 1 and 2 amounts to 6870 MW, hence the failure to meet the 10000 MW target of GH2 power demand in these simulation cases is due to the lack of renewable energy generation capacity. This goes along with the expected output from the method and algorithm applied in this thesis, given that new GH2 loads are supposed to be fed by renewable generators only.

In contrast, the grid evolution towards the "NEP2035" scenario allows to attain the pre-set target of 10000 MW, both when using only 110 kV buses as well as when allowing the use of buses in the three voltage levels, resulting in ten and four GH2 loads respectively. Consequently, this scenario allows for higher GH2 power demand distributed in fewer locations, meaning larger GH2 plants than the ones achieved for the "Status Quo" scenario.

In this scenario, the increase in power demand due to GH2 is met almost exclusively by wind generation. Simulation case "HLHW NE 110" (case 3) presents increments of 5396 MW and 3020 MW in onshore and offshore wind generation outputs, plus the incorporation of 1370 MW from biogas plants generation as well as marginal increases in hydropower and solar generation, as depicted in Figure 5.3.

Moreover, simulation case "HLHW NE All" (case 4) only proposes connections to the 380 kV grid, and therefore the majority of the increment in power demand is covered by offshore wind energy generation, increasing from 2201 MW in the base case to 9888 MW (7687 MW increment). Additionally, onshore wind energy

generation rises by 1886 MW, while other renewables such as hydro and solar show a slight increase in their output.

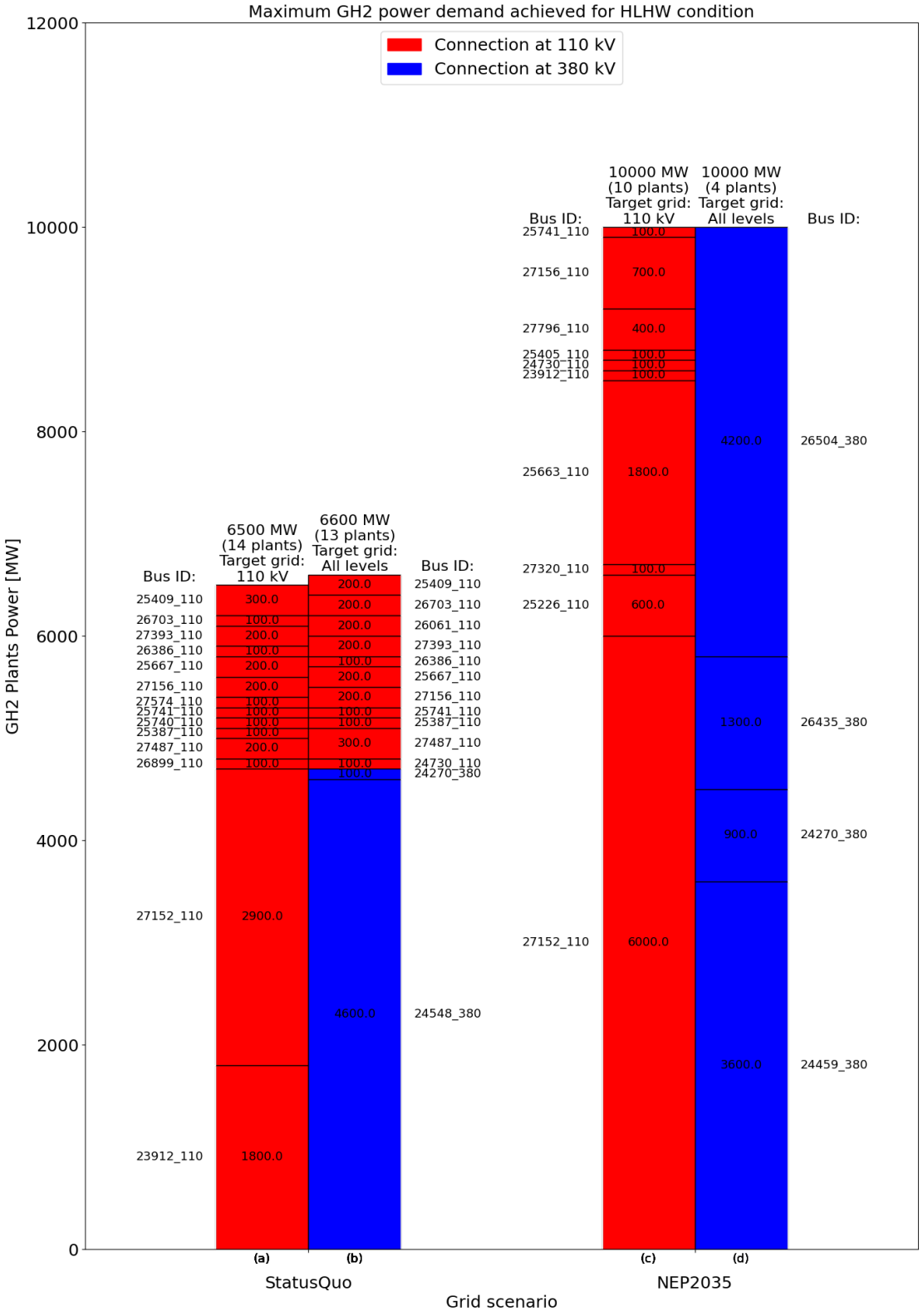

Figure 5.1. Resultant GH2 power, achieved from simulation cases 1 to 4: (a) HLHW SQ 110, (b) HLHW SQ All, (c) HLHW NE 110, (d) HLHW NE All.

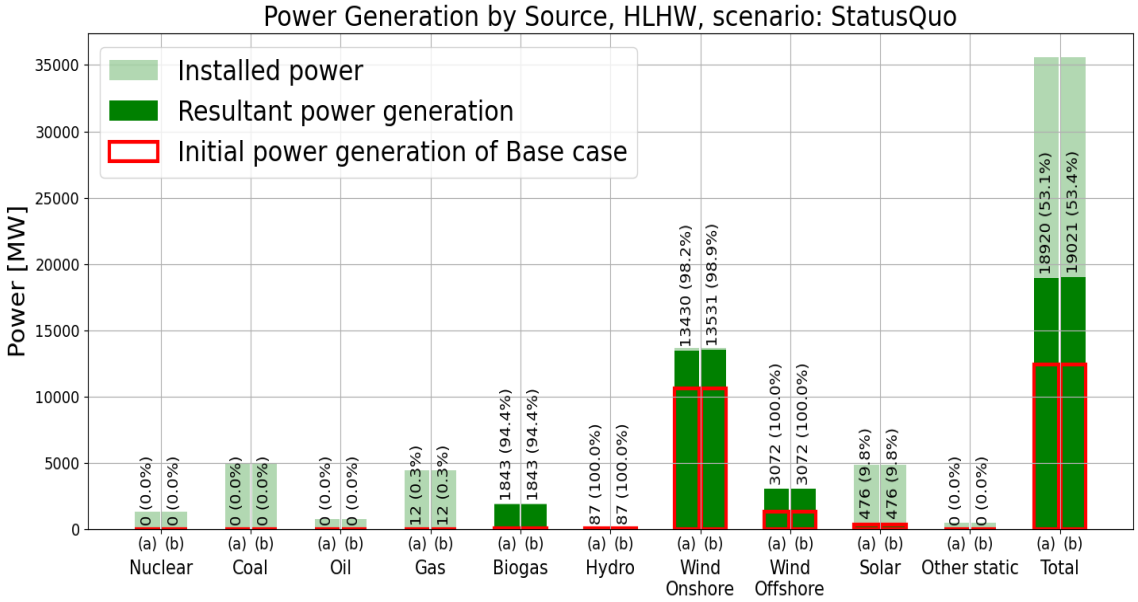

Figure 5.2. Resultant power generation, by energy source, for simulation cases 1 and 2: (a) HLHW SQ 110, (b) HLHW SQ All.

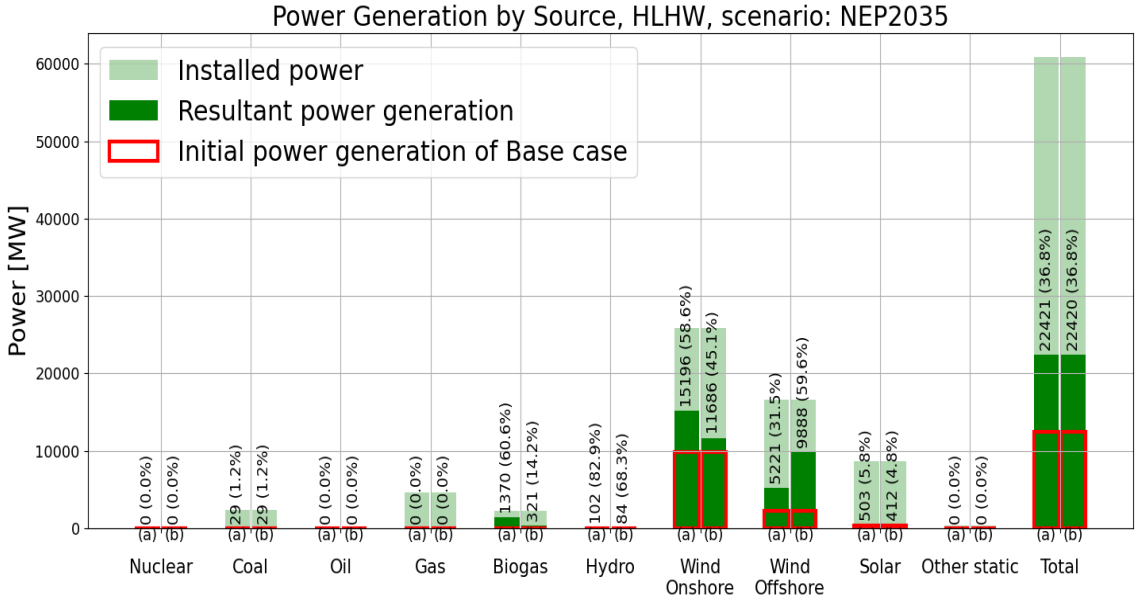

Figure 5.3. Resultant power generation, by energy source, for simulation cases 3 and 4: (a) HLHW NE 110, (b) HLHW NE All.

5.1.1.1. Resultant geographic distribution of GH2 plants in cases 1 and 2

As it can be observed in Figure 5.4, proposed GH2 plant locations for high load and high wind availability conditions in scenario "Status Quo" are distributed among the coastal districts of Schleswig-Holstein and the west part of Lower Saxony. Fourteen new GH2 loads are incorporated when only allowing their connection to 110 kV (simulation case 1: "HLHW SQ 110"), with the highest GH2 power demand being achieved in the district of Leer with 2900 MW, followed by Stade with 1800 MW, these two districts comprising 72 % of the total GH2 demand for this simulation case. Smaller GH2 loads are found in the following districts: Dithmarschen (600 MW), Nordfriesland (500 MW), Schleswig-Flensburg (400 MW), Emsland (100 MW), Ostholstein (100 MW) and Rendsburg-Eckernförde (100 MW). This GH2 power demand distribution is illustrated in Figure 5.6.

Meanwhile, in case "HLHW SQ All" (simulation case 2), where connection to all voltage levels is permitted, thirteen new GH2 loads are incorporated (two connected at 380 kV and eleven at 110 kV). The distribution of GH2 loads includes a GH2 power demand of 4600 MW in the district of Emsland, this alone accounting for almost 70 % of the new GH2 demand, as is depicted in Figure 5.6. Other districts that receive GH2 loads are Dithmarschen (700 MW), Nordfriesland (500 MW), Schleswig-Flensburg (500 MW), Ostholstein (100 MW), Rendsburg-Eckernförde (100 MW), Steinburg (100 MW).

5.1.1.2. Resultant geographic distribution of GH2 plants in cases 3 and 4

The proposed distribution for grid scenario "NEP2035" contemplates fewer GH2 loads of higher power demand to achieve the 10000 MW target (ten GH2 loads when connection is restricted to 110 kV and four GH2 loads when connection is allowed to all voltage levels), which are connected to different buses located in Schleswig-Holstein and the west part of Lower Saxony, as depicted in Figure 5.5.

As it can be noted from Figure 5.7, the highest GH2 load in case "HLHW NE 110" (simulation case 3), is achieved once again in the district of Leer (6000 MW), followed by Schleswig-Flensburg (1800 MW), together accounting for 78 % of the GH2 demand for this simulation case. Smaller GH2 loads are allocated to the districts of Dithmarschen (700 MW), Emsland (700 MW), Nordfriesland (500 MW), Rendsburg-Eckernförde (100 MW), Stade (100 MW) and Steinburg

(100 MW). Meanwhile, for case "HLHW NE All" (simulation case 4), all new GH2 loads are connected to the 380 kV level, with the district of Emsland receiving the largest one (4200 MW), followed by Dithmarschen (3600 MW) and Steinburg (2200 MW), as illustrated in Figure 5.7.

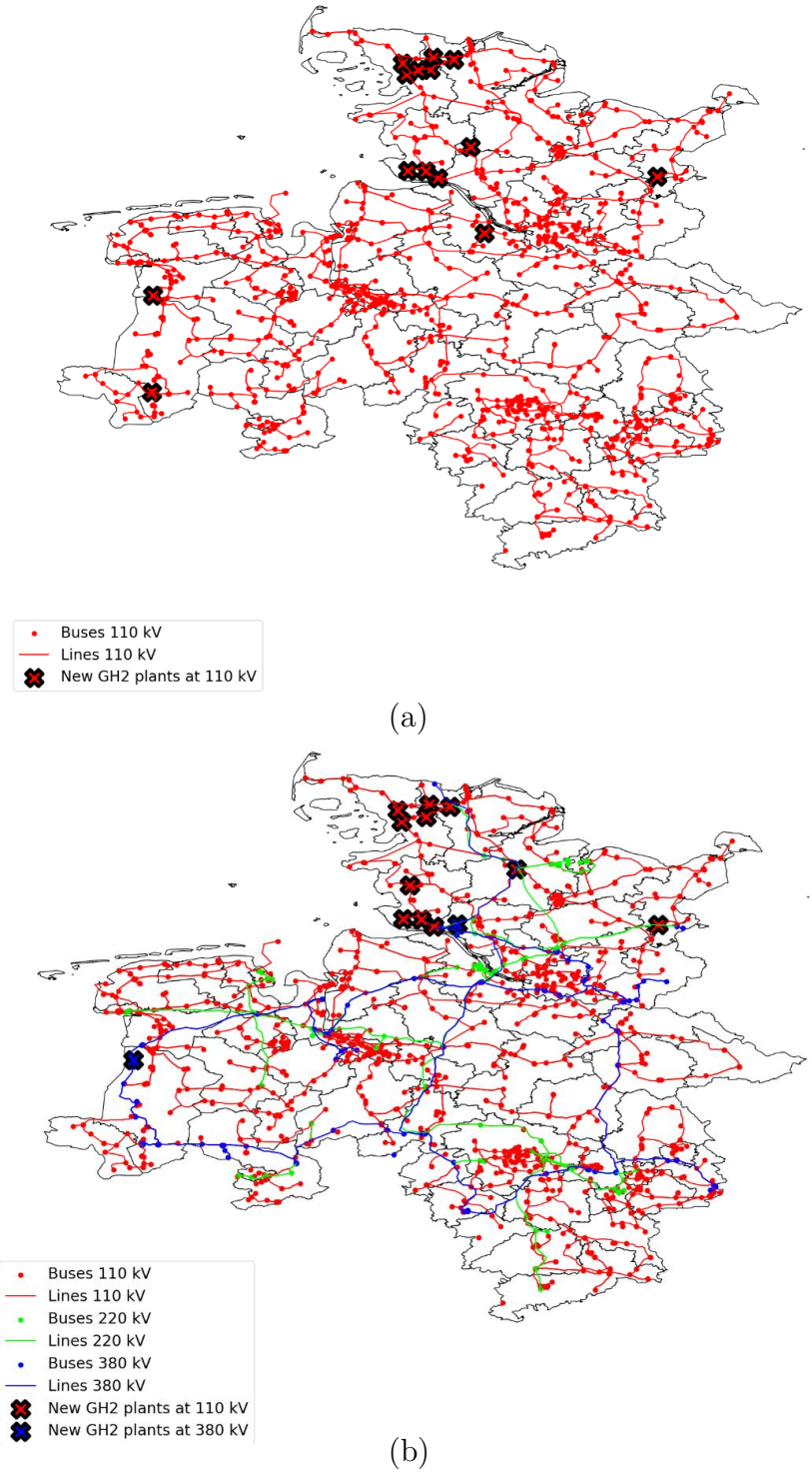

Figure 5.4. Geographic representation of GH2 plants connection points to the power grid simulation cases 1 and 2 (Status Quo): (a) HLHW SQ 110, (b) HLHW SQ All.

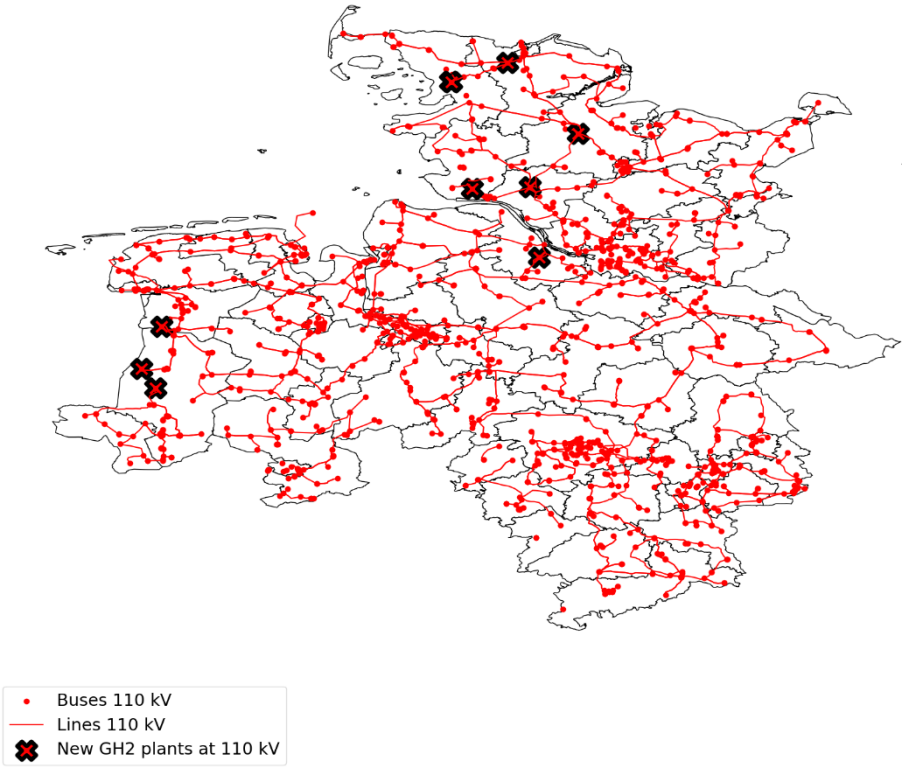

(a)

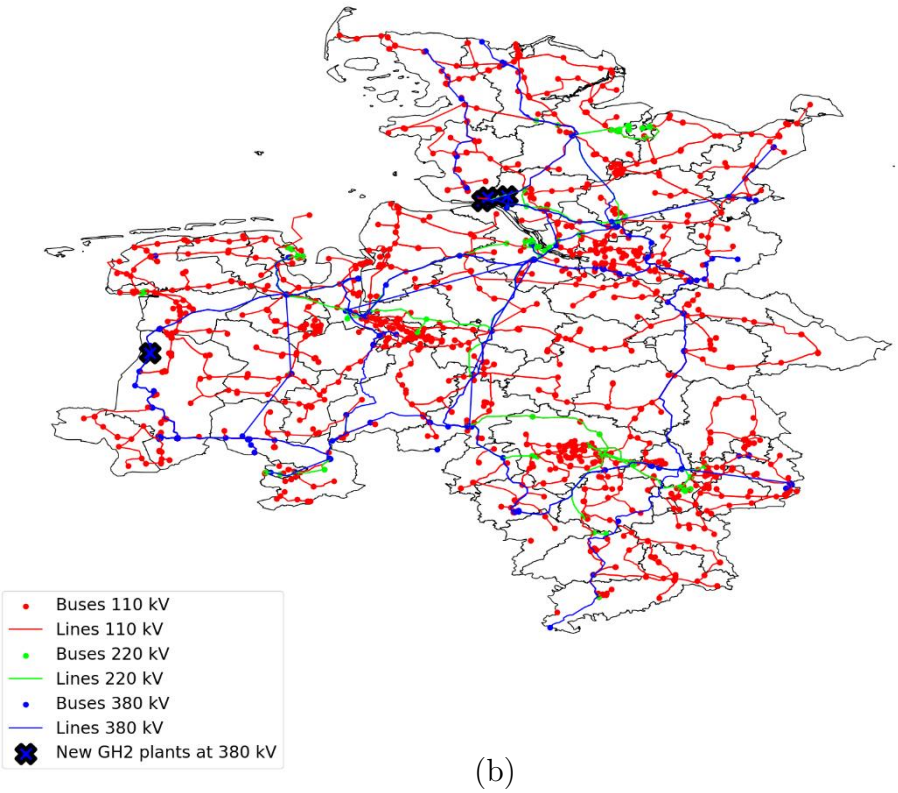

(b)

Figure 5.5. Geographic representation of GH2 plants connection points to the power grid simulation cases 3 and 4 (NEP2035): (a) HLHW NE 110, (b) HLHW NE All.

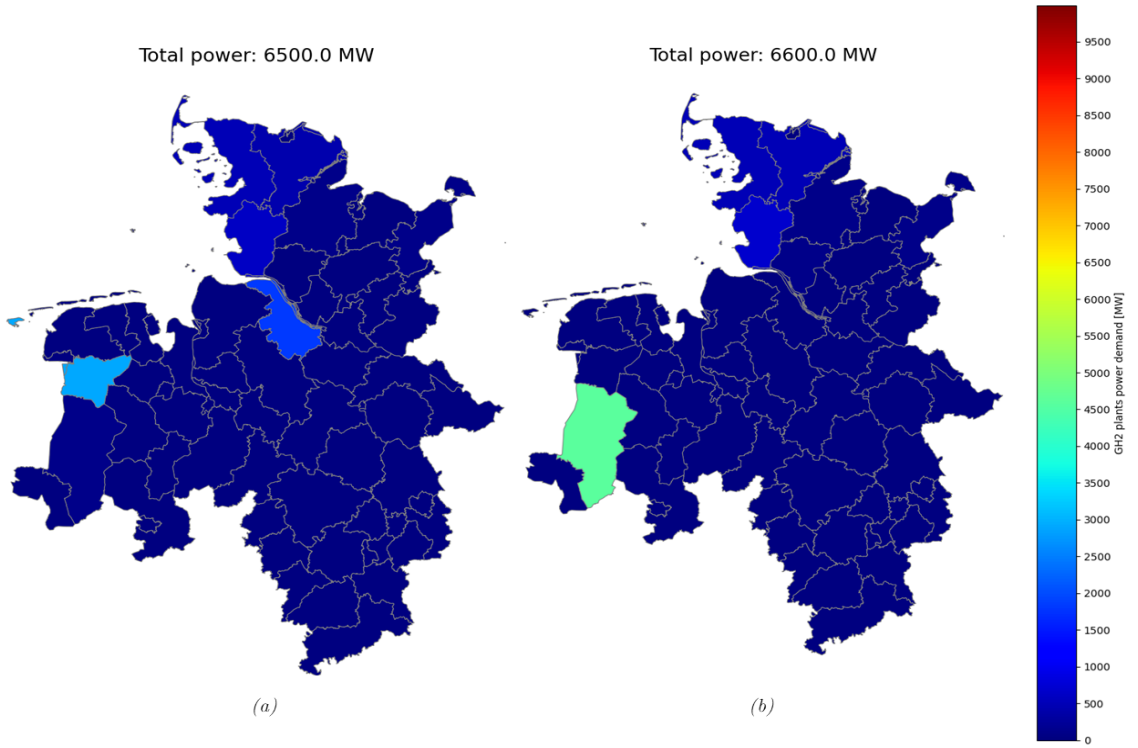

Figure 5.6. Resultant GH2 power, by district (germ. *Landkreis*), achieved from simulation cases 1 and 2 (Status Quo): (*a*) HLHW SQ 110, (*b*) HLHW SQ All.

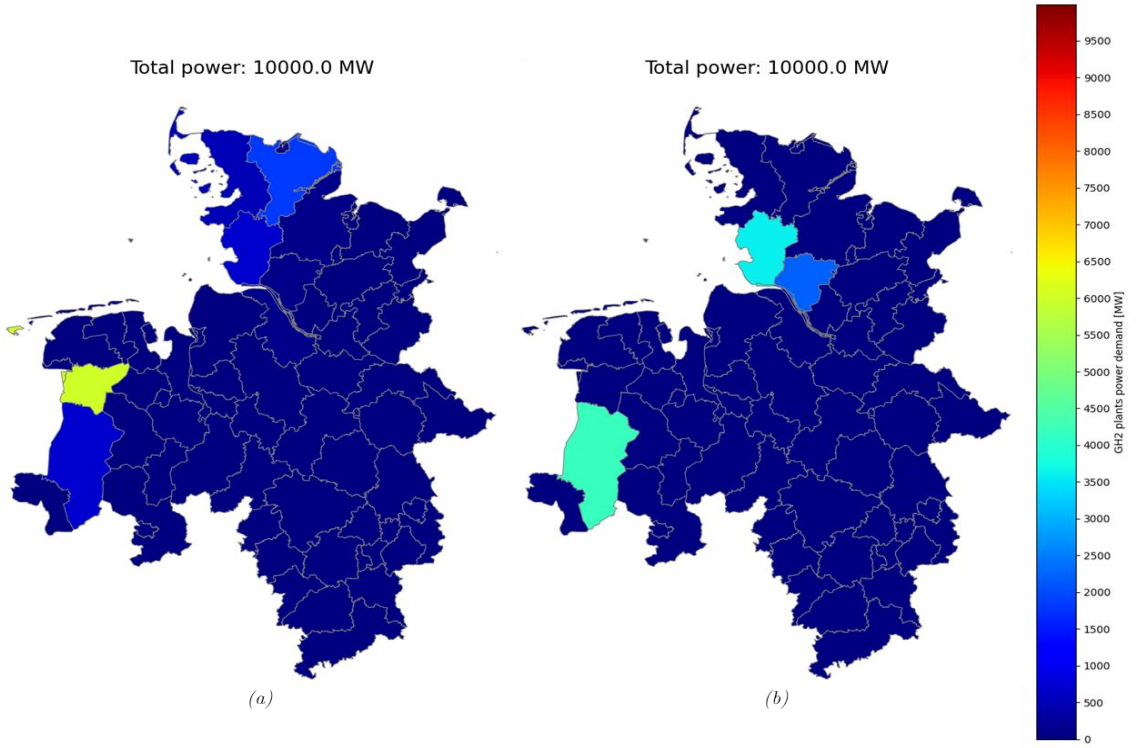

Figure 5.7. Resultant GH2 power, by district (germ. *Landkreis*), achieved from simulation cases 3 and 4 (NEP2035): (*a*) HLHW NE 110, (*b*) HLHW NE All.

5.1.2. Low power demand and high wind energy availability: Simulation cases 5 to 8

This section presents the results of simulation cases 5 to 8, as shown in Table 4.7: "LLHW SQ 110", "LLHW SQ All", "LLHW NE 110", and "LLHW NE All", which represent conditions of low initial power demand and high wind energy availability. These results indicate the highest GH2 power demand and distribution achieved in the previously mentioned simulation cases.

As depicted in Figure 5.8, for low power demand and high wind energy availability conditions (LLHW) in the "Status Quo" scenario, the 10000 MW target *RP* was successfully met. This was accomplished when either limiting new GH2 load connections to the 110 kV grid (case 5: "LLHW SQ 110") or permitting connections across all voltage levels (case 6: "LLHW SQ All"). Nine GH2 loads were integrated to meet the GH2 power demand in case "LLHW SQ 110", whereas in case "LLHW SQ All", only two GH2 loads were needed.

In simulation case "LLHW SQ 110" where connections were restricted to the 110 kV grid, three major GH2 loads of 6000 MW, 2000 MW, and 1000 MW were incorporated, supplemented by other six smaller GH2 loads varying between 100 MW and 300 MW. Contrastingly, simulation case "LLHW SQ All", which considered connections across the entire power grid, proposed only two GH2 loads of 6600 MW and 3400 MW on the 380 kV grid. Thus, by permitting connections across all voltage levels under the "Status Quo" scenario, GH2 power demand can centralized more significantly than if connections were restricted to 110 kV.

The power required to fulfil the new GH2 demand in the "Status Quo" scenario for cases 5 and 6 is indicated in Figure 5.9. For "LLHW SQ 110", onshore wind generation rose by 6089 MW, and offshore wind generation by 2341 MW. Additionally, biogas plants are ramped up to 1280 MW, supplemented by minor increases in hydro and solar generation. Case "LLHW SQ All" exhibited a similar trend, with wind generators providing 97 % of the GH2 demand (6611 MW from onshore and 3072 MW from offshore), supplemented by minor boosts in solar and hydropower generation.

From Figure 5.9 and Table 5.1 it can be inferred that the available power from RES for feeding new GH2 loads in cases 5 and 6 amounts to nearly 14000 MW, exceeding the *RP* target by 40 %. Although the utilization of this available power could be limited by the maximum permissible loading of transmission lines, the low power demand cases depicted in Figure 4.14 display a reduced utilization of

transmission lines for feeding initial loads compared to the high power demand cases, leaving room for demand expansion due to GH2.

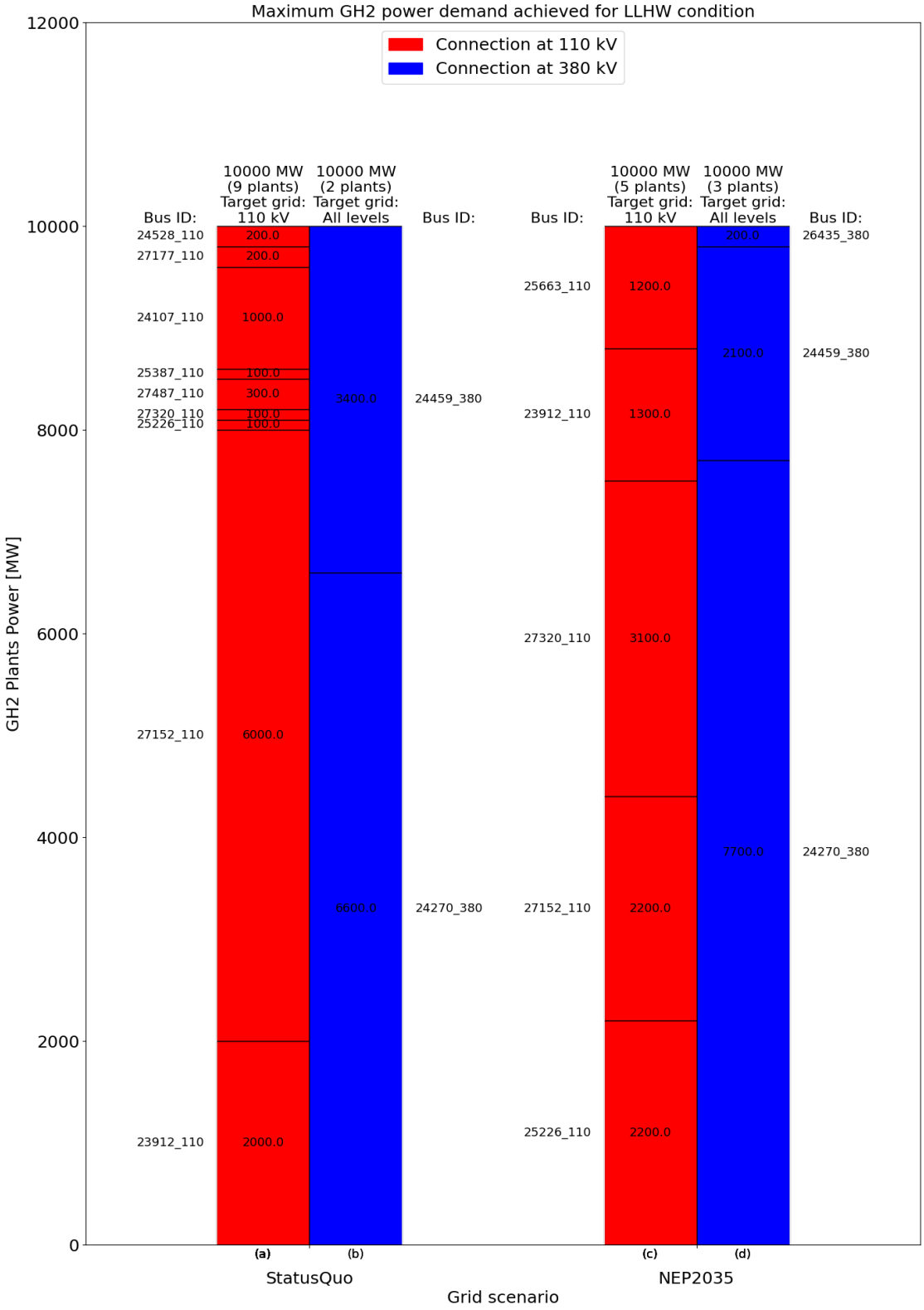

Figure 5.8. Resultant GH2 power, achieved from simulation cases 5 to 8: (a) LLHW SQ 110, (b) LLHW SQ All, (c) LLHW NE 110, (d) LLHW NE All.

Similarly, the "NEP2035" grid scenario meets the pre-set 10000 MW target, both when limiting connections to 110 kV buses (resulting in five GH2 loads) or when allowing connections across all voltage levels (resulting in three GH2 loads connected to the 380 kV level). Here, the increase in power demand due to GH2 is predominantly offset by substantial increments in wind energy generation. As Figure 5.10 shows, case "LLHW NE 110" (case 7) presents increases of 6780 MW and 2816 MW in onshore and offshore wind generation, supplemented by minor increases in hydro and solar. Similarly, case "LLHW NE All" (case 8) reports an increase of 6158 MW and 2789 MW in onshore and offshore wind generation respectively, along with an increase of 720 MW in biogas generation and marginal increases in hydro and solar.

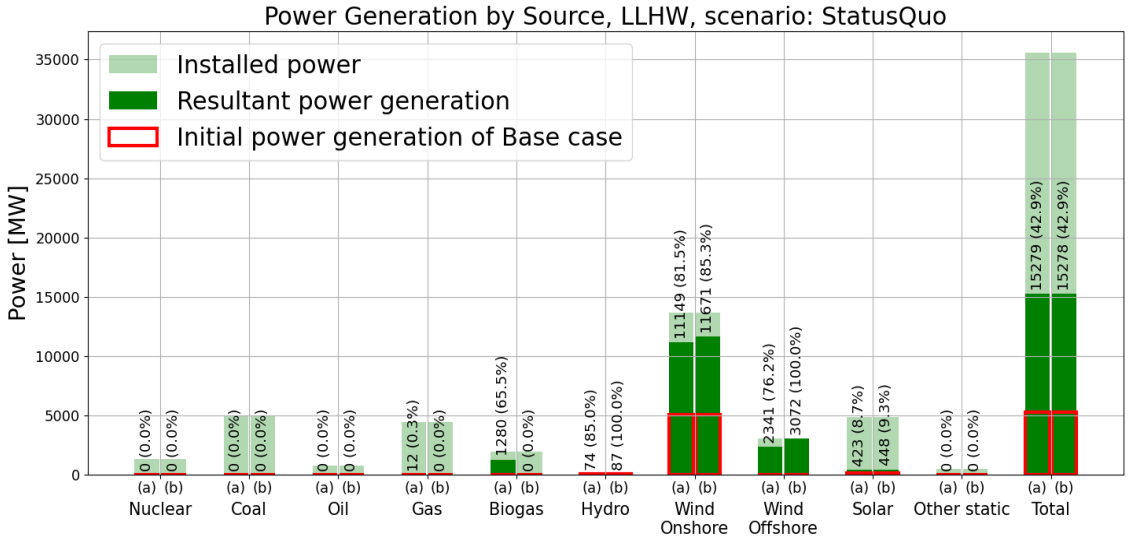

Figure 5.9. Resultant power generation, by energy source, for simulation cases 5 and 6: (a) LLHW SQ 110, (b) LLHW SQ All.

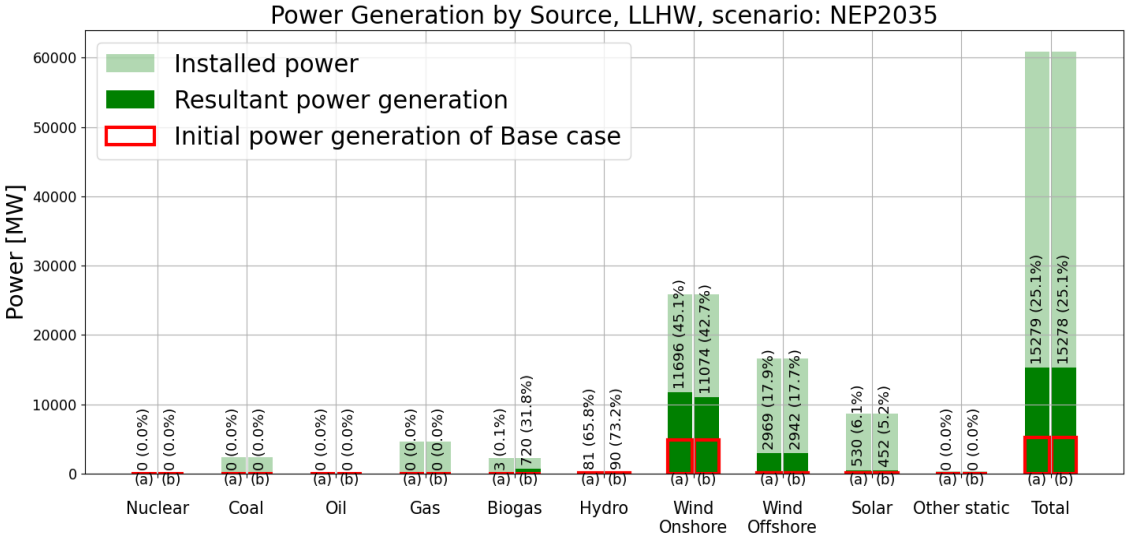

Figure 5.10. Resultant power generation, by energy source, for simulation cases 7 and 8: (a) LLHW NE 110, (b) LLHW NE All.

5.1.2.1. Resultant geographic distribution of GH2 Plants in Cases 5 and 6

Figure 5.11 reveals the proposed locations for GH2 plants under LLHW conditions in the "Status Quo" scenario, primarily distributed across the western and northern districts of Schleswig-Holstein and Lower Saxony.

In case "LLHW SQ 110" (simulation case 5), which only allows new GH2 loads to connect at 110 kV, nine new GH2 plants are incorporated, with the largest GH2 power demand emerging at the district of Leer (6000 MW), followed by Stade (2000 MW). These districts account for 80 % of the total GH2 demand in this simulation case. Smaller demands appear in other districts like Wilhelmshaven (1000 MW), Schleswig-Flensburg (300 MW), Emsland (200 MW), Friesland (200 MW), Steinburg (200 MW), and Dithmarschen (100 MW), as it can be observed in Figure 5.13.

On the other hand, case "LLHW SQ All" (simulation case 6), which allows connections at all voltage levels, proposes two GH2 loads (both connected at 380 kV) in the districts of Steinburg and Dithmarschen located in the western side of Schleswig-Holstein, with achieved power demands of 6600 MW and 3400 MW respectively (Figure 5.13).

5.1.2.2. Resultant geographic distribution of GH2 Plants in Cases 7 and 8

Under the "NEP2035" grid scenario, case "LLHW NE 110" (simulation case 7) suggests five GH2 loads connecting to various buses located in Schleswig-Holstein and Lower Saxony at 110 kV (Figure 5.12). The district of Emsland receives the highest GH2 demand (5300 MW), followed by Leer (2200 MW), Stade (1300 MW), and Schleswig-Flensburg (1200 MW); this distribution of GH2 power demand is presented in Figure 5.14.

In contrast, case "LLHW NE All" (simulation case 8) concentrates GH2 power demand in three closely positioned connection points at 380 kV, located in the neighbouring districts of Steinburg and Dithmarschen, as depicted in Figure 5.12. In this case the district of Steinburg receives a GH2 power demand of 7900 MW, while Dithmarschen receives 2100 MW. This distribution of GH2 plant is depicted in Figure 5.14.

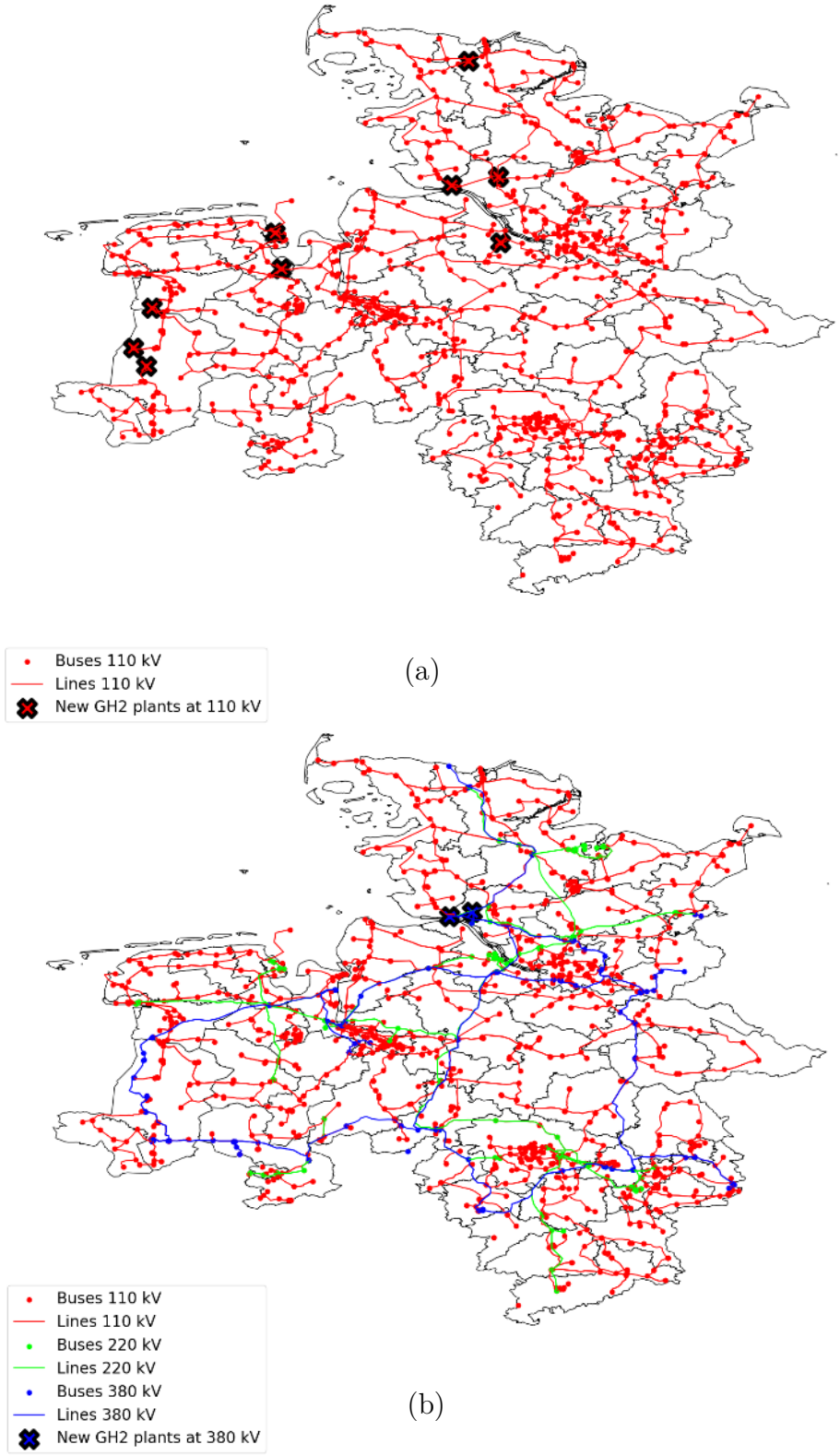

Figure 5.11. Geographic representation of GH2 plants connection points to the power grid simulation cases 5 and 6 (Status Quo): (a) LLHW SQ 110, (b) LLHW SQ All.

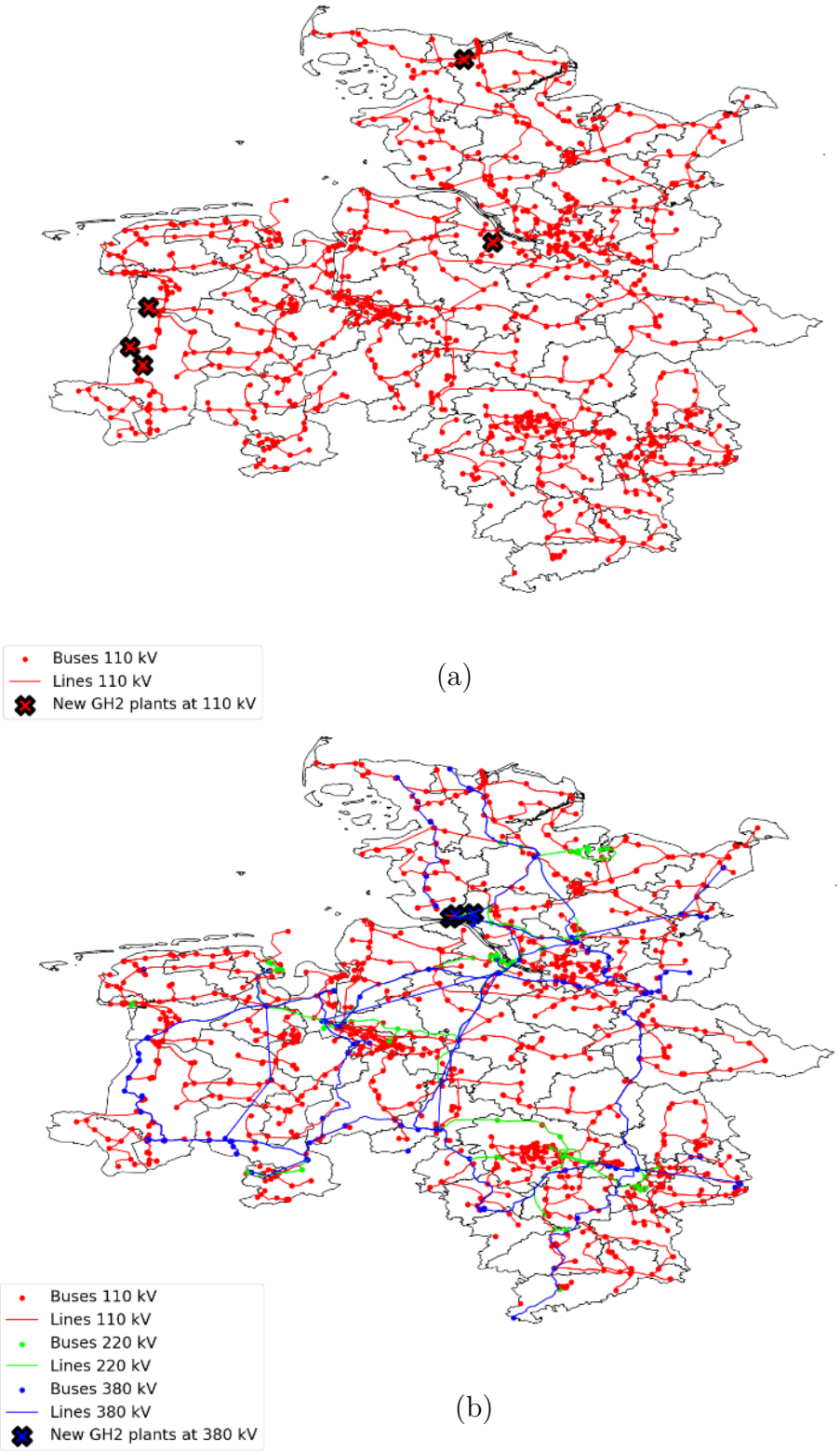

Figure 5.12. Geographic representation of GH2 plants connection points to the power grid simulation cases 7 and 8 (NEP2035): (a) LLHW NE 110, (b) LLHW NE All.

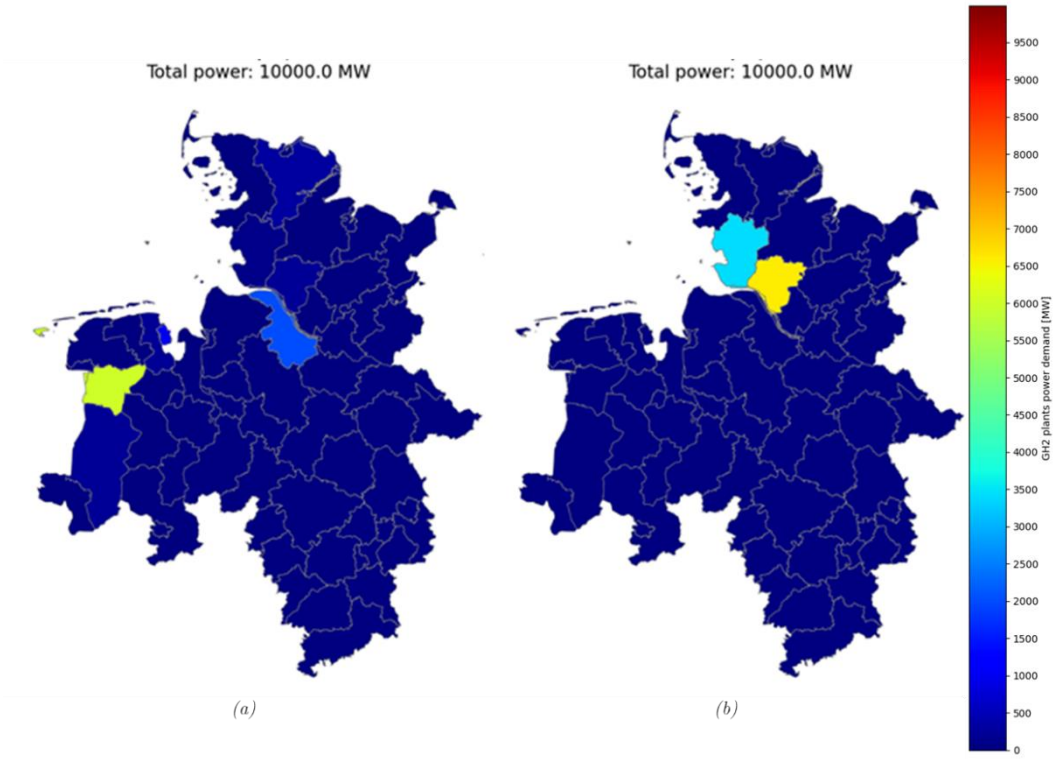

Figure 5.13. Resultant GH2 power, by district (germ. *Landkreis*), achieved from simulation cases 5 and 6 (Status Quo): (*a*) LLHW SQ 110, (*b*) LLHW SQ All.

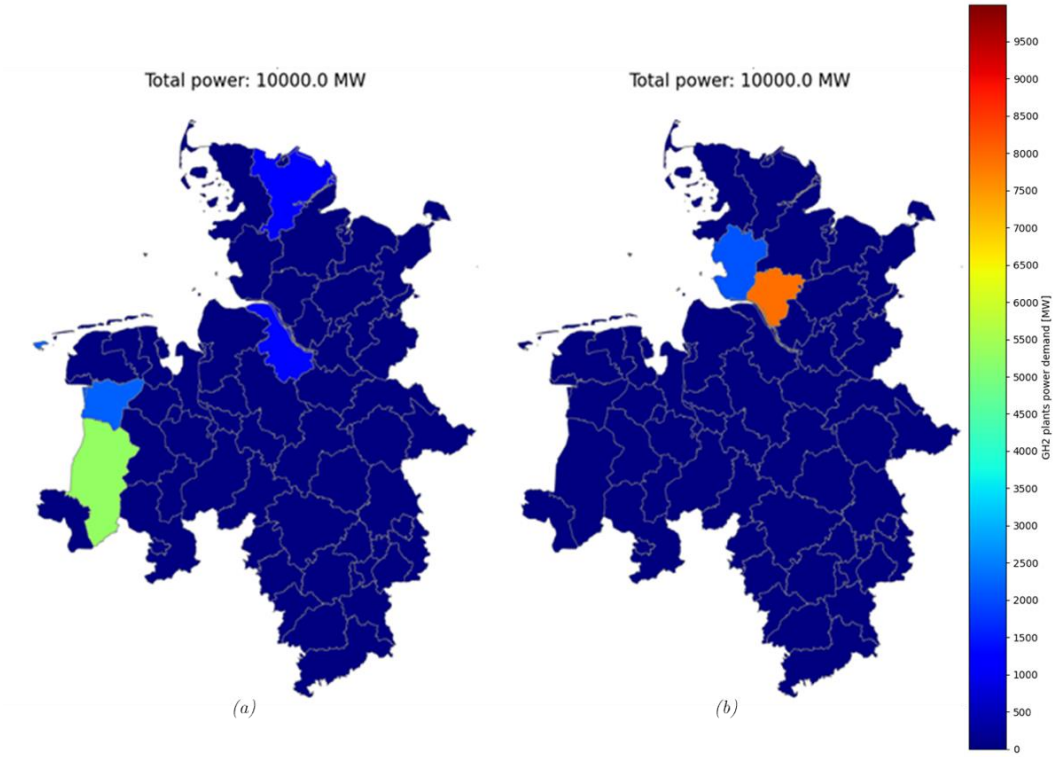

Figure 5.14. Resultant GH2 power, by district (germ. *Landkreis*), achieved from simulation cases 7 and 8 (NEP2035): (*a*) LLHW NE 110, (*b*) LLHW NE All.

5.1.3. High power demand and limited wind energy availability: Simulation cases 9 to 12

This section elucidates the outcomes of simulation cases 9 through 12, denoted as "HLLW SQ 110", "HLLW SQ All", "HLLW NE 110", and "HLLW NE All" in Table 4.7, addressing conditions characterized by high initial power demand and limited wind energy availability. These results present the maximum attainable GH2 power demand and required distribution within the cited simulation cases.

Figure 5.15 demonstrates that in cases of high initial power demand and limited wind energy availability, specifically in the "Status Quo" context (cases 9 and 10), it is not feasible to incorporate any new GH2 load. Figure 5.16 and Table 5.1 indicate that renewable energy generators were operating at available capacity, supplying power to the initial system loads in the respective base case. Moreover, the overall output of coal-fired power plants is 75 % of their full capacity, contributing 3726 MW of the 12420 MW required by the system loads.

As a result, there is no surplus of renewable energy to accommodate new GH2 loads. This observation aligns with the expected outcomes derived from the methodology and algorithm employed to assess and plan the strategic allocation of GH2 loads among the selected buses in this thesis, given that GH2 demand should solely be fulfilled by renewable sources.

In contrast, the "NEP2035" grid scenario allows the addition of 4200 MW of GH2 power demand when limiting connections to 110 kV buses (case 11), resulting in five GH2 loads. When permitting connections across all voltage levels (case 12), 7300 MW can be incorporated, also resulting in five GH2 loads (four connected at 380 kV and one at 110 kV). As highlighted in Figure 5.17, simulation case "HLLW NE 110" (case 11) mostly compensates for the GH2-related increment in power demand by considerably increasing onshore wind energy (2250 MW) and biogas generation (2229 MW), along with minor increases in solar and hydropower. Interestingly, a decrease of 477 MW in offshore wind generation is also observed.

This unexpected situation of increased biogas generation and reduced offshore wind output is not immediately intuitive. Given that biogas generation costs are higher than those of offshore wind (as shown in Table 4.5), the assumption would be that offshore wind would be prioritized during the OPF calculation process to determine generator outputs. Nevertheless, the feasibility assessment and cost optimization stages conducted in PowerFactory ensures the ramp up of biogas plants is used to supply GH2 loads that otherwise could not be fed using cheaper RES without violating pre-set constraints (such as maximum line loading at 100 %). The increase

in onshore wind generation, which is closer to the loads (at 110 kV), heavily contributes to the slight reduction in offshore wind output.

Conversely, in simulation case 12 ("HLLW NE All"), the increased demand brought on by new GH2 loads is catered to by a 2258 MW and 2664 MW surge in onshore and offshore wind generation, complemented by a 2183 MW boost in biogas generation and small increases in hydro and solar energy.

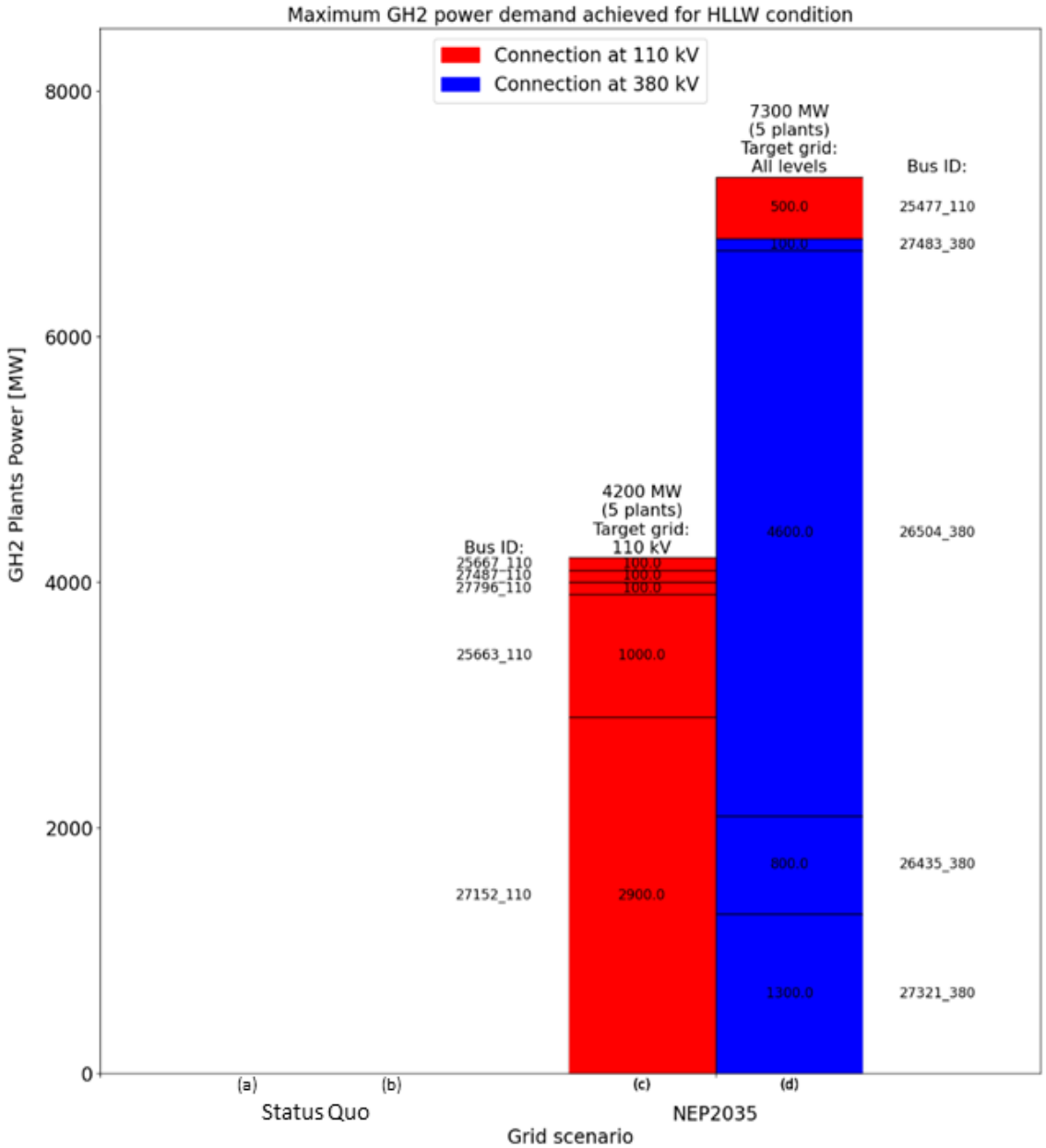

Figure 5.15. Resultant GH2 power, achieved from simulation cases 9 to 12: (a) HLLW SQ 110, (b) HLLW SQ All, (c) HLLW NE 110, (d) HLLW NE All.

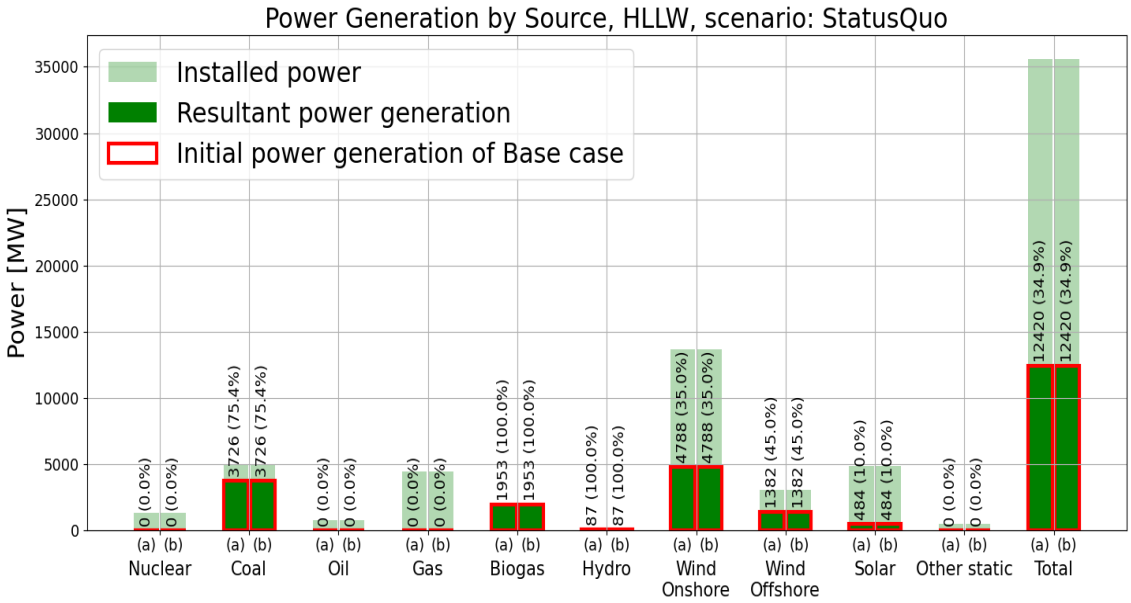

Figure 5.16. Resultant power generation, by energy source. Simulation cases 9 and 10: (a) HLLW SQ 110, (b) HLLW SQ All.

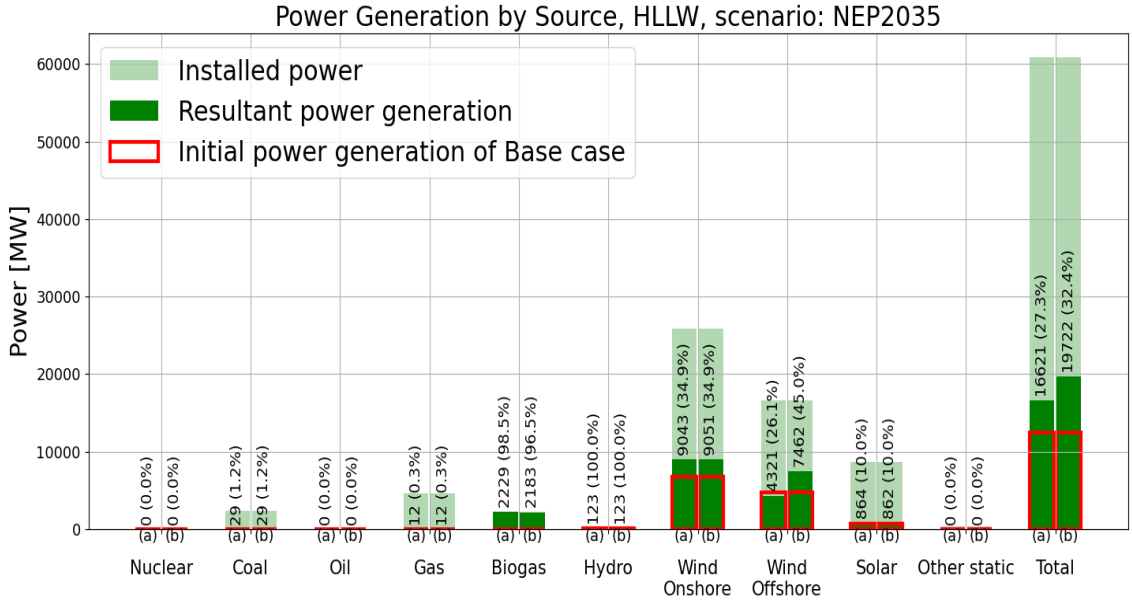

Figure 5.17. Resultant power generation, by energy source. Simulation cases 11 and 12: (a) HLLW NE 110, (b) HLLW NE All.

5.1.3.1. Resultant geographic distribution of GH2 Plants in Cases 9 and 10

For cases 9 and 10, the geographical distribution of GH2 plants is illustrated in Figure 5.18, which shows no GH2 load connected to the power grid. Figure 5.20 further highlights the lack of GH2 demand in any district.

5.1.3.2. Resultant geographic Distribution of GH2 Plants in Cases 11 and 12

Under the "NEP2035" grid scenario, simulation case 11 ("HLLW NE 110") proposes five new GH2 loads connected to multiple buses situated in the north and west of Schleswig-Holstein and the western part of Lower Saxony at 110 kV, as depicted in Figure 5.19. The district of Leer in Lower Saxony accommodates the largest GH2 power demand (2900 MW), followed by Schleswig-Flensburg (1200 MW) and Nordfriesland (100 MW); this distribution is represented in Figure 5.21. Similarly, simulation case 12 ("HLLW NE All") also sees five GH2 loads distributed across the north and west of Schleswig-Holstein and the western part of Lower Saxony (four connected at 380 kV and one at 110 kV), as shown in Figure 5.19. This time, the district of Emsland receives the largest share of GH2 power demand with 5900 MW (80 % of the total), succeeded by Steinburg (800 MW), Dithmarschen (500 MW), and Schleswig-Flensburg (100 MW), as depicted in Figure 5.21.

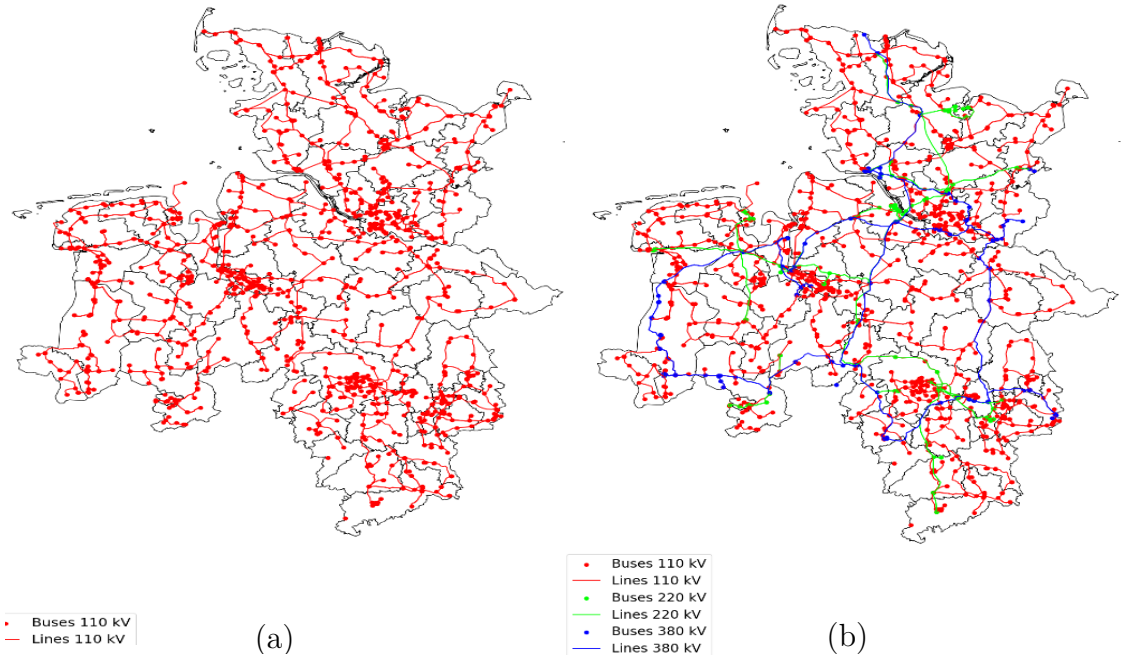

Figure 5.18. Geographic representation of GH2 plants connection points to the power grid simulation cases 5 and 6 (Status Quo): (a) LLHW SQ 110, (b) LLHW SQ All.

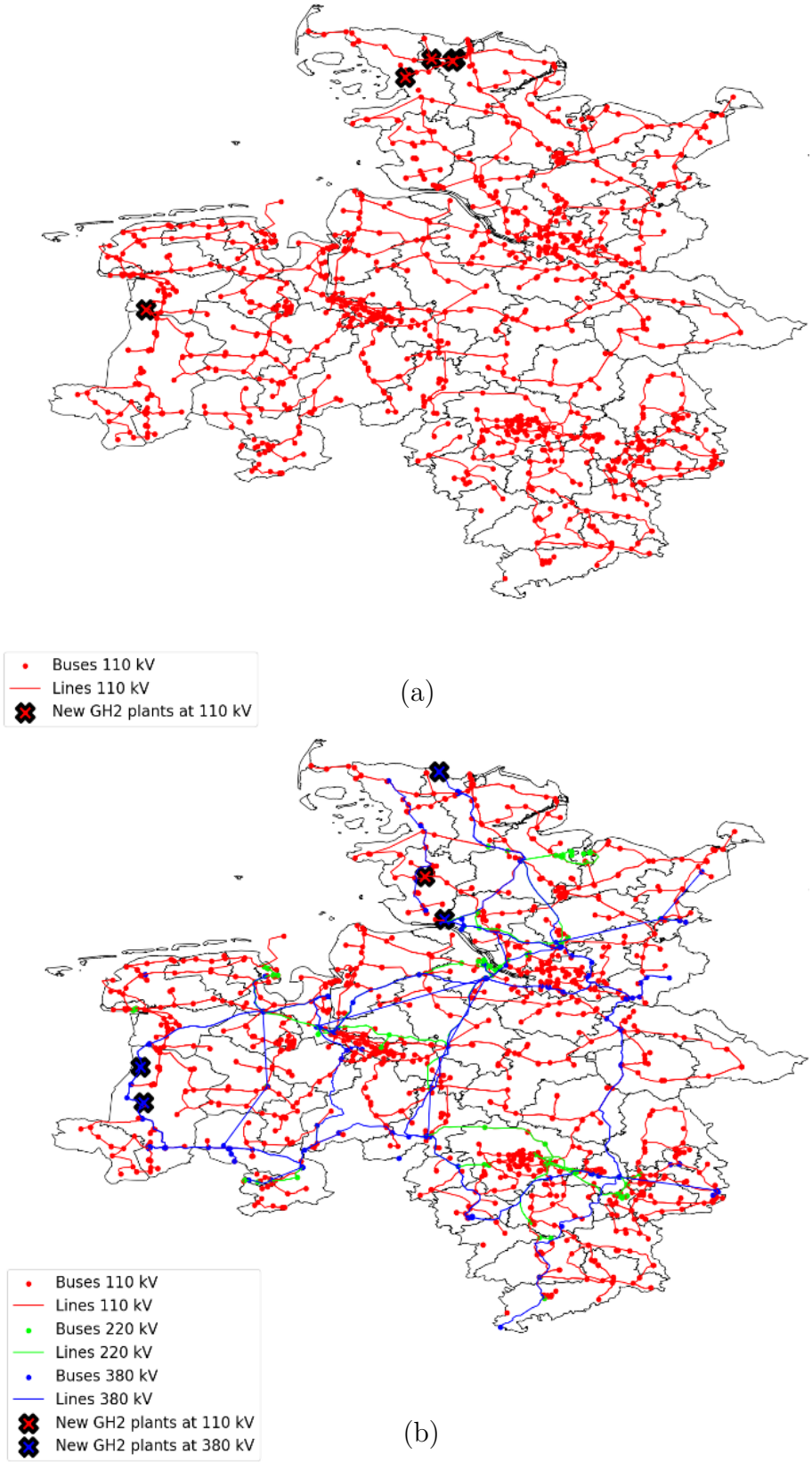

Figure 5.19. Geographic representation of GH2 plants connection points to the power grid simulation cases 7 and 8 (NEP2035): (a) LLHW NE 110, (b) LLHW NE All.

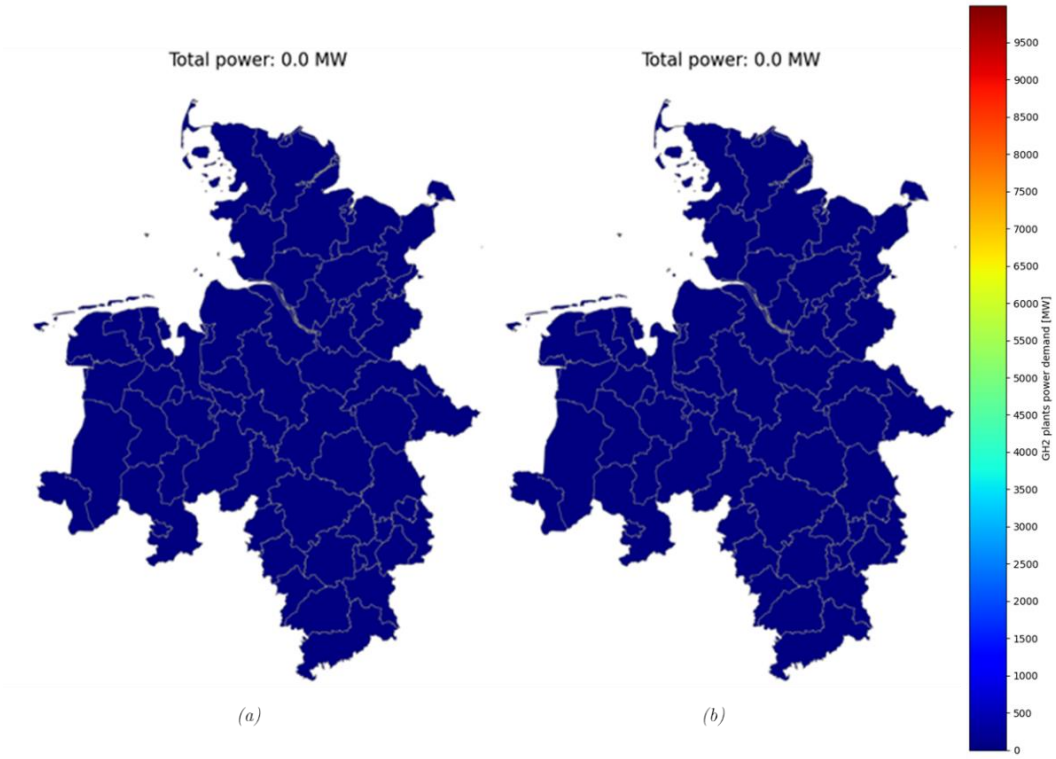

Figure 5.20. Resultant GH2 power, by district (germ. *Landkreis*), achieved from simulation cases 9 and 10 (Status Quo): (*a*) HLLW SQ 110, (*b*) HLLW SQ All.

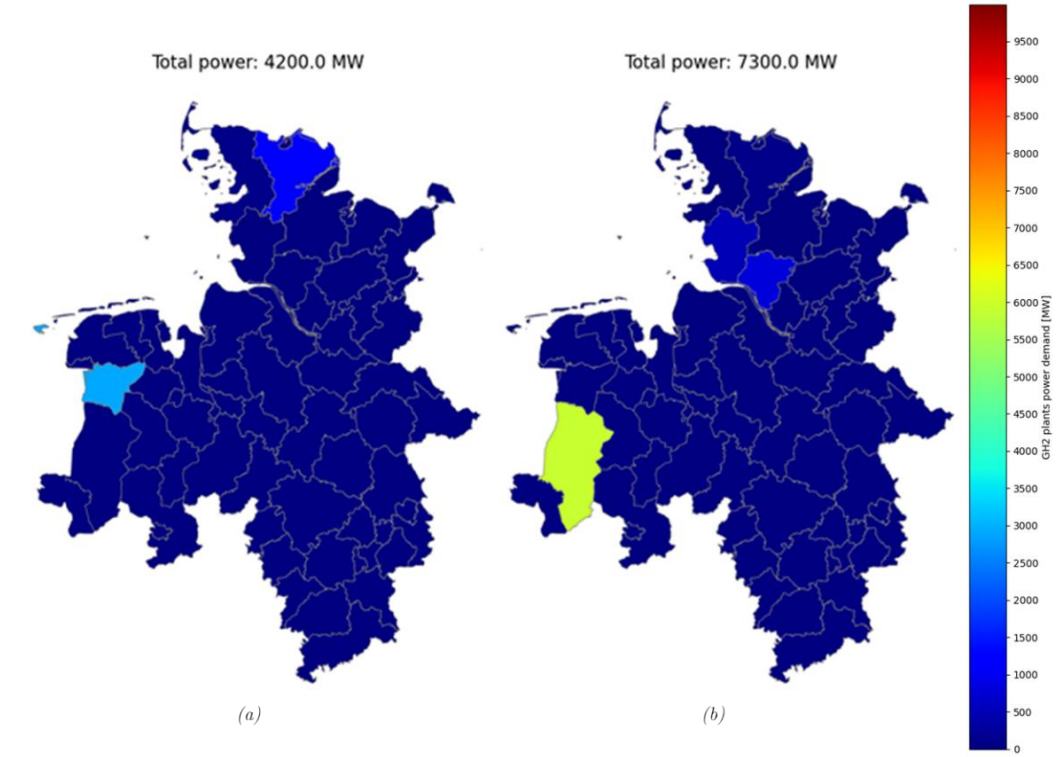

Figure 5.21. Resultant GH2 power, by district (germ. *Landkreis*), achieved from simulation cases 11 and 12 (NEP2035): (*a*) HLLW NE 110, (*b*) HLLW NE All.

5.1.4. Low power demand and limited wind energy availability: Simulation cases 13 to 16

This section details the outcomes of simulation cases 13 to 16, identified as "LLLW SQ 110", "LLLW SQ All", "LLLW NE 110", and "LLLW NE All" (refer to Table 4.7), which examine instances of low initial power demand and limited wind energy availability. These results showcase the highest GH2 power demand achieved in the mentioned simulation cases.

As evidenced by Figure 5.22, in the "Status Quo" scenario under conditions of low power demand and limited wind energy availability (LLLW), the target *RP* of 10000 MW was unattainable, peaking at just 3400 MW. This GH2 power demand was achieved whether connections were limited to the 110 kV grid (case 13: "LLLW SQ 110") or allowed at all voltage levels (case 14: "LLLW SQ All"). To achieve this level of GH2 power, two major GH2 loads of 1800 MW and 1600 MW are required for case "LLLW SQ 110" Contrarily, a singular load linked to the 380 kV grid is incorporated in simulation case "LLLW SQ All", leading to a higher centralization of GH2 power demand.

As illustrated in Figure 5.23, the necessary power to meet the new GH2 demand in these two simulation cases of the "Status Quo" scenario is derived from renewable energy sources (RES), primarily from an increase in biogas generation of 1937 MW. This is supplemented by onshore and offshore wind generators, which contribute an additional 393 MW and 1024 MW respectively, along with minor boosts in solar and hydropower. The power surplus from RES to supply new GH2 loads in cases 13 and 14 totals slightly above 3400 MW, as inferred from Figure 5.23 as well as from Table 5.1. Consequently, the inability to reach the 10000 MW target of GH2 power demand in these cases is caused by insufficient renewable energy generation capacity. This outcome aligns with the expected results from the employed methodology and algorithm, since new GH2 loads should be exclusively fed by renewable generators.

On the other hand, the progression towards the "NEP2035" scenario enables the inclusion of a greater GH2 power demand, achieving 9900 MW spread across sixteen loads when connections are limited to the 110 kV buses (case 15: "LLLW NE 110"). Moreover, it fulfils the 10000 MW *RP* target when access to buses at all three voltage levels is allowed (case 16: "LLLW NE All"), resulting in four GH2 loads connected at 380 kV. Consequently, this grid scenario facilitates a larger GH2 power demand, centralized in more substantial GH2 plants than those achieved for the "Status Quo" scenario.

As portrayed in Figure 5.24, simulation case “LLLW NE 110” (case 15) sees increases of 4519 MW and 2637 MW in onshore and offshore wind generation outputs, accompanied by the addition of 2224 MW from biogas plants generation, and roughly 500 MW cumulative increase in hydropower and solar generation. Furthermore, simulation case “LLLW NE All” (case 16), which only proposes connections to the 380 kV grid, accommodates the corresponding demand increase from the four new GH2 loads mainly through increases of 6578 MW and 2122 MW in offshore and onshore wind energy generation. Additionally, biogas generation rises by 943 MW, with the remainder being supplied by other renewables like hydro and solar, which experience a minor increase in their output.

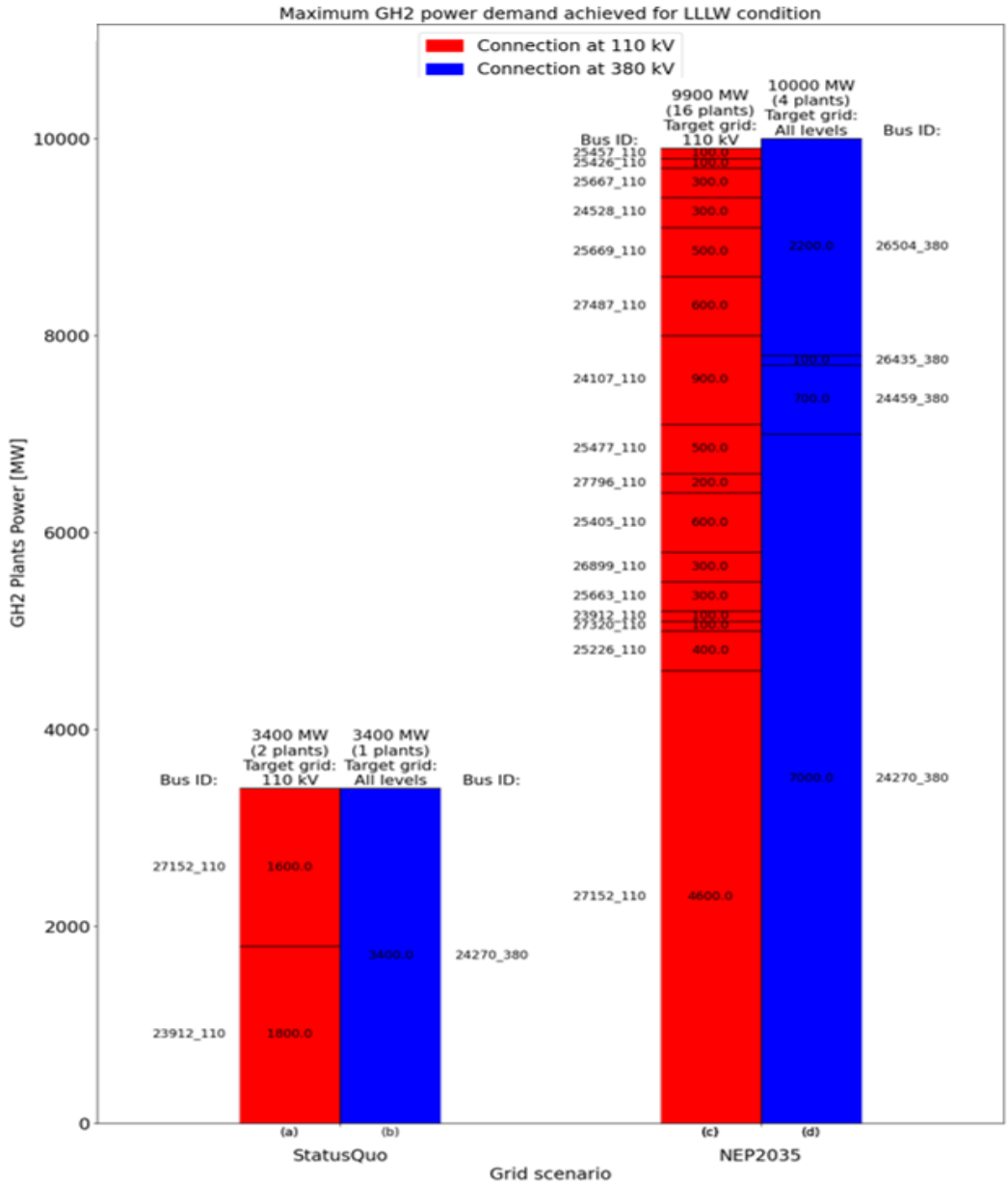

Figure 5.22. Resultant GH2 power, achieved from simulation cases 13 to 16: (a) LLLW SQ 110, (b) LLLW SQ All, (c) LLLW NE 110, (d) LLLW NE All.

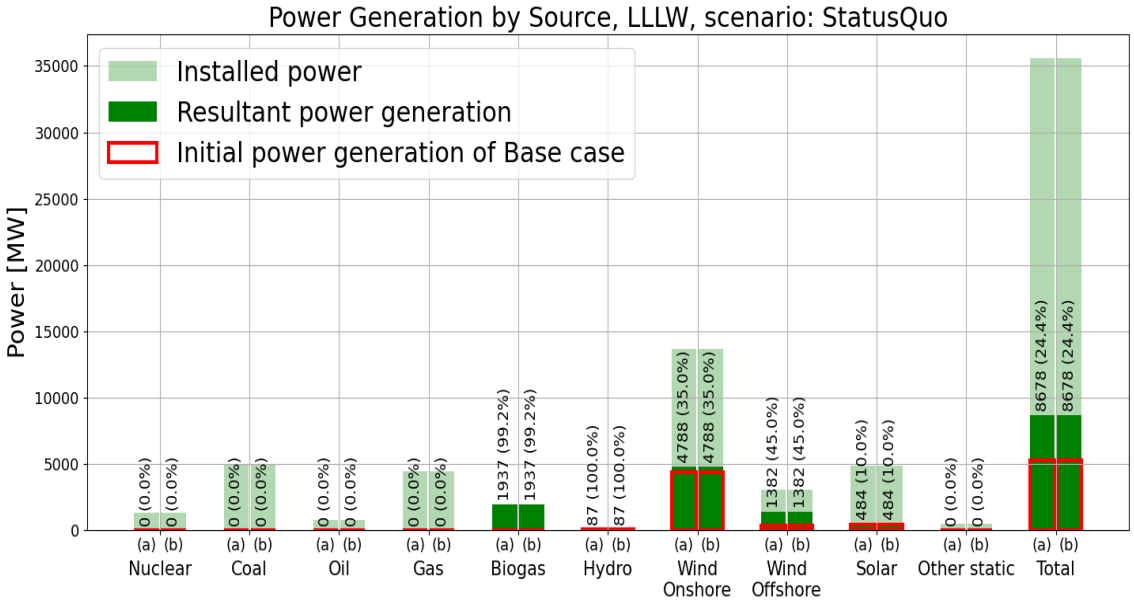

Figure 5.23. Resultant power generation, by energy source. Simulation cases 13 and 14: (a) LLLW SQ 110, (b) LLLW SQ All.

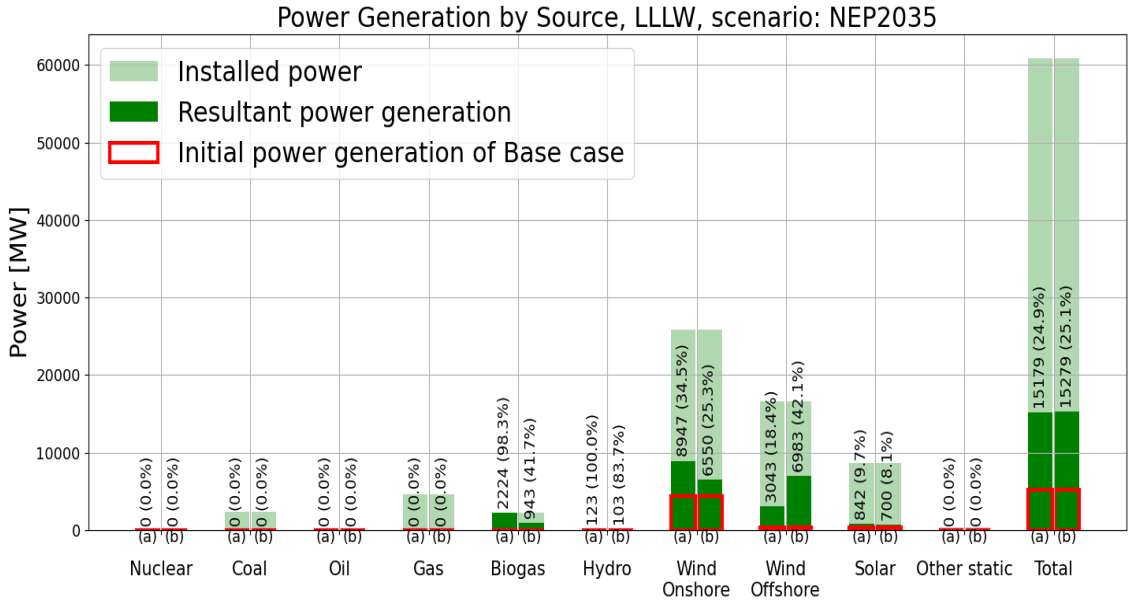

Figure 5.24. Resultant power generation, by energy source. Simulation cases 15 and 16: (a) HLLW NE 110, (b) HLLW NE All.

5.1.4.1. Resultant geographic distribution of GH2 plants in cases 13 and 14

Figure 5.25 indicates that the proposed GH2 plant locations for the "Status Quo" scenario under conditions of low demand and limited wind availability are concentrated in the north and west of Lower Saxony. In simulation case "LLLW SQ 110" (case 13), the GH2 power demand of 3400 MW is divided between two loads connected at 110 kV, which are located in the districts of Stade (1800 MW) and Leer (1600 MW).

Conversely, in simulation case "LLLW SQ All" (case 14), where connection to all voltage levels is allowed, the sole incorporated GH2 load of 3400 MW is situated in the district of Steinburg, connected to the 380 kV grid, as it can be observed in Figure 5.25.

The distribution of GH2 power demand by district (germ. *Landkreis*) for these simulation cases in scenario "Status Quo" is depicted in Figure 5.27.

5.1.4.2. Resultant geographic distribution of GH2 plants in cases 15 and 16

Under the "NEP2035" grid scenario, case "LLLW NE 110" (simulation case 15) suggests sixteen new GH2 loads distributed across various buses located in Schleswig-Holstein and Lower Saxony, connected at 110 kV (Figure 5.26). Gigawatt-level power demand is incorporated in the districts of Leer (4700 MW), Schleswig-Flensburg (1200 MW) and Wilhelmshaven (1000 MW), with 69 % of the total achieved GH2 power demand being concentrated in these three districts. Other GH2 loads are distributed among the districts of Emsland (800 MW), Nordfriesland (700 MW), Steinburg (600 MW), Dithmarschen (500 MW), Friesland (300 MW), and Stade (100 MW). This distribution of GH2 power demand by district (germ. *Landkreis*) is presented in Figure 5.28.

As demonstrated in Figure 5.26, case "LLLW NE All" (simulation case 16) results in four new GH2 loads, which are connected at 380 kV. In this simulation case, 78 % of the GH2 power demand is divided between the districts of Steinburg (7100 MW) and Dithmarschen (700 MW) in Schleswig-Holstein, while the remaining 22 % is incorporated in the district of Emsland in Lower Saxony (2200 MW), as depicted in Figure 5.28.

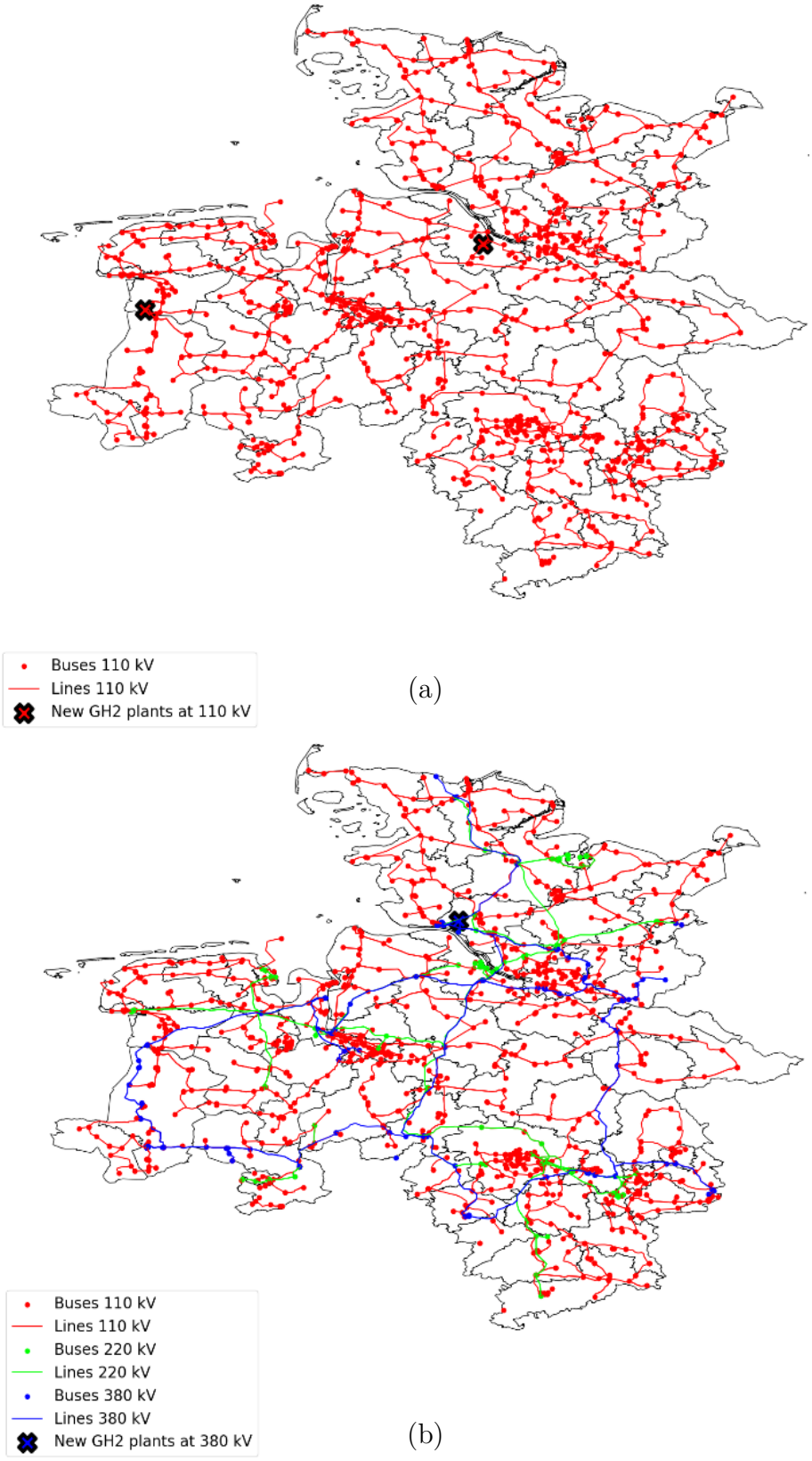

Figure 5.25. Geographic representation of GH2 plants connection points to the power grid simulation cases 13 and 14 (Status Quo): (a) LLLW SQ 110, (b) LLLW SQ All.

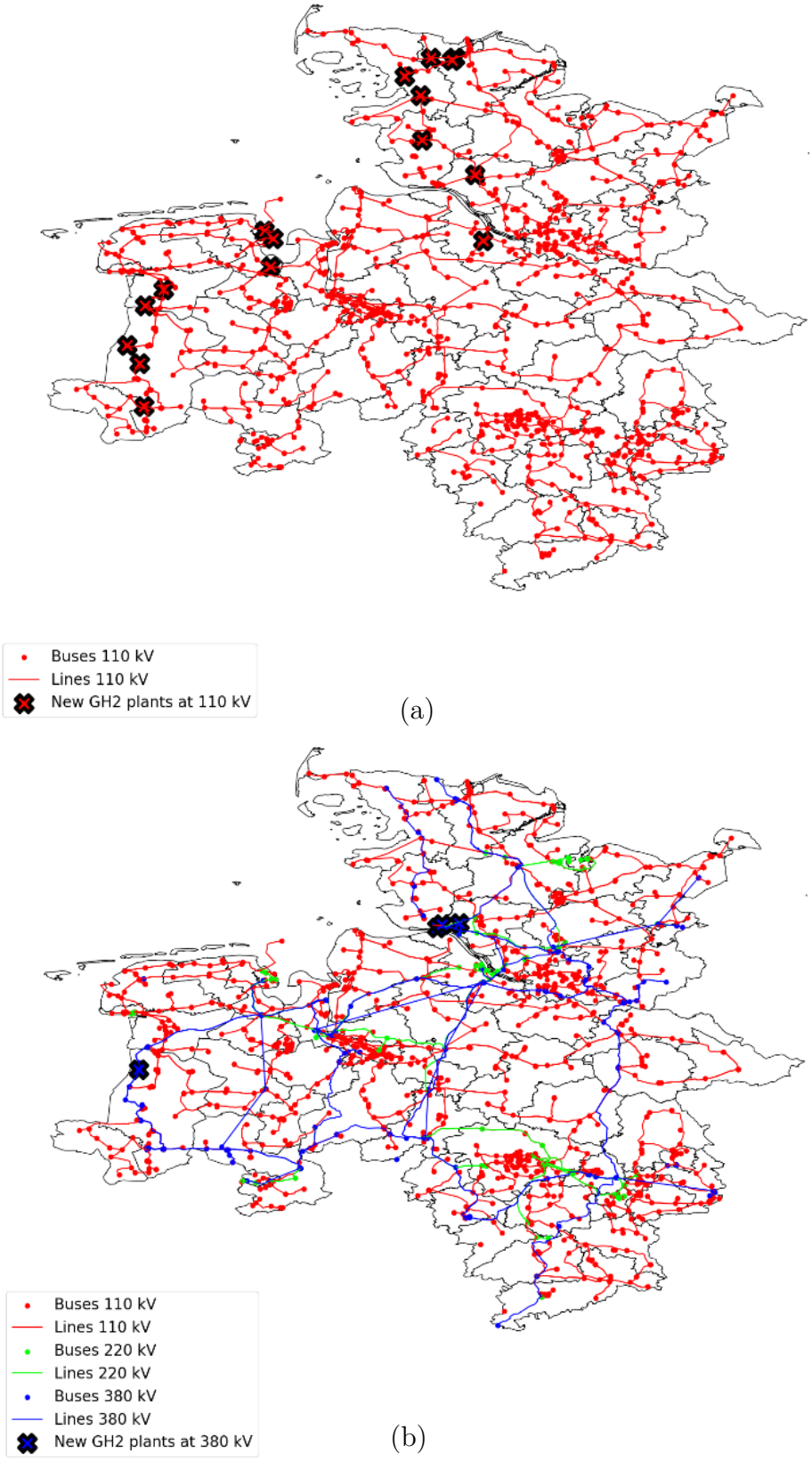

Figure 5.26. Geographic representation of GH2 plants connection points to the power grid. Simulation cases 7 and 8 (NEP2035): (a) LLHW NE 110, (b) LLHW NE All.

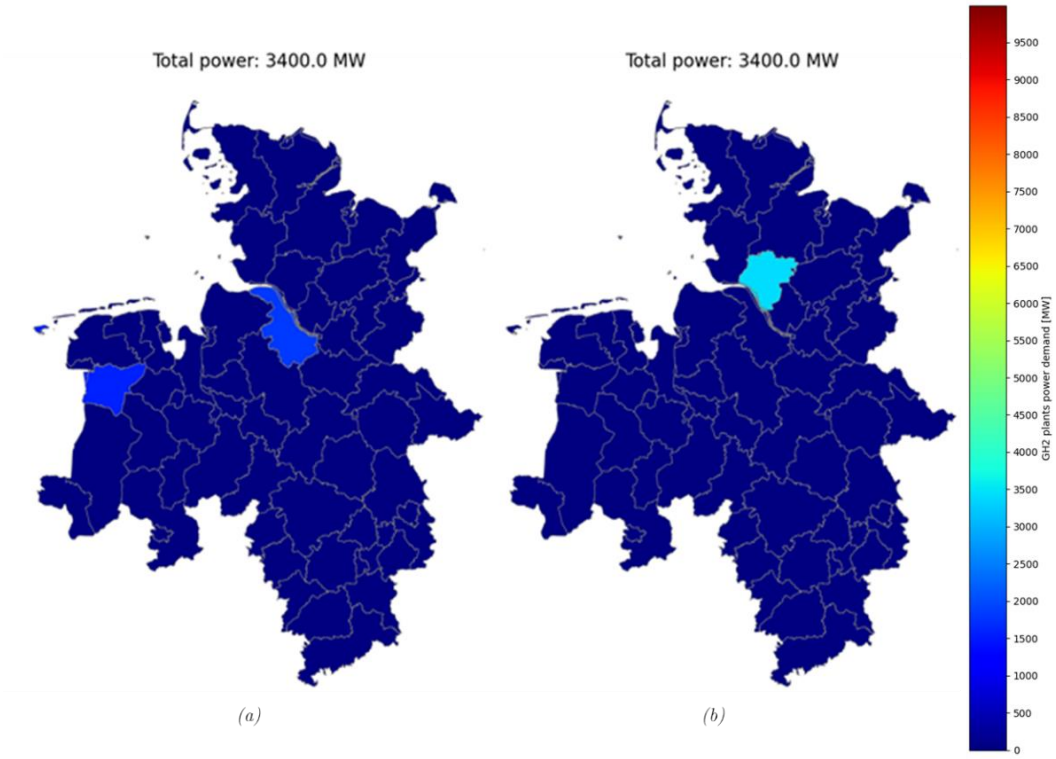

Figure 5.27. Resultant GH2 power, by district (germ. *Landkreis*), achieved from simulation cases 13 and 14 (Status Quo): (*a*) LLLW SQ 110, (*b*) LLLW SQ All.

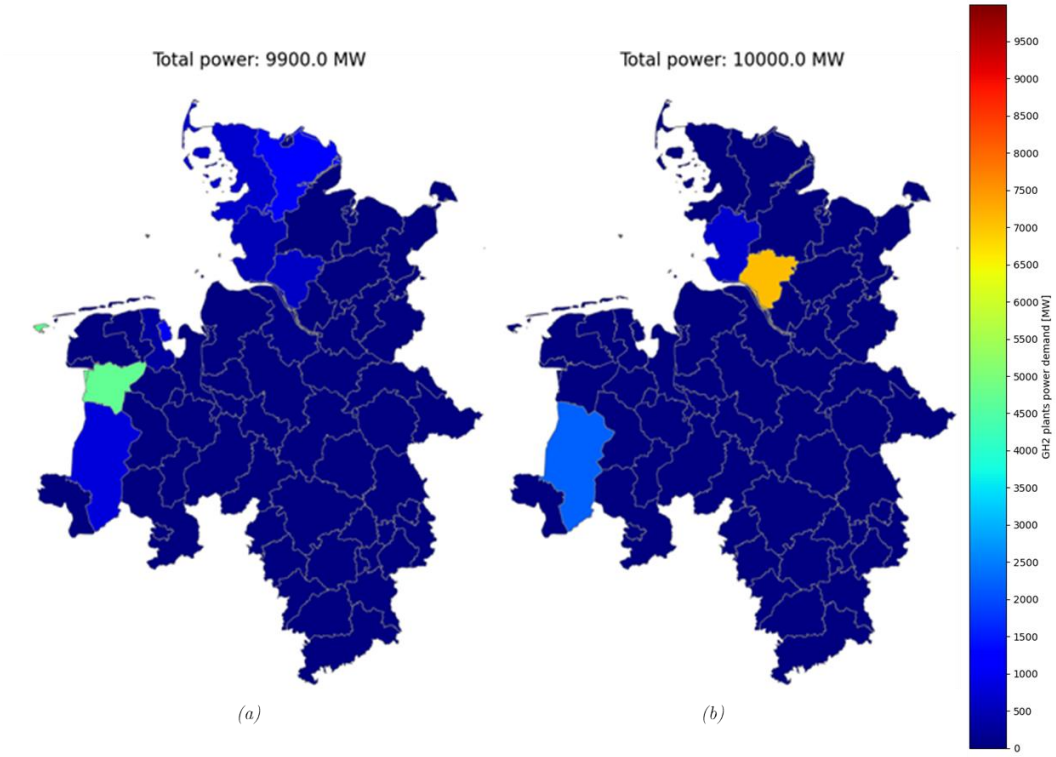

Figure 5.28. Resultant GH2 power, by district (germ. *Landkreis*), achieved from simulation cases 15 and 16 (NEP2035): (*a*) LLLW NE 110, (*b*) LLLW NE All.

5.2. Case comparison

This section provides a comparative analysis of the different simulation cases discussed in sections 5.1.1 to 5.1.4, encompassing cases 1 to 16. Examining the results from these simulations offers insightful information about the achieved GH2 power demand and the required number of GH2 loads for the different operating conditions and grid development scenarios that were considered.

When focusing on the achieved GH2 demand, it is evident that in grid scenario "Status Quo" the incorporation of new large-scale GH2 loads is not always attainable. This is observed in cases 9 and 10 where the system operates under high power demand from its original loads combined with limited availability of the wind resource, conditions that fully restrict the system's ability to incorporate large loads for green hydrogen production. Other cases show the incorporation of GH2 loads is possible, although the target RP of 10000 MW could only be achieved in cases 5 and 6, i.e. under conditions of low power demand from the system loads, coupled with high wind energy availability. Therefore, the observed behaviour indicates higher GH2 power demand is achieved when wind energy availability is higher, while high load conditions (which already exert pressure on RES and transmission lines) hinder the ability of the system to incorporate large-scale GH2 loads. This behaviour aligns with intuition, since high wind availability can be associated to a higher capacity for GH2 production. A summary of the incorporated GH2 power demand in each simulation case is illustrated in Figure 5.29 and Table 5.1.

The observed behaviour under the "Status Quo" grid scenario serves as a useful indicator of the performance of the method and algorithm employed to identify the maximum size and connection point of the GH2 loads in each simulation case. The logical results and discernible system changes align with expectations and can be easily rationalized.

In contrast, the "NEP2035" scenario consistently accommodates the incorporation of GH2 loads, with only cases 11, 12 (HLLW), and 15 (LLLW) falling short of the RP target.

In terms of the number of GH2 loads added to the grid in each simulation case to achieve the respective GH2 power demand, after analysing the geographic distributions of GH2 loads presented in section 5.1, and drawing inferences from Figure 5.30, it is observable that allowing connection of GH2 loads to all voltage levels produces higher centralization of the GH2 power demand for each grid scenario, i.e. greater amounts of power distributed among fewer loads, allowing

larger GH2 plants to be incorporated. Meanwhile, allowing connection only at 110 kV results in a more distributed allocation of GH2 loads.

Table 5.1. Summary of Achieved GH2 power demand in all simulation cases.

N°	Case designation	N° of GH2 plants	Achieved GH2 power [MW]	Available Power from RES [MW]*	Available Power from WEG** [MW]*
1	HLHW SQ 110	14	6500	6870	4839
2	HLHW SQ All	13	6600		
3	HLHW NE 110	10	10000	33368	30511
4	HLHW NE All	4	10000		
5	LLHW SQ 110	9	10000	13999	11694
6	LLHW SQ All	2	10000		
7	LLHW NE 110	5	10000	40582	37543
8	LLHW NE All	3	10000		
9	HLLW SQ 110	0	0	1	1
10	HLLW SQ All	0	0		
11	HLLW NE 110	5	4200	7403	4946
12	HLLW NE All	5	7300		
13	LLLW SQ 110	2	3400	3417	1418
14	LLLW SQ All	1	3400		
15	LLLW NE 110	16	9900	14508	11704
16	LLLW NE All	4	10000		

*Power that can be used to feed GH2 loads.

** WEG: Wind energy generators.

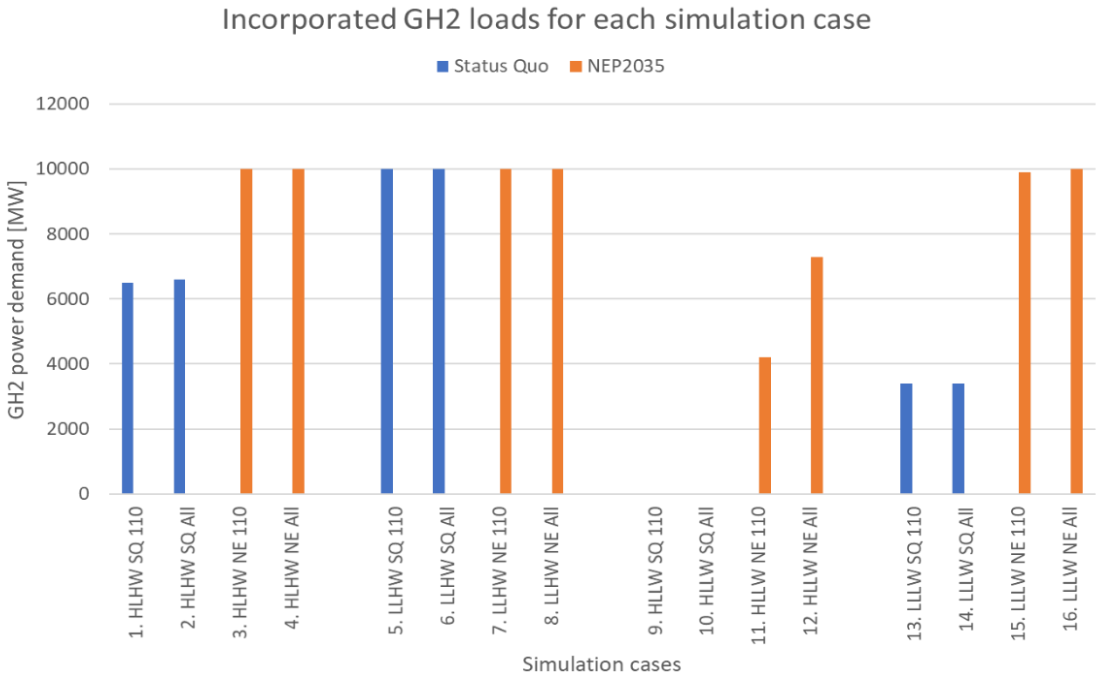

Figure 5.29. Summary of incorporated GH2 loads for each simulation case.

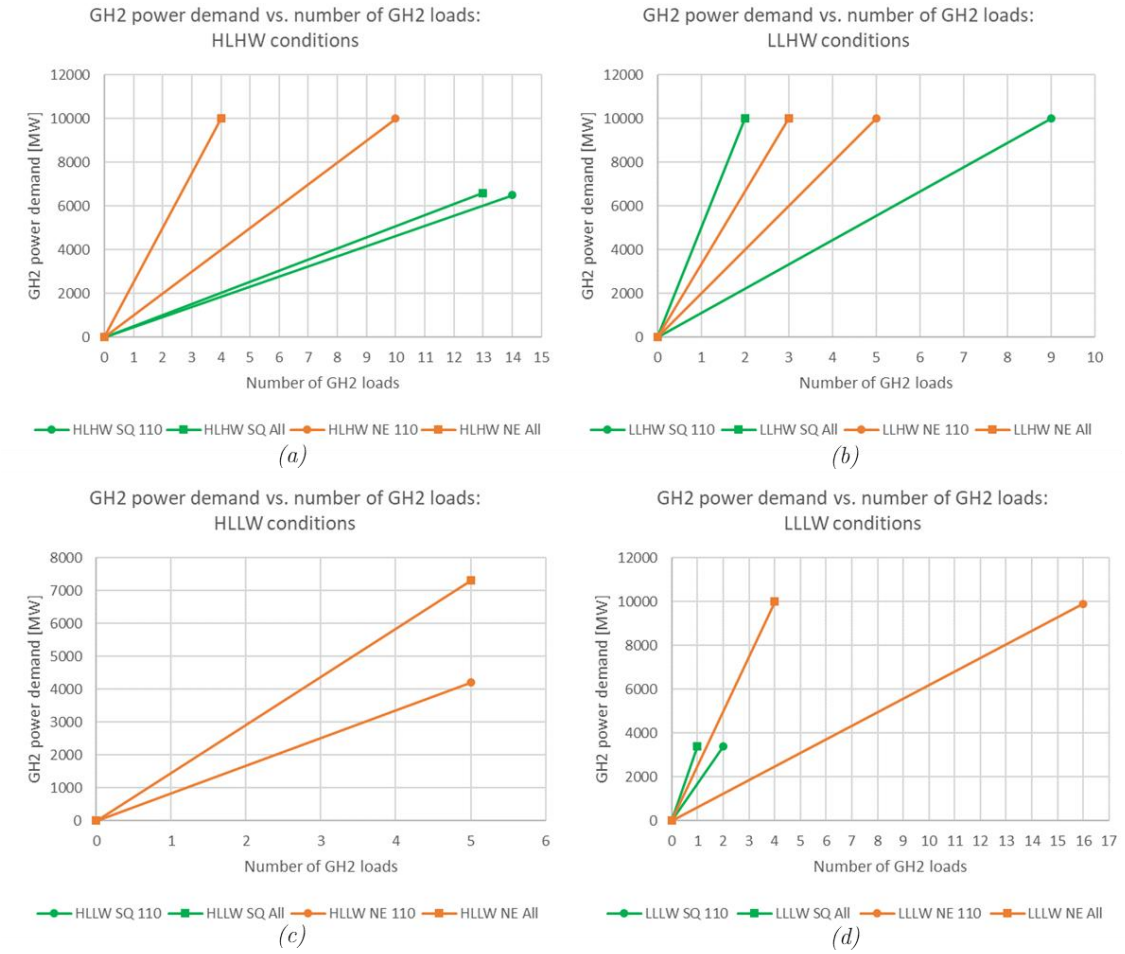

Figure 5.30. Correlation between achieved GH2 power demand and number of incorporated GH2 loads, for all scenarios, grouped by operative condition:
(*a*) HLHW, (*b*) LLHW, (*c*) HLLW, (*d*) LLLW.

It is interesting to see in Figure 5.30 (*b*) that under conditions of low initial power demand and high wind energy availability (LLHW), when allowing connections of new GH2 loads to all voltage levels (case 6: "LLHW SQ All" and case 8: "LLHW NE All"), although the 10000 MW pre-set target was achieved in both scenarios, case "LLHW SQ All" results in fewer GH2 loads (two) than case "LLHW NE All" (three). This indicates that the same power can be achieved with fewer GH2 plants in scenario "Status Quo", which is differs from the results obtained under other operative conditions.

As it can be observed in Figure 5.8, "LLHW NE All" allows for the incorporation of a major 7700 MW GH2 load, requiring other two GH2 loads of 2100 MW and 200 MW to attain the 10000 MW target. Meanwhile the highest GH2 load achieved in "LLHW SQ All" was 6600 MW (1100 MW lower than the highest in "LLHW NE All"), followed by another GH2 load of 3400 MW.

Since both cases have common buses in their selection of connection points, the causes of this behaviour can be rapidly investigated: after being able to initially incorporate the first GH2 load, case "LLHW NE All" (first GH2 load: 7700 MW) presents a higher utilization of transmission lines than "LLHW SQ All" (first GH2 load: 6600 MW), with more transmission lines operating at 100% capacity.

A higher line loading in case "LLHW NE All" hinders the system's ability to integrate further GH2 loads in other connection points without violating operative constraints, which restricts the achievable power demand of the second incorporated GH2 load to just 2100 MW. Thus, a third load of 200 MW in yet another connection point was required to attain the 10000 MW target.

Conversely, in case "LLHW SQ All", a resultant lower transmission line utilization after incorporating the first 6600 MW GH2 load, leaves room to supply more power to new GH2 loads in other buses, enabling the inclusion of a second GH2 load of higher power (3400 MW) than the corresponding one in case "LLHW NE All".

This situation suggests that in certain cases, incorporating the highest achievable GH2 power demand in the most stable bus (which is the expected output from the developed algorithm) could actually restrict the size of other GH2 loads in subsequent connection points, therefore increasing the number of GH2 loads required for achieving the pre-set target. To address this issue, the inclusion of a size optimization stage to the algorithm might prove beneficial in achieving a specific target with fewer GH2 loads, or alternatively, the opposite approach. This avenue of investigation could serve as a continuation of this thesis.

5.2.1. First steps in the incorporation of new GH2 Plants

The application of the methodology (and algorithm) presented in this thesis to determine the size and location of new GH2 plants resulted in a different combination of GH2 power demand and geographic distribution for every tested operative condition and grid scenario. While achieving a definitive optimal distribution of GH2 plants throughout the region of analysis will necessitate further steps, the data derived from these simulation cases can inform strategic resource allocation for the development of new GH2 facilities. This data can guide the prioritization of locations and grid connection points capable of supplying power to large-scale GH2 loads under a wide range of operative scenarios.

As highlighted in Figure 5.31, of almost two hundred potential connection points (or buses), only thirty-five are utilized across all simulation cases. Thus, if connection of new GH2 plants were restricted to the 110 kV grid, bus 27152_110,

located in the district of Leer, could be prioritized to receive resources related to the implementation of new GH2 facilities, provided this bus was considered as a connection point for new GH2 loads in all simulation cases where only connections to 110 kV was allowed and GH2 loads incorporation was possible. For operation under "Status Quo", another example of a connection point that appears in several operative conditions is bus 23912_110 (located in Stade), while for operation in "NEP2035" (once the grid infrastructure has evolved) bus 25663_110 (located in Schleswig-Flensburg) consistently features in all related simulation cases.

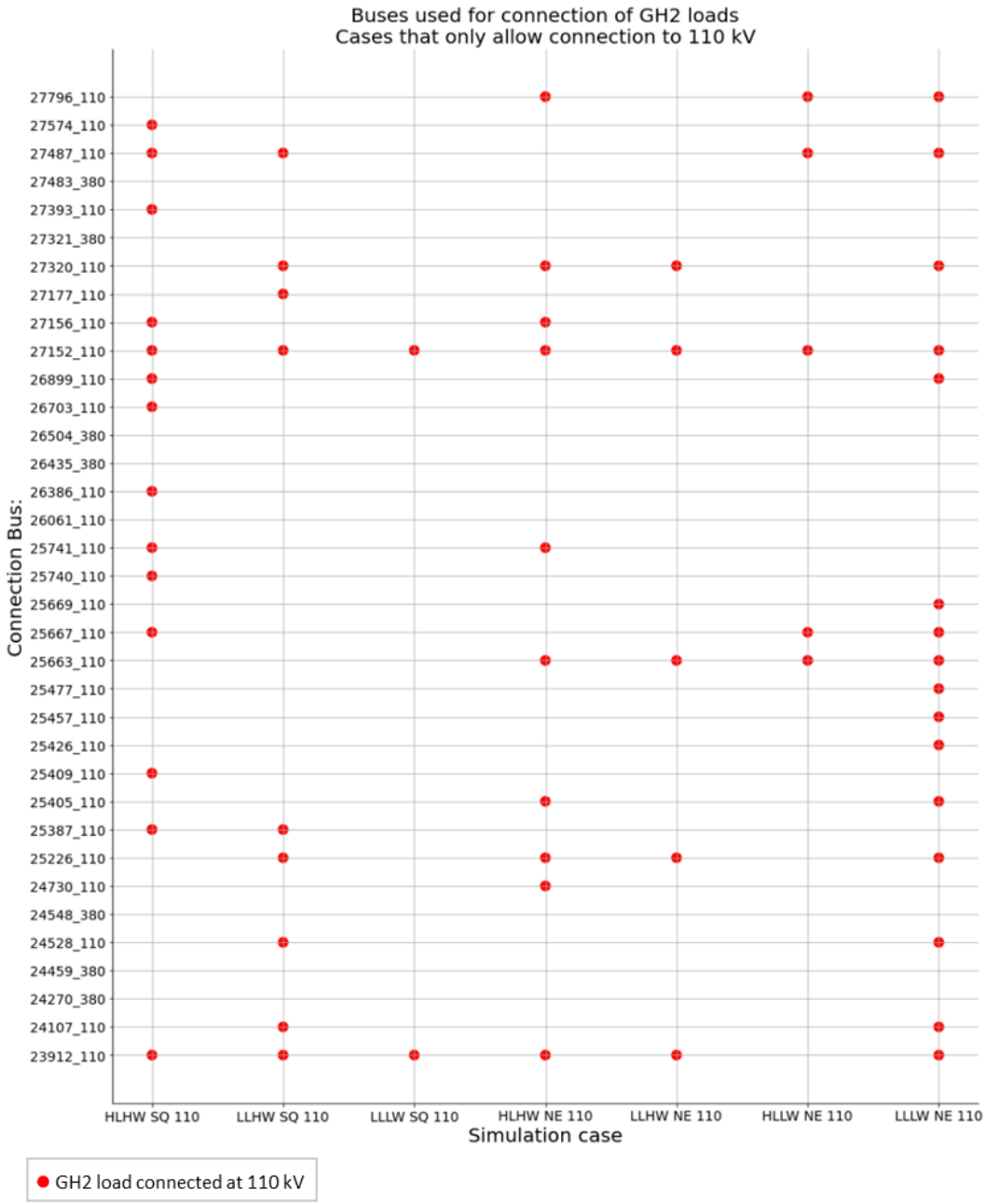

Figure 5.31. Connection points of new GH2 plants in simulation cases that only allow connection to 110 kV.

As depicted in Figure 5.32, when connections of new GH2 loads are permitted at all voltage levels, bus 24270_380 (located in Steinburg) is the most commonly recurring connection point across the simulation cases. Moreover, upon adaptation of the grid to the "NEP2035" scenario, bus 26435_380 (also located in Steinburg) presents a prime option for the prioritized allocation of resources for integration of new GH2 loads.

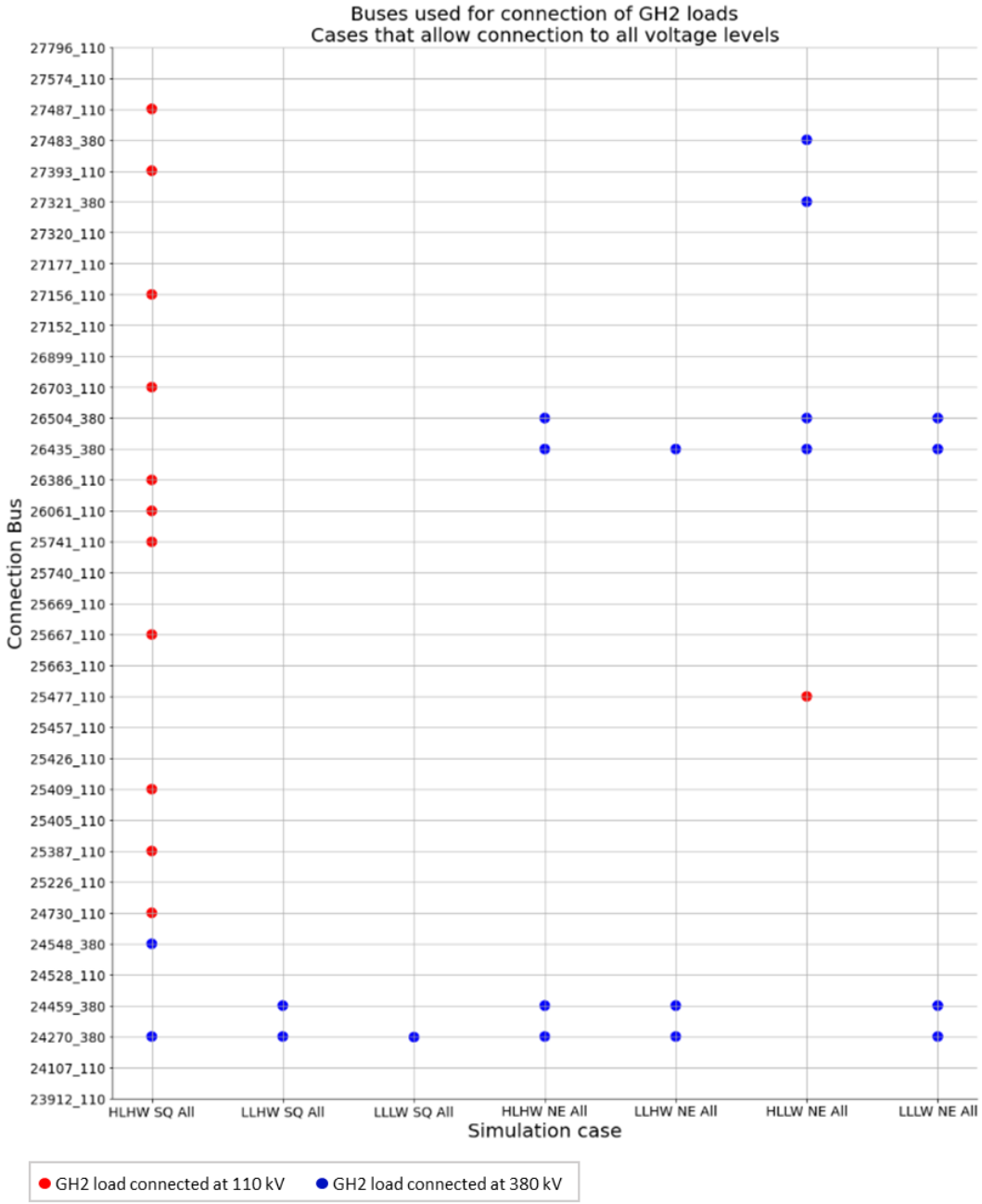

Figure 5.32. Connection points of new GH2 plants in simulation cases that allow connection to all voltage levels.

6. Conclusions

This thesis has successfully introduced and applied a method for determining a power-system-friendly distribution of new large-scale GH2 plants among nodes of interest in the northwest German high voltage power grid. This method was realized through an algorithm that strategically identified beneficial connection points for GH2 production facilities across the specified power grid nodes.

This algorithm determined the maximum GH2 plant size that could be sustainably connected to buses of interest, leveraging the benefits of implementing large-scale GH2 production facilities in both economic and logistical contexts. To achieve this, the *V-P* characteristic analysis was satisfactorily used to determine the connection points that could provide higher amounts of power without producing voltage collapse, achieving the incorporation of GH2 loads of up to 7700 MW while keeping stable power system operation in steady state.

Constrained power flow calculation enabled the incorporation of these large-scale loads to the power system without producing transmission line overloads. Moreover, optimal power flow calculations (OPF) optimized power allocation to generators based on generation costs, thereby prioritizing the use of Renewable Energy Sources (having the lowest generation costs) as outlined in our base case scenarios.

The implemented method and accompanying algorithm achieved the primary goal of proposing a strategic distribution of GH2 loads across the targeted grid for diverse operative conditions, drawing power exclusively from RES to meet the increase in power demand. Moreover, through the application of the *V-P* characteristic analysis, concentration of GH2 production in few connection points is produced, which is seen as a positive outcome due to the advantages of larger plant sizes as suggested in [14]. However, additional constraints such as available space, hydrogen storage capacity, and substation expansion capacity may limit the maximum GH2 plant size attainable at a particular location, which may well be considered for further studies.

The analysed model of the northwest German high voltage grid proves capable of accommodating new large-scale GH2 plants in several different operating conditions. However, under grid scenario “Status Quo” it is not always feasible to supply new GH2 loads. In this scenario, high load and low wind conditions demonstrated to fully prohibit the incorporation of new GH2 loads. Meanwhile, important GH2 power demand could be achieved in other operative situations, even

reaching the 10000 MW pre-set target when the system operates under low initial demand and full wind energy availability (extremely favourable conditions). Conversely, under "NEP2035" it was possible to incorporate new large-scale GH2 loads in every tried simulation case. Moreover, the German national target of 10000 MW for the year 2035 is consistently achieved in this scenario for all operative conditions but one (high initial load and low wind availability), although up to 7300 MW are achieved for this.

Two potential pathways for connecting new large-scale GH2 production facilities to the HV grid were proposed in this thesis: restriction to connect plants solely at the 110 kV level, and the unrestricted option allowing connections at all voltage levels. It was observed that enabling GH2 load connections at all voltage levels leads to more centralized GH2 power demand, i.e., larger GH2 plants.

The method outlined in this thesis serves as a tool for identifying the power capacity and beneficial locations of new large-scale hydrogen production facilities in Germany. In this regard, the application of the algorithm to the developed model of the northwest German high voltage grid rendered different combinations of plant sizes and connection points for the various evaluated cases. Therefore, a final answer to a definitive distribution of GH2 plants in the subject grid is yet to be established, which invites further research, that may include (apart from power system adequacy assessment to accommodate GH2 loads as in this thesis) evaluation of other criteria, such as gas infrastructure and environmental regulations, as well as optimization for maximum GH2 production and cost minimization. Despite these future challenges, a preliminary strategy to prioritize resource allocation for the implementation of new GH2 plants to connection points that were repetitively selected among all simulation cases has been proposed in section 5.2.1, highlighting buses 27152_110, 23912_110, 25663_110, 24270_380 and 26435_380 as connection points that consistently are utilized to incorporate GH2 loads through the simulation cases.

7. Future Work and Opportunities for Improvement

Continued advancements and extensions to this project may encompass additional development and validation of the northwest German high voltage grid model. This could involve the integration of transformers tap changer characteristics, as well as the inclusion of reactive power compensation components such as shunt and series capacitors, reactors, SVCs (static VAR compensator), and other FACTS (flexible alternating current transmission system) devices prevalent in the power grid. This would permit the deployment of reactive power management and voltage regulation strategies, factors that could influence the *V*-*P* characteristics calculations, which the algorithm in this thesis relies on to choose suitable connection points for new GH2 loads.

The inclusion of reactive power compensation devices could enhance the algorithm's functionality by enabling the implementation of AC optimal power flow. This would provide the capability to calculate reactive power flows within the system, thereby improving the significance of the results.

Besides, as this thesis only focus on the evaluation of steady state conditions, future developments may include dynamic analysis of system stability, providing information on the ability of the system to achieve and maintain steady state normal operation.

Moreover, future work could also contemplate the inclusion of other regions of the interconnected German (and broader European) power grid. Consideration of various contingency scenarios and the incorporation of *N*-1 congestion verification within the algorithm might also prove beneficial for further investigations.

Furthermore, GH2 plant size optimization considering voltage levels, overall power demand, internal component scaling (transformers, compressors, pumps, filters and electrolytic cells) for cost reduction and operative efficiency could be incorporated as additional stages to the presented algorithm.

Lastly, it would be advantageous to consider other criteria such as gas infrastructure, storage capacity, substation expansion capability, water availability, environmental constraints, and urban planning in the identification of interest buses as viable connection points for new GH2 facilities.

Appendix A

Buses of Interest:

Scenario "Status Quo"			Scenario "NEP2035"		
Bus ID	**District**	**Voltage Level**	**Bus ID**	**District**	**Voltage Level**
23744_110	Stade	110 kV	23744_110	Stade	110 kV
23806_110	Wittmund	110 kV	23806_110	Wittmund	110 kV
23808_110	Friesland	110 kV	23808_110	Friesland	110 kV
23825_110	Wilhelmshaven	110 kV	23825_110	Wilhelmshaven	110 kV
23912_110	Stade	110 kV	23912_110	Stade	110 kV
24107_110	Wilhelmshaven	110 kV	24107_110	Wilhelmshaven	110 kV
24137_110	Schleswig-Flensburg	110 kV	24137_110	Schleswig-Flensburg	110 kV
24270_380	Steinburg	380 kV	24270_380	Steinburg	380 kV
24314_110	Emsland	110 kV	24314_110	Emsland	110 kV
24315_110	Emsland	110 kV	24315_110	Emsland	110 kV
24350_110	Steinburg	110 kV	24350_110	Steinburg	110 kV
24352_110	Steinburg	110 kV	24352_110	Steinburg	110 kV
24446_110	Stade	110 kV	24446_110	Stade	110 kV
24451_110	Wesermarsch	110 kV	24451_110	Wesermarsch	110 kV
24459_380	Dithmarschen	380 kV	24457_110	Dithmarschen	110 kV
24528_110	Friesland	110 kV	24459_380	Dithmarschen	380 kV
24546_110	Friesland	110 kV	24528_110	Friesland	110 kV
24548_380	Emsland	380 kV	24546_110	Friesland	110 kV
24558_110	Wesermarsch	110 kV	24548_380	Emsland	380 kV
24622_110	Schleswig-Flensburg	110 kV	24558_110	Wesermarsch	110 kV
24630_110	Stade	110 kV	24622_110	Schleswig-Flensburg	110 kV
24634_110	Stade	110 kV	24630_110	Stade	110 kV
24648_110	Rendsburg-Eckernförde	110 kV	24634_110	Stade	110 kV
24663_110	Plön	110 kV	24648_110	Rendsburg-Eckernförde	110 kV
24669_110	Plön	110 kV	24663_110	Plön	110 kV
24674_110	Rendsburg-Eckernförde	110 kV	24669_110	Plön	110 kV
24698_110	Wesermarsch	110 kV	24674_110	Rendsburg-Eckernförde	110 kV
24709_110	Emden	110 kV	24698_110	Wesermarsch	110 kV
24715_110	Plön	110 kV	24709_110	Emden	110 kV

Scenario "Status Quo"			Scenario "NEP2035"		
Bus ID	**District**	**Voltage Level**	**Bus ID**	**District**	**Voltage Level**
24730_110	Rendsburg-Eckernförde	110 kV	24715_110	Plön	110 kV
24748_110	Plön	110 kV	24730_110	Rendsburg-Eckernförde	110 kV
24777_110	Friesland	110 kV	24748_110	Plön	110 kV
24778_110	Wittmund	110 kV	24777_110	Friesland	110 kV
24780_110	Emden	110 kV	24778_110	Wittmund	110 kV
24785_110	Plön	110 kV	24780_110	Emden	110 kV
24795_110	Wittmund	110 kV	24785_110	Plön	110 kV
24800_110	Wittmund	110 kV	24795_110	Wittmund	110 kV
24801_110	Aurich	110 kV	24800_110	Wittmund	110 kV
24802_110	Aurich	110 kV	24801_110	Aurich	110 kV
24803_110	Aurich	110 kV	24802_110	Aurich	110 kV
24805_110	Aurich	110 kV	24803_110	Aurich	110 kV
24806_110	Aurich	110 kV	24805_110	Aurich	110 kV
24807_110	Aurich	110 kV	24806_110	Aurich	110 kV
24808_110	Aurich	110 kV	24807_110	Aurich	110 kV
24821_110	Leer	110 kV	24808_110	Aurich	110 kV
24822_110	Leer	110 kV	24821_110	Leer	110 kV
24823_110	Leer	110 kV	24822_110	Leer	110 kV
24836_110	Cuxhaven	110 kV	24823_110	Leer	110 kV
24839_110	Wesermarsch	110 kV	24836_110	Cuxhaven	110 kV
24846_110	Wesermarsch	110 kV	24839_110	Wesermarsch	110 kV
24853_110	Leer	110 kV	24846_110	Wesermarsch	110 kV
24861_110	Leer	110 kV	24853_110	Leer	110 kV
24943_110	Nordfriesland	110 kV	24861_110	Leer	110 kV
24973_110	Rendsburg-Eckernförde	110 kV	24943_110	Nordfriesland	110 kV
24999_110	Bremerhaven	110 kV	24973_110	Rendsburg-Eckernförde	110 kV
25081_110	Wesermarsch	110 kV	24999_110	Bremerhaven	110 kV
25122_110	Steinburg	110 kV	25081_110	Wesermarsch	110 kV
25226_110	Emsland	110 kV	25122_110	Steinburg	110 kV
25227_380	Emsland	380 kV	25226_110	Emsland	110 kV
25240_110	Grafschaft Bentheim	110 kV	25227_380	Emsland	380 kV
25242_110	Emsland	110 kV	25240_110	Grafschaft Bentheim	110 kV
25244_110	Emsland	110 kV	25242_110	Emsland	110 kV
25245_110	Emsland	110 kV	25244_110	Emsland	110 kV
25286_110	Cuxhaven	110 kV	25245_110	Emsland	110 kV

Scenario "Status Quo"			Scenario "NEP2035"		
Bus ID	**District**	**Voltage Level**	**Bus ID**	**District**	**Voltage Level**
25302_110	Grafschaft Bentheim	110 kV	25286_110	Cuxhaven	110 kV
25387_110	Dithmarschen	110 kV	25302_110	Grafschaft Bentheim	110 kV
25402_110	Rendsburg-Eckernförde	110 kV	25387_110	Dithmarschen	110 kV
25405_110	Steinburg	110 kV	25402_110	Rendsburg-Eckernförde	110 kV
25406_220	Steinburg	220 kV	25405_110	Steinburg	110 kV
25409_110	Dithmarschen	110 kV	25406_220	Steinburg	220 kV
25410_110	Dithmarschen	110 kV	25409_110	Dithmarschen	110 kV
25414_110	Emsland	110 kV	25410_110	Dithmarschen	110 kV
25425_110	Wilhelmshaven	110 kV	25414_110	Emsland	110 kV
25430_110	Aurich	110 kV	25425_110	Wilhelmshaven	110 kV
25435_110	Emsland	110 kV	25426_110	Wilhelmshaven	110 kV
25438_110	Dithmarschen	110 kV	25428_110	Wittmund	110 kV
25457_110	Leer	110 kV	25430_110	Aurich	110 kV
25473_110	Dithmarschen	110 kV	25435_110	Emsland	110 kV
25476_110	Dithmarschen	110 kV	25438_110	Dithmarschen	110 kV
25477_110	Dithmarschen	110 kV	25457_110	Leer	110 kV
25493_110	Rendsburg-Eckernförde	110 kV	25473_110	Dithmarschen	110 kV
25500_110	Ostholstein	110 kV	25476_110	Dithmarschen	110 kV
25518_110	Leer	110 kV	25477_110	Dithmarschen	110 kV
25519_110	Rendsburg-Eckernförde	110 kV	25493_110	Rendsburg-Eckernförde	110 kV
25532_110	Lübeck	110 kV	25500_110	Ostholstein	110 kV
25535_110	Lübeck	110 kV	25518_110	Leer	110 kV
25569_110	Schleswig-Flensburg	110 kV	25519_110	Rendsburg-Eckernförde	110 kV
25570_110	Aurich	110 kV	25532_110	Lübeck	110 kV
25617_110	Aurich	110 kV	25535_110	Lübeck	110 kV
25640_110	Ostholstein	110 kV	25569_110	Schleswig-Flensburg	110 kV
25641_110	Ostholstein	110 kV	25570_110	Aurich	110 kV
25642_110	Ostholstein	110 kV	25617_110	Aurich	110 kV
25643_110	Ostholstein	110 kV	25640_110	Ostholstein	110 kV
25644_110	Ostholstein	110 kV	25641_110	Ostholstein	110 kV
25645_110	Ostholstein	110 kV	25642_110	Ostholstein	110 kV
25662_110	Schleswig-Flensburg	110 kV	25643_110	Ostholstein	110 kV

Scenario "Status Quo"			Scenario "NEP2035"		
Bus ID	**District**	**Voltage Level**	**Bus ID**	**District**	**Voltage Level**
25663_110	Schleswig-Flensburg	110 kV	25644_110	Ostholstein	110 kV
25666_110	Schleswig-Flensburg	110 kV	25645_110	Ostholstein	110 kV
25667_110	Schleswig-Flensburg	110 kV	25662_110	Schleswig-Flensburg	110 kV
25668_110	Schleswig-Flensburg	110 kV	25663_110	Schleswig-Flensburg	110 kV
25669_110	Nordfriesland	110 kV	25666_110	Schleswig-Flensburg	110 kV
25670_110	Nordfriesland	110 kV	25667_110	Schleswig-Flensburg	110 kV
25701_110	Rendsburg-Eckernförde	110 kV	25668_110	Schleswig-Flensburg	110 kV
25705_110	Emsland	110 kV	25669_110	Nordfriesland	110 kV
25706_110	Nordfriesland	110 kV	25670_110	Nordfriesland	110 kV
25723_110	Nordfriesland	110 kV	25701_110	Rendsburg-Eckernförde	110 kV
25724_110	Nordfriesland	110 kV	25705_110	Emsland	110 kV
25739_110	Dithmarschen	110 kV	25706_110	Nordfriesland	110 kV
25740_110	Rendsburg-Eckernförde	110 kV	25723_110	Nordfriesland	110 kV
25741_110	Nordfriesland	110 kV	25724_110	Nordfriesland	110 kV
25751_110	Schleswig-Flensburg	110 kV	25739_110	Dithmarschen	110 kV
25752_110	Nordfriesland	110 kV	25740_110	Rendsburg-Eckernförde	110 kV
25753_110	Nordfriesland	110 kV	25741_110	Nordfriesland	110 kV
25789_110	Nordfriesland	110 kV	25751_110	Schleswig-Flensburg	110 kV
25884_110	Stade	110 kV	25752_110	Nordfriesland	110 kV
25931_110	Ostholstein	110 kV	25753_110	Nordfriesland	110 kV
25980_110	Rendsburg-Eckernförde	110 kV	25789_110	Nordfriesland	110 kV
25991_110	Emsland	110 kV	25884_110	Stade	110 kV
26031_110	Lübeck	110 kV	25931_110	Ostholstein	110 kV
26039_110	Schleswig-Flensburg	110 kV	25980_110	Rendsburg-Eckernförde	110 kV
26040_110	Schleswig-Flensburg	110 kV	25991_110	Emsland	110 kV
26061_110	Dithmarschen	110 kV	26031_110	Lübeck	110 kV
26083_110	Emsland	110 kV	26039_110	Schleswig-Flensburg	110 kV

Scenario "Status Quo"			Scenario "NEP2035"		
Bus ID	**District**	**Voltage Level**	**Bus ID**	**District**	**Voltage Level**
26139_110	Wesermarsch	110 kV	26040_110	Schleswig-Flensburg	110 kV
26166_110	Cuxhaven	110 kV	26061_110	Dithmarschen	110 kV
26194_110	Wesermarsch	110 kV	26083_110	Emsland	110 kV
26215_110	Cuxhaven	110 kV	26134_110	Emden	110 kV
26227_110	Nordfriesland	110 kV	26139_110	Wesermarsch	110 kV
26251_110	Cuxhaven	110 kV	26166_110	Cuxhaven	110 kV
26252_110	Bremerhaven	110 kV	26194_110	Wesermarsch	110 kV
26263_110	Cuxhaven	110 kV	26215_110	Cuxhaven	110 kV
26285_110	Emsland	110 kV	26227_110	Nordfriesland	110 kV
26310_110	Flensburg	110 kV	26251_110	Cuxhaven	110 kV
26386_110	Ostholstein	110 kV	26252_110	Bremerhaven	110 kV
26435_380	Steinburg	380 kV	26263_110	Cuxhaven	110 kV
26504_380	Emsland	380 kV	26285_110	Emsland	110 kV
26549_110	Steinburg	110 kV	26310_110	Flensburg	110 kV
26678_110	Grafschaft Bentheim	110 kV	26386_110	Ostholstein	110 kV
26679_110	Grafschaft Bentheim	110 kV	26435_380	Steinburg	380 kV
26693_110	Flensburg	110 kV	26504_380	Emsland	380 kV
26703_110	Nordfriesland	110 kV	26549_110	Steinburg	110 kV
26889_110	Stade	110 kV	26678_110	Grafschaft Bentheim	110 kV
26893_110	Bremerhaven	110 kV	26679_110	Grafschaft Bentheim	110 kV
26899_110	Emsland	110 kV	26693_110	Flensburg	110 kV
26917_110	Steinburg	110 kV	26703_110	Nordfriesland	110 kV
26918_110	Schleswig-Flensburg	110 kV	26889_110	Stade	110 kV
26942_110	Aurich	110 kV	26893_110	Bremerhaven	110 kV
26946_110	Nordfriesland	110 kV	26899_110	Emsland	110 kV
27030_110	Leer	110 kV	26917_110	Steinburg	110 kV
27152_110	Leer	110 kV	26918_110	Schleswig-Flensburg	110 kV
27153_380	Leer	380 kV	26942_110	Aurich	110 kV
27156_110	Dithmarschen	110 kV	26943_110	Wittmund	110 kV
27161_110	Cuxhaven	110 kV	26946_110	Nordfriesland	110 kV
27177_110	Steinburg	110 kV	27030_110	Leer	110 kV
27242_110	Cuxhaven	110 kV	27152_110	Leer	110 kV
27320_110	Emsland	110 kV	27153_380	Leer	380 kV
27321_380	Emsland	380 kV	27156_110	Dithmarschen	110 kV
27334_110	Lübeck	110 kV	27161_110	Cuxhaven	110 kV

Scenario "Status Quo"			Scenario "NEP2035"		
Bus ID	**District**	**Voltage Level**	**Bus ID**	**District**	**Voltage Level**
27346_110	Cuxhaven	110 kV	27177_110	Steinburg	110 kV
27358_110	Schleswig-Flensburg	110 kV	27242_110	Cuxhaven	110 kV
27383_110	Nordfriesland	110 kV	27320_110	Emsland	110 kV
27393_110	Nordfriesland	110 kV	27321_380	Emsland	380 kV
27435_110	Steinburg	110 kV	27334_110	Lübeck	110 kV
27478_110	Schleswig-Flensburg	110 kV	27346_110	Cuxhaven	110 kV
27483_380	Schleswig-Flensburg	380 kV	27358_110	Schleswig-Flensburg	110 kV
27487_110	Schleswig-Flensburg	110 kV	27383_110	Nordfriesland	110 kV
27519_110	Steinburg	110 kV	27393_110	Nordfriesland	110 kV
27552_110	Wittmund	110 kV	27435_110	Steinburg	110 kV
27558_110	Emsland	110 kV	27478_110	Schleswig-Flensburg	110 kV
27574_110	Nordfriesland	110 kV	27483_380	Schleswig-Flensburg	380 kV
27606_110	Plön	110 kV	27487_110	Schleswig-Flensburg	110 kV
27650_110	Stade	110 kV	27500_110	Emsland	110 kV
27663_110	Aurich	110 kV	27519_110	Steinburg	110 kV
27664_110	Cuxhaven	110 kV	27552_110	Wittmund	110 kV
27680_110	Aurich	110 kV	27558_110	Emsland	110 kV
27684_110	Nordfriesland	110 kV	27574_110	Nordfriesland	110 kV
27686_110	Steinburg	110 kV	27606_110	Plön	110 kV
27687_110	Friesland	110 kV	27650_110	Stade	110 kV
27690_110	Steinburg	110 kV	27663_110	Aurich	110 kV
27692_110	Rendsburg-Eckernförde	110 kV	27664_110	Cuxhaven	110 kV
27703_110	Wittmund	110 kV	27680_110	Aurich	110 kV
27734_110	Schleswig-Flensburg	110 kV	27684_110	Nordfriesland	110 kV
27796_110	Nordfriesland	110 kV	27686_110	Steinburg	110 kV
27808_110	Emsland	110 kV	27687_110	Friesland	110 kV
27834_110	Stade	110 kV	27690_110	Steinburg	110 kV
27941_110	Nordfriesland	110 kV	27692_110	Rendsburg-Eckernförde	110 kV
28172_110	Emsland	110 kV	27703_110	Wittmund	110 kV
28309_110	Ostholstein	110 kV	27734_110	Schleswig-Flensburg	110 kV
28357_110	Stade	110 kV	27796_110	Nordfriesland	110 kV

Scenario "Status Quo"			Scenario "NEP2035"		
Bus ID	**District**	**Voltage Level**	**Bus ID**	**District**	**Voltage Level**
28360_110	Grafschaft Bentheim	110 kV	27808_110	Emsland	110 kV
28403_110	Ostholstein	110 kV	27834_110	Stade	110 kV
			27941_110	Nordfriesland	110 kV
			28172_110	Emsland	110 kV
			28309_110	Ostholstein	110 kV
			28357_110	Stade	110 kV
			28360_110	Grafschaft Bentheim	110 kV
			28403_110	Ostholstein	110 kV

References

[1] H.-O. Pörtner, D. C. Roberts, E. S. Poloczanska, K. Mintenbeck, M. Tignor, A. Alegría, M. Craig, S. Langsdorf, S. Löschke and V. Möller, "IPCC, 2022: Summary for policymakers," in *Climate Change 2022: Impacts, Adaptation, and Vulnerability*, Cambridge, UK and New York, NY, USA, Cambridge University Pres, 2022, pp. 3-33.

[2] Federal Ministry for the Environment, Nature Conservation, Building and Nuclear Safety (BMUB), "Climate Action Plan 2050," Berlin, 2016.

[3] International Energy Agency, "Germany 2020 - Energy Policy Review," IEA, 2020.

[4] B. Burger, "Net Electricity Generation in Germany in 2022: Significant Increase in Generation from Wind and PV," Fraunhofer Institute for Solar Energy Systems ISE, Freiburg, Germany, 2023.

[5] C. Flachsland and S. Levi, "Germany's Federal Climate Change Act," *Environmental Politics,* vol. 30, no. sup1, pp. 118-140, 2021.

[6] Fraunhofer ISE, "Net installed electricity generation capacity in Germany in 2023," Fraunhofer ISE, 2023. [Online]. Available: https://energy-charts.info/charts/installed_power/chart.htm?l=en&c=DE&chartColumnSorting=default. [Accessed 2023].

[7] F. Cebulla, J. Haas, J. Eichman, W. Nowak and P. Mancarella, "How much electrical energy storage do we need? A synthesis for the U.S., Europe, and Germany," *Journal of Cleaner Production,* vol. 181, 2018.

[8] A. Rabiee, A. Keane and A. Soroudi, "Green hydrogen: A new flexibility source for security constrained scheduling of power systems with renewable energies," *International Journal of Hydrogen Energy,* vol. 46, no. 37, pp. 19270-19284, 2021.

[9] International Energy Agency, "The Future of Hydrogen : Seizing today's opportunities," IEA, Paris, 2019.

[10] Federal Ministry for Economic Affairs and Energy, "The National Hydrogen Strategy," Federal Ministry for Economic Affairs and Energy, Public Relations Division, Berlin, 2020.

[11] M. Takach, M. Sarajlić, D. Peters, M. Kroener, F. Schuldt and K. von Maydell, "Review of Hydrogen Production Techniques from Water Using Renewable Energy Sources and Its Storage in Salt Caverns," *Energies (Basel),* vol. 15, no. 4, p. 1415, 2022.

[12] 50Hertz Transmission GmbH, Amprion GmbH, TenneT TSO GmbH, TransnetBW GmbH, "Netzentwicklungsplan Strom 2035, Version 2021," 2021.

[13] Gasunie Deutschland Transport Services GmbH, TenneT TSO GmbH, Thyssengas GmbH, "Quo Vadis, Elektrolyse? Identifikation gesamtenergiesystemdienlicher Power-to-Gas-Standorte in der Potentialregion nordwestliches Niedersachsen und Schleswig-Holstein," 2022.

[14] E. R. Morgan, J. F. Manwell and J. G. McGowan, "Opportunities for economies of scale with alkaline electrolyzers," *International Journal of Hydrogen Energy,* vol. 38, no. 36, pp. 15903-15909, 2013.

[15] P. S. Kundur, Power system stability and control, N. J. Balu and M. G. Lauby, Eds., Mc Graw Hill, 1994.

[16] N. T. Linh, "Voltage stability analysis of grids connected wind generators," *2009 4th IEEE Conference on Industrial Electronics and Applications,* pp. 2657-2660, 2009.

[17] A. Siritaratiwat and N. Thasnas, "Static Voltage Stability Margin Enhancement Using Shunt Capacitor, SVC and STATCOM," *Applied Mechanics and Materials (Advanced Engineering Research),* vol. 781, pp. 288-291, 2015.

[18] A. Fateh, M. Nor and M. Sulaiman, "Identification of Weak Buses in Electrical Power System," *ARPN Journal of Engineering and Applied Sciences,* vol. 14, no. 7, pp. 1377-1384, 2019.

[19] J. J. Grainger and W. D. Stevenson, Power Systems Analysis, McGraw-Hill, 1994.

[20] M. Crappe, Electric power systems, Hoboken, NJ: Wiley, 2008.

[21] Federal Ministry for Economic Affairs and Climate Action, "Grids and infrastructure," 2023. [Online]. Available: https://www.bmwk.de/Redaktion/EN/Artikel/Energy/electricity-grids-of-the-future-01.html. [Accessed 2023].

[22] B. Stott, "Review of load-flow calculation methods," *Proceedings of the IEEE,* vol. 62, no. 7, pp. 916-929, 1974.

[23] D. I. Sun, B. Ashley, B. Brewer, A. Hughes and W. F. Tinney, "Optimal Power Flow By Newton Approach," *IEEE Transactions on Power Apparatus and Systems,* Vols. PAS-103, no. 10, pp. 2864-2880, 1984.

[24] S. Nuthalapati, Use of Voltage Stability Assessment and Transient Stability Assessment Tools in Grid Operations, 1st ed. 2021. ed., Springer International Publishing, 2021.

[25] P. Kundur, J. Paserba, Ajjarapu, G. Andersson, A. Bose, C. Canizares, N. Hatziargyriou, D. Hill, A. Stankovic, C. Taylor, T. Van Cutsem and Vittal, "Definition and classification of power system stability," *IEEE transactions on power systems,* vol. 19, no. 3, pp. 1387-1401, 2004.

[26] B. Gao, G. K. Morison and P. Kundur, "Towards the development of a systematic approach for voltage stability assessment of large-scale power systems," *IEEE Transactions on Power Systems,* vol. 11, no. 3, pp. 1314-1324, 1996.

[27] J. Brauns and T. Turek, "Alkaline water electrolysis powered by renewable energy: A review," *Processes,* vol. 8, no. 2, 2020.

[28] T. Wang, X. Cao and L. Jiao, "PEM water electrolysis for hydrogen production: fundamentals, advances, and prospects," *Carbon Neutrality,* vol. 1, no. 1, p. 21, 2022.

[29] K. Belmokhtar, M. L. Doumbia and K. Agbossou, "Dynamic model of an alkaline electrolyzer based on artificial neural networks," in *Eighth International Conference and Exhibition on Ecological Vehicles and Renewable Energies (EVER)*, Monte Carlo, Monaco, 2013.

[30] A. Ursúa and P. Sanchis, "Static–dynamic modelling of the electrical behaviour of a commercial advanced alkaline water electrolyser," *International Journal of Hydrogen Energy,* vol. 37, no. 24, pp. 18598-18614, 2012.

[31] M. Chen, S.-F. Chou, F. Blaabjerg and P. Davari, "Overview of Power Electronic Converter Topologies Enabling Large-Scale Hydrogen Production via Water Electrolysis," *Applied Sciences,* vol. 12, no. 4, 2022.

[32] C. d. Boor, A Practical Guide to Splines, New York: Springer Verlag, 2001.

[33] P. Virtanen, "SciPy 1.0: fundamental algorithms for scientific computing in Python," *Nature Methods,* vol. 17, no. 3, pp. 261-272, 2020.

[34] A. Quarteroni, Numerical Mathematics, R. Sacco and F. Saleri, Eds., New York, NY: Springer, 2007.

[35] C. R. Harris, "Array programming with NumPy," *Nature,* vol. 585, no. 7825, pp. 357-362, 2020.

[36] International Renewable Energy Agency, "Green Hydrogen Cost Reduction: Scaling up Electrolysers to Meet the 1.5ºC Climate Goal," Abu Dhabi, 2020.

[37] DIgSILENT GmbH, PowerFactory 2022 User Manual, Gomaringen, Germany: DIgSILENT GmbH, 2022.

[38] open_eGo: open electricity grid optimization, "Open Energy Platform," [Online]. Available: https://openenergy-platform.org/. [Accessed 2023].

[39] U. P. Müller, B. Schachler, W. D. Bunke, J. Bartels, M. Glauer, C. Büttner, K. E. Günther Stephan, I. Cussmann, L. Hülk, M. Scharf and others, "Netzebenenübergreifendes Planungsinstrument-zur Bestimmung des optimalen Netz-und Speicherausbaus in Deutschland-integriert in einer OpenEnergy-Plattform," Hochschule Flensburg – University of Applied Sciences, Flensburg, 2019.

[40] F. Kaspar, M. Borsche, U. Pfeifroth, J. Trentmann, J. Drücke and P. Becker, "A climatological assessment of balancing effects and shortfall risks of photovoltaics and wind energy in Germany and Europe," *Advances in Science and Research,* vol. 16, pp. 119-128, 2019.

[41] L. Barroso and H. Rudnick, "The Growth of Renewables: Zero-Marginal-Cost Electricity Markets [Guest Editorial]," *IEEE Power and Energy Magazine,* vol. 19, no. 1, pp. 16-18, 2021.

[42] C. Kost, S. Shammugam, V. Fluri, D. Peper, A. D. Memar and T. Schlegel, "Levelized Cost of Electricity-Renewable Energy Technologies," Fraunhofer Institute for Solar Energy Systems ISE, Freiburg, 2021.

Declaration of Authorship

I, Orlando Antonio Pereira Leon, declare that this thesis titled, "Power-Grid-Friendly Placement of Large-Scale Hydrogen Production Facilities in the Northwest German High Voltage Grid" and the work presented in it are my own.

I hereby confirm that this thesis is entirely my own work. I confirm that no part of the document has been copied from either a book or any other source – including the internet – except where such sections are clearly shown as quotations and the sources have been correctly identified within the text or in the list of references.

Moreover, I confirm that I have taken notice of the "Leitlinien guter wissenschaftlicher Praxis" of the University of Oldenburg.

Oldenburg, 09.08.2023

Place, date.

Author's signature.